Dissertation

submitted to the

Combined Faculties for the Natural Sciences and for Mathematics

of the Ruperto-Carola University Heidelberg, Germany

for the degree of

Doctor of Natural Science

Presented by:

Master of Science Sabrina Schröder

Born in: Bochum

Oral-examination:

……

Functional Analysis of Sam68 during Forebrain and Oligodendrocyte Development

Referees: Prof. Dr. Ulrike Müller

PD Alexander von Holst

Content

List of Figures

Abbreviations

BMP	Bone Morphogenic Protein
bp	Base pairs
BSA	Bovine Serum Albumine
CDM	Chemically Defined Medium
CDM_Diff.	CDM Differentiation Medium
CDM_Prol.	CDM Proliferation Medium
cDNA	Copy DNA
CGE	Caudal Ganglionic Eminence
CNS	Central Nervous System
CP	Cortical Plate
Cy2	Carbocyanine
Cy3	Indocarbocyanine
DMEM	Dulbeccos Modified MEM
dNTP	Deoxyribonucleotide-triphosphate
ECL	Enhanced Chemiluminescence
ECM	Extracellular Matrix
EDTA	Ethylenediaminetetraacetic acid
EGFP	Enhanced GFP
FCS	Fetal Calf Serum
FITC	Fluorescein Isothiocyanate
FGF	Fibroblast Growth Factor
GCL	Ganglion Cell Layer
GE	Ganglionic Eminence
GFAP	Glial Fibrillary Acidic Protein
GFP	Green Fluorescent Protein
Gly	Glycin
h	Hour
HEK293	Human Embryonic Kidney Cells
HEPES	4-(2-hydroxyethyl)-1-piperazineethanesulfonic acid

hnRNP	Heterogenous Nuclear Protein
HRP	Horseraddish peroxydase
Golli	Genes of oligodendrocyte lineage
Ig	Immunglobulin
IGF-1	Insulin like Growth Factor 1
IP	Intermediate Progenitor Cells
IR	Insulin Receptor
IRS-1	Insulin Receptor Substrate 1
KRH	Krebs-Ringer-HEPES
KRH/A	KRH with BSA
kDa	Kilodalton
LB	Lysogeny Broth
LGE	Lateral Ganglionic Eminence
MAG	Myelin-associated Glycoprotein
MBP	Myelin Basic Protein
MEM	Minimal Essential Medium
MGC	Mixed Glial Culture Medium
MGE	Medial Ganglionic Eminence
mRNA	Messenger RNA
NSC	Neural Stem Cell
OPC	Oligodendrocyte Precursor Cell
ONL	Outer Nuclear Layer
P	Postnatal Day
PAGE	Polyacrylamide gel electrophoresis
PBS	Phosphate-buffered saline
PBS/A	PBS with BSA
PBT1	PBS with TritonX100
PBT01	PBT with L-lysine
PBT/IM	PBT with Serum
PCR	Polymerase Chain Reaction
PDGF-AA	Plateled-derived Growth Factor
PDGFRα	PDGF receptor alpha
PDL	Poly-D-Lysin

PFA	Paraformaldehyd
PLP	Proteolipid Protein
PORN	Poly-Ornithin
P/S	Penicillin/Streptavidin
PVDF	Polyvinylidenfluoride
RNP	Ribonucleoprotein
ROI	Region of Interest
rpm	Rounds per minute
RT	Room temperature
RT-PCR	Reverse Transcriptase PCR
Sam68	Src-associated substrate in mitosis of 68kDa
SD	Standard deviation
SDS	Sodium Dodecyl Sulfate
SHH	Sonic Hedgehog Protein
siRNA	Small interfering RNA
Slm-1	Sam68 like mammalian Protein-1
Slm-2	Sam68 like mammalian Protein-2
STAR	Signal transduction and activation of RNA
T3	Triiodothyronin
T4	Thyroxin
TAE	Tris-acetate-EDTA
TBS	Tris-buffered saline
TBST	TBS with Tween20
TE	Trypsin-EDTA
TEMED	N,N,N',N'-Tetramethylethylendiamine
Tris	2-Amino-2-(hydroxymethyl)-propane-1,3-diol
TE	Trypsin EDTA
Tnc	Tenascin-C
Tnr	Tenascin-R
U	Unit
ZNS	Zentrales Nervensystem

Abstract

During the development of the central nervous sytem (CNS) the maturation of oligodendrocytes occurs through the tightly regulated activity of diverse intrinsic and extrinsic signalling factors. Our group identified the STAR-family protein Sam68 as one of those intrinsic cues involved in oligodendrocyte differentiation. The level of Sam68 increases with ongoing maturation and it regulates the expression of Myelin Basic Protein (MBP). Despite its role in OPC (oligodendrocyte precursor cells) maturation, previous studies already identified Sam68 as a promotor of neural stem cell (NSC) differentiation and as a Tenascin-C- regulated target gene. However, the mechanism(s) how Sam68 regulates NSC and particularly oligodendrocyte development remained incompletely understood. This thesis provides completely new insights into the role of Sam68 during forebrain and particularly, oligodendrocyte development. Furthermore, my results exhibit hnRNPA1 as a new interaction partner of Sam68 in oligodendrocyte development and provide a basic concept for the regulation of MBP-expression through both proteins.

Our group already investigated the general expression pattern of the three STAR-family members, Sam68, Slm-1 and Slm-2 and showed a specific expression of all three proteins during forebrain development. The present thesis characterised for the first time the identity of Sam68 expressing cells during forebrain development. Neuroepithelial, radial glia cells and their derivative cell types were exhibited to express Sam68. Furthermore, time-dependent cell culture experiments revealed a significant shift in the expression pattern towards differentiating cells. These findings supported earlier studies of our group indicating a promotive role of Sam68 in cell differentiation.

The second part describes a successfully established method for the high efficiency transfection of non-adherent primary rat OPCs. This new transfection protocol enables for the first time the reproducible transfection of non-adherent OPCs with a high viability, a regular maturation pattern and an acceptable transfection efficiency. Regarding the time-consuming and low yield isolation of OPCs, this method represents a big advantage and provides the basis for the main goal of this thesis, which displays the determination of the role of Sam68 during oligodendrocyte development. Although oligodendrocytes count to the best characterised cell types within the CNS, many intracellular signalling pathways regulating their development and differentiation remained elusive. Here, I discovered the

respective Sam68 domains which modulates cell growth, MBP-expression and myelin-sheet formation. The complete RNA-binding domain and the NLS-sequence were shown to be relevant for the regulation of MBP-expression as well as for the formation of myelin-sheets. The relevance of the NLS-sequence and the knowledge about Sam68 as a regulator of alternative splicing events led to the assumption that Sam68 may regulate MBP-expression through modulating its splicing. The well-studied splicing regulator hnRNPA1 was already shown to regulate the alternative splicing of myelin-associated glycoprotein in cooperation with the STAR-family member Quaking I. Thus, I assumed a similar interaction of Sam68 and hnRNPA1 in the regulation of MBP expression. Indeed, MBP-level was downregulated after an hnRNPA1 knockdown and this effect was intensified after an additional overexpression of Sam68. These results provide a good basis to unravel the very complex regulation between Sam68 and hnRNPA1 in oligodendrocyte development.

Zusammenfassung

Während der Entwicklung des zentralen Nervensystems (ZNS) wird die Reifung von Oligodendrozyten durch die Aktivität diverser intrinsischer und extrinsischer Signalmoleküle gesteuert. Unserer Arbeitsgruppe gelang es, das STAR-Family Protein Sam68 als einen solchen intrinsischen Faktor, im Rahmen der Oligodendrozyten Differenzierung zu identifizieren. Mit voranschreitender Reifung steigt das Sam68-Level in Oligodendrozyten an und die MBP-Expression wird gesteigert. Neben dieser Funktion während der Oligodendrozyten Entwicklung, konnten vorherige Studien auch zeigen, dass Sam68 die neurale Stammzell (NSC)- Differenzierung fördert und durch Tenascin-C reguliert wird. Die exakten Mechanismen, wie Sam68 die NSC und besonders die Oligodendrozyten Entwicklung reguliert, sind allerdings noch unverstanden. Die in dieser Arbeit präsentierten Ergebnisse liefern komplett neue Erkenntnisse über die Funktion von Sam68 während der Vorderhirn- und besonders der Oligodendrozytenentwicklung. Weitergehend wurde hnRNPA1 als Interaktionspartner von Sam68 identifiziert und eine Hypothese zur Regulation der MBP-expression durch diese beiden Faktoren aufgestellt.

Studien unserer Arbeitsgruppe zeigten bereits ein spezifisches Expressionsmuster der drei STAR-family Proteine Sam68, Slm-1 und Slm-2 während der Vorderhirn Entwicklung. In dieser Arbeit wurden zum ersten Mal Sam68 exprimierende Zellen im Vorderhirn im Hinblick auf ihre zelluläre Identität charakterisiert. Diese Ergebnisse zeigten eine Expression von Sam68 in neuroepithelialen und radialen glia Zellen und in aus diesen Vorläufern hervorgehenden Zelltypen. In weiterführenden Zell-Kultur Experimenten wurde im Rahmen einer zeitabhängigen Studie festgestellt, dass sich die Sam68-Expression in Vorläuferzellen zu differenzierenden Zellen hin verschiebt. Diese Ergebnisse unterstützen vorherige Studien unserer Arbeitsgruppe, die eine fördernde Funktion von Sam68 im Rahmen der Zelldifferenzierung vermuten lassen.

Im zweiten Teil dieser Arbeit wird der Etablierungsprozess für die Methode der hoch effizienten Transfektion von nicht adherenten primären Oligodendrozyten Vorläuferzellen beschrieben. Diese neue Transfektionsmethode ermöglicht zum ersten Mal die reproduzierbare Elektroporation von geringen Zellzahlen und bietet daher im Hinblick auf die sehr zeitaufwändige und ertragsarme Isolierung von primären Oligodendrozyten aus Ratten einen enormen Vorteil.

Diese Methode bot die Grundlage für die Untersuchungen zur Rolle von Sam68 während der Oligodendrozytenentwicklung, welche den Hauptbestandteil dieser Arbeit darstellt. Obwohl Oligodendrozyten zu den am besten charakterisierten Zelltypen des ZNS zählen, sind viele intrazelluläre Signalwege, die ihre Entwicklung und Differenzierung regulieren, noch völlig unklar. In dieser Arbeit konnte ich die Sam68 Domänen ermitteln, die das Zellwachstum, die MBP-Expression und die Myelin-Membran Bildung modulieren. Die komplette RNA-bindende Domäne und die Kern-Lokalisierungssequenz sind für diese Funktionen relevant. Sam68 ist ein bekannter Splicing Regulator und die Relevanz der Kern-Lokalisierungssequenz führte zu der Vermutung, dass Sam68 die MBP-expression durch diesen Mechanismus steuert. Der Splicing Regulator hnRNPA1 kontrolliert zusammen mit dem STAR-family Protein Quaking I das alternative Splicen des Myelin-associated Glykoprotein. Eine ähnliche Wechselwirkung wurde zwischen Sam68 und hnRNPA1 vermutet und untersucht. Tatsächlich konnte ich in dieser Arbeit eine Runterregulation des MBP-Levels nach einem hnRNPA1 knockdown zeigen. Dieser Effekt wurde durch die zusätzliche Überexpression von Sam68 verstärkt. Diese Ergebnisse liefern erste Rückschlüsse auf die vermutlich sehr komplexe Regulation zwischen Sam68 und hnRNPA1 während der Entwicklung von Oligodendrozyten.

1. Introduction

1.1. Development of the Central Nervous System

In the last not even 100 years the fundamental knowledge about the development of the central nervous system (CNS) increased drastically. Beginning in the 1930' where neural induction was discovered by Spemann and Mangold showing that transplanted dorsal blastopore lip tissue can induce the host ventral ectoderm to form a complete secondary dorsal axis. These transplantation experiments with amphibians were performed during gastrulation, the early embryonic phase giving rise to the three germinal layers: ectoderm, endoderm and mesoderm. Meso -and endoderm develop into skeleton, heart and muscle tissues whereas the ectoderm gives rise to neural and epidermal tissue. The eye is almost entirely composed of the three ectodermal derivatives of the embryo, namely the neuroectoderm, the head surface ectoderm and the neural crest (Saha et al., 1989). The molecular mechanism of the Speemans organizer remained elusive until in the 1990' the first biochemical pathways involved in this neural induction process were discovered. Noggin, chordin and follistatin were discovered as neural inducers (Lamb et al., 1993, Smith et al., 1993, Hemmati-Brivanlou et al., 1994, Sasai et al., 1994) and as inhibitors of bone morphogenic protein (BMP) signalling pathway. This inhibition of BMP induces neural differentiation of the ectoderm leading to the formation of the neural tube. This process is called neurulation and leads to the formation of the entire CNS. The neural plate rolls up into a tube separating from the rest of the ectoderm. The notochord is formed by the involute cells concentrated underneath the neural plate and it is the origin of sonic hedgehog (SHH) proteins. The BMP signalling from ectoderm and SHH proteins synthesised by the notochord result in the dorso-ventral patterning of the neural tube. After the neural induction, the neuroectoderm consists of a homogenous layer of radially aligned neuroepithelial cells. These cells are the principle progenitor cells of all neural cell types and are characterised by the expression of distinct marker molecules for instance the intermediate filament protein Nestin (Hockfield and McKay, 1985, Lendahl et al., 1990). Most of the neural tube gives rise to the spinal cord, whereas the rostral end enlarges to form the three primary brain vesicles: prosencephalon (forebrain), mesencephalon (midbrain) and rhombencephalon (hindbrain). During embryonic forebrain development the symmetric division of neural progenitors leads

to a tissue expansion and is followed by the neurogenic phase. In this phase, around E9-10, neurons are generated directly from symmetric and asymmetric dividing neuroepithelial cells. As the developing brain epithelium thickens, neuroepithelial cells elongate and convert into radial glial cells expressing Pax6 (Gotz et al., 1998). In the eye, Pax6 is initially expressed throughout the whole ocular cup and is required for the differentiation of most retinal lineages. At E12.5, when retinogenesis is near completion, Pax6 becomes expressed in high levels in amacrine cells, radial ganglion cells and horizontal cells (Hsieh and Yang, 2009). This prominent role becomes clear regarding the severe effects in the *pax6* knockout mouse where the eyes are completely absent (Stoykova et al., 1996). Pax6 expressing cells in the brain and the eye own a neuronal fate (Shaham et al., 2012, Manuel et al., 2015). In the brain the asymmetric division of radial glial cells generate neurons either directly or indirectly through intermediate progenitor cells (IP) (Noctor et al., 2001). Radial glial cells contain a regional specification and differ regarding the neuronal subtypes they generate in the telencephalon. With ongoing neurogenesis radial glial cells differentiate from neuroepithelial cells by acquiring glial hallmarks, such as e.g. expression of vimentin and glial fibrillary acidic protein (GFAP) (Dimou and Gotz, 2014). However, neurons migrate from their origin in the embryonic ventricular zone of the forebrain to their final place of destination in the different cortical layers. They do so by migrating along the processes of the radial glial cells (Nadarajah, 2003, Paridaen and Huttner, 2014) (Figure 1). In the dorsal telencephalon and the ganglionic eminence (GE) they generate glutamatergic pyramidal projection neurons identified by the transcription factor Pax6 (Dimou and Gotz, 2014). Finally, in the gliogenic phase around birth, macroglia arise from radial glial cells directly or through IP cells (Kriegstein and Alvarez-Buylla, 2009) (Figure 1). These are the star-shaped astrocytes, implicated in ion and metabolic brain homeostasis, microglia important in phagocytosis and defense and lastly the myelinating glial cells. Schwann cells are the myelinating cells of the peripheral nervous system, whereas oligodendrocytes fulfil this function in the CNS. Recently additionally NG2-glia were discovered identified by NG2 antibody recognizing the chondroitin sulfate proteoglycan 4 (Levine and Nishiyama, 1996, Dimou and Gotz, 2014).

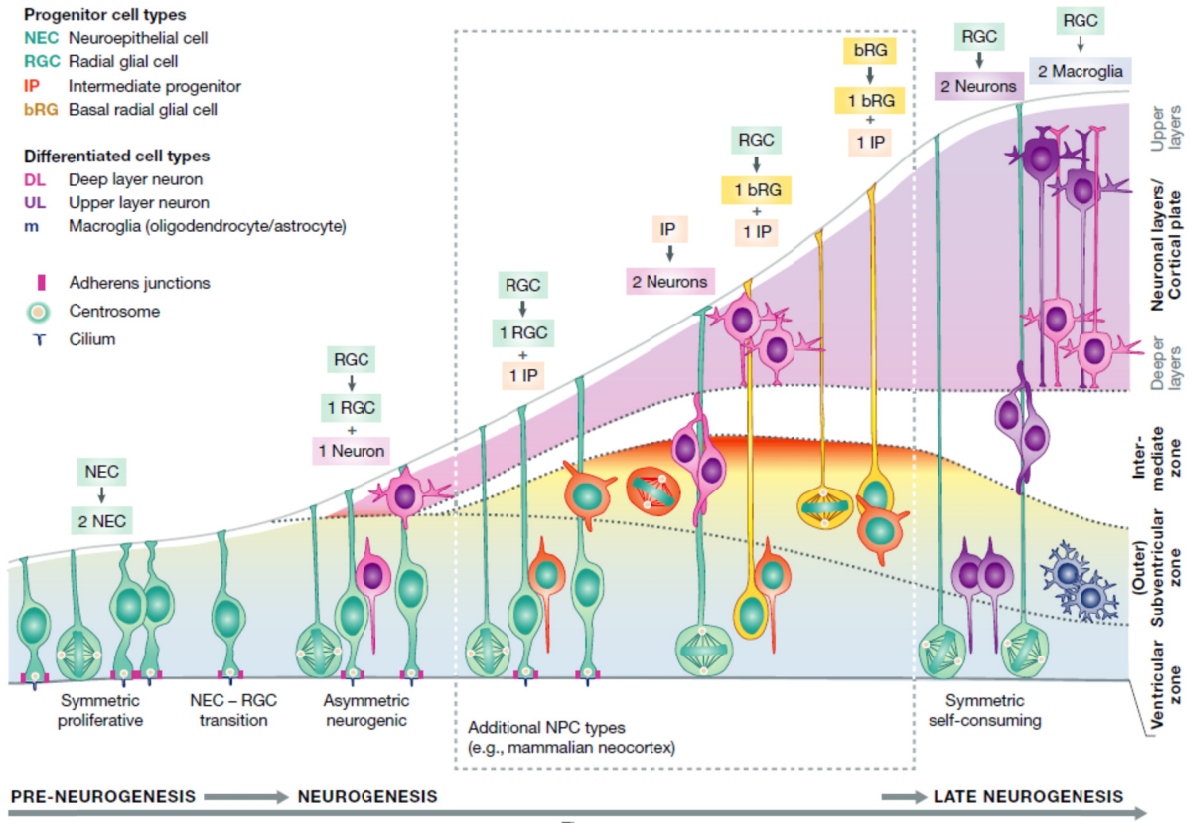

Figure 1. Development of the cerebral cortex

The schematic drawing illustrates the cortical development in a time-dependent manner. During the pre-neurogenesis the ventricular zone consist of a neuroepithelial monolayer. At this point the cells divide symmetrically and result in an expansion of the cortical tissue. At E9-E10 neurogenesis starts by the asymmetric division of some radial glial cells giving rise to neurons, either directly or indirectly through IPs. Young neurons migrate along the radial glia processes to their point of destination causing the neuron complexity of the cortex. Around birth, gliogenesis starts and macroglia arise either directly from radial glial cells, e.g. astrocytes or indirectly through IP cells in the case of oligodendrocytes (Paridaen and Huttner, 2014).

1.1.1. Glial stem and progenitor cells in development

The knowledge about glial cell function changed drastically within the last 150 years beginning with the first description of neuroglia by Rudolf Virchow. From the opinion that glial cells are only responsible for supporting neurons and maintaining stability, this view changed discovering that glial cells actively contribute to synaptic communication as direct synaptic partners (Kettenmann and Verkhratsky, 2008). Tripartite synapses contain either two neuronal elements (pre-and postsynaptic endings) or a presynaptic neuronal element and cells of the target organ, and a glial part. Additionally glial cells forming and receiving

synapses were discovered, such as NG2-glia (Butt et al., 2005, Rivers et al., 2008). The function of oligodendrocytes is also more complex than just isolating axons, the role initially suggested by Pedro Ramon y Cajal. They serve as metabolic supporters by supplying lactate to neurons through their myelin sheets (Lee et al., 2012).

1.2. Oligodendrocyte Development and Differentiation

As mentioned above, oligodendrocytes develop from oligodendrocyte precursor cells. These in turn are detectable only few days after the start of neurogenesis in the endopeduncular area, a subfield of the medial ganglionic eminence (MGE). This first wave of OPCs generates from *Nkx2.1*-expressing cells around E12.5 and they subsequently migrate into all parts of telencephalon and finally enter the cerebral cortex after E16. By postnatal day 10 the number of *Nkx2.1* cells declines and is overtaken by OPCs derived from *GSh2*-precursors in the LGE and caudal ganglionic eminence (CGE). Finally in a third wave OPCs emerge from *Emx1*-positive cells in the cortex itself. Those later born OPCs contribute to the total OPC number in the adult brain by replacing the earlier generated OPCs (Kessaris et al., 2006, Dimou and Gotz, 2014). The differentiation from a bipolar OPC to a complex branched shape in the mature, myelinating oligodendrocyte follows stepwise morphological changes accompanied with a highly specific marker profile. Biopolar progenitors express typical surface molecules, for instance the plated derived growth factor receptor α (PDGFRα) (Pringle and Richardson, 1993), the NG2-proteoglykan (Levine and Stallcup, 1987, Stallcup and Beasley, 1987) and the tetrasialyganlioside recognized by the A2B5 antibody (Eisenbarth et al., 1979). The differentiation to a pre-oligodendrocyte is accompanied with formation of complex branches and a change in the antigen profile. Progenitor molecules like PDGFRα and A2B5 are downregulated and instead the glycolipid sulfatide is expressed, which is recognized by the O4-antibody (Sommer and Schachner, 1981). With the formation of axon wrapping membranes, the expression of galactocerebroside (GalC), the major glycolipid in myelin, starts and can be followed with the monoclonal antibody O1 (Sommer and Schachner, 1981) and GalC (Ranscht et al., 1982). Finally, the expression of major myelin proteins such as myelin associated glycoprotein (MAG) (Poltorak et al., 1987) and myelin basic protein (MBP) (Barbarese and Pfeiffer, 1981) characterise mature oligodendrocytes.

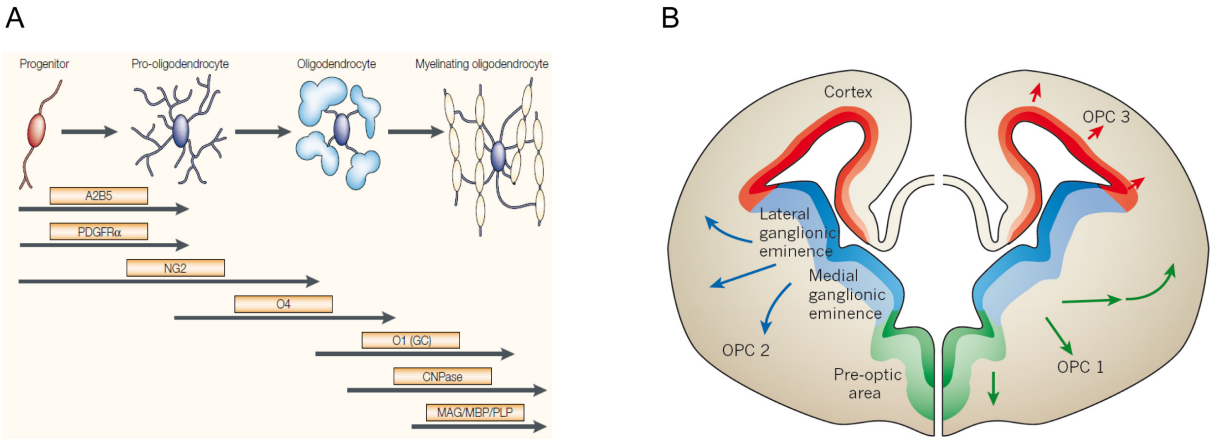

Figure 2. Oligodendroglia development and distinct marker profile

(A) The cartoon illustrates the stepwise morphological transformation from bipolar progenitors to myelinating oligodendrocytes accompanied with a change in the sequential expression of molecular markers. Adopted from (Zhang, 2001). (B) This scheme shows a coronal view of an embryonic forebrain demonstrating the time-dependent migration of OPCs from the three ganglionic eminences. The green, blue and red shaded areas illustrate the pre-optic area, medial/lateral GE and neocortex. The first wave arises from *Nkx2.1*-expressing precursors in the MGE at E12.5. Around E15.5 *Gsx2* precursors in the LGE and MGE gives rise to the second wave. The last OPCs arise from *Emx*1 expressing cells in the cortex, starting around birth. Adopted from (Rowitch and Kriegstein, 2010).

1.2.1. MBP Synthesis and myelin sheet formation

The mechanism by which oligodendrocytes extend their plasma membrane to wrap axons and generate multi-layered compact myelin sheath is still unresolved. Recent studies revealed new insights into this complex process. In principal, myelin is an insulating membrane formed by oligodendrocytes wrapping their plasma membrane multiple times around an axon resulting in a multi-layered stack of compacted membranes (Bunge, 1968, Remahl and Hildebrand, 1982). Only few proteins reside within compacted myelin, MBP (Myelin Basic Protein) is one of these two abundant proteins. Hence, MBP needs to be transported to myelin. During development this occurs by the transport of its messenger RNA (mRNA) within cytoplasmic granules (Colman et al., 1983, Ainger et al., 1993). Already 30 years ago, the transport of *MBP* mRNA in RNA granules to the myelin compartments and a local translation was postulated by microinjection experiments (Colman et al., 1983). The transport depends on two regions within the 3'UTR. The 21-nucleotide RNA trafficking sequence (RTS), being important for the cell body to oligodendrocyte branches transport and the RNA localisation element (RLR), which is important for the final transport into the

myelin sheet (Ainger et al., 1997). Oligodendrocytes form myelin-like membranes in the absence of neurons, thus the capacity to differentiate into mature oligodendrocytes is intrinsic and furthermore depends on interactions between OPCs (Sarlieve et al., 1983, Yang et al., 2011). Nevertheless, coculture-experiments with neurons increase myelin gene expression, such as *PLP*, *MBP*, and *MAG* indicating the importance of axon-glia communication (Macklin et al., 1986, Kidd et al., 1990). The axon-glia communication is not only necessary for myelin production but also for axon survival. Exosome mediated neurotransmitter release from oligodendrocytes to neurons for instance is crucial for axon survival (Fruhbeis et al., 2013). However, the amount of myelin at axonal segments varies. Therefore oligodendrocytes need to regulate the production of myelin responsive to local axonal requirements. Regarding OPC differentiation, the general idea is that neuronal contact and signals control the morphological transformation to myelin-forming oligodendrocytes (Hardy and Friedrich, 1996). In the peripheral system, neuregulin-1 controls the myelination of schwann-cells (Grigoryan and Birchmeier, 2015). Such a single key player is currently not known in the CNS. Moreover, signals from inhibitory neurons are important for OPCs to exit a repressed state (Bergles et al., 2000, Emery, 2010). These inhibitory signals (e.g. Jagged, PSA-NCAM, and LINGO-1) activate transcriptional regulators, like *Sox5/6*, *Hes5* and *Id2/4*. These in turn prevent OPCs from entering their terminal differentiation (Piaton et al., 2010, Taveggia et al., 2010, Simons and Nave, 2015). Besides the axonal influence on OPCs, extrinsic signalling mechanisms also control oligodendrocyte differentiation and myelination. Fyn kinase, as a member of the Src-family kinases, is an important regulator of myelination. It causes the phosphorylation of hnRNPA2 and the release of hnRNPA2 and hnRNP-E1 from mRNA-transport granules (White et al., 2008). Both proteins are crucial trans-acting factors regulating the transport and the translation of *MBP*-mRNA (Torvund-Jensen et al., 2014). Subsequently, the local transition of MBP is initiated at the tip of the oligodendrocyte branches (White et al., 2008, Laursen et al., 2011, Wake et al., 2011). The classic multifunctional MBP protein expressed by myelinating oligodendrocytes arises from a gene complex called *Golli* (genes of oligodendrocyte lineage), which also gives rise to Golli(-MBP) family of proteins. The *Golli* gene contains three different transcriptional start sites enabling the expression of the two distinct subfamilies of proteins, classic MBP proteins and Golli(-MBP) proteins (Campagnoni et al., 1993, Muller et al., 2013). The existence of classical MBP-proteins is restricted to myelinating cells, whereas Golli(-MBP) proteins were also found in other neural and non-neural cells (Givogri et al., 2001, Marty et al., 2002). Classic MBP-isoforms are encoded by exons I, III, IV and VII,

whereas exon II, V and VI are only found in specific splice variants. The different sizes of MBP-isoforms in the mouse have a molecular weight of 14, 17.22, 17.24, 18.5, 20.2 and 21.5 kDa, whereas the biggest predicted MBP-isoform of a rat is supposed to have a molecular weight of 35.86 kDa. The relative abundance of isoforms containing exon II is higher during myelinogenesis, whereas the presence of isoforms lacking this exon is increased in compact myelin sheets (Ozgen et al., 2014). In the first case, MBP as a positively charged protein is proposed to function in the compaction of myelin membranes by associating with the negatively charged oligodendroglial phospholipids (Nawaz et al., 2009) and bringing the opposing cytoplasmic surfaces of the myelin membrane closely together (Roach et al., 1983). Therefore, most soluble and membrane proteins must be depleted from the membrane. MBP is regulating this depletion process by the formation of a mesh-like network of MBP-molecules acting as a diffusion barrier. Larger proteins are extruded or bound to MBP, whereas small molecules diffuse through the pores (Aggarwal et al., 2013). Consequentially, compact myelin becomes a protein-poor membrane lacking major glycoproteins at the extracellular leaflet promoting the association of two bilayers (Bakhti et al., 2013, Simons and Nave, 2015).

The compacted myelin provides the high electrical resistance and low capacitance essential for saltatory impulse propagation. Most oligodendrocytes generate between 20-60 myelinating processes with intermodal lengths of 20-200 µm and up to 100 membrane turns (Matthews and Duncan, 1971, Hildebrand et al., 1993). The surface area of one oligodendrocyte can reach up to 5-50x10^3 µm^2, making them unique in their size compared to all other cell types of our body (Pfeiffer et al., 1993, Baron and Hoekstra, 2010). In zebrafish oligodendrocytes wrap single axonal segments and produce all myelin sheaths in only five hours (Czopka and Lyons, 2011, Czopka et al., 2013).

1.2.2. Regulation of OPC differentiation

In vitro oligodendrocytes produce myelin-like membranes in the absence of axons and in the absence of neighbouring cells and mitogens. Although OPCs divide in the presence of mitogens, the number of cell divisions is limited (Temple and Raff, 1985, 1986). One regulator of this limitation is the cyclin-dependent kinase inhibitor $p27^{Kipl}$. With ongoing OPC proliferation, $p27^{Kipl}$ accumulates, resulting in cell cycle exit (Durand et al., 1997). A combination of distinct mitogens enables the unlimited proliferation of OPCs *in vitro* (Tang et al., 2001). Beside PDGF-AA, FGF-2 (Bogler et al., 1990, McKinnon et al., 1990, Chen et al., 2015), insulin-like growth factor 1 (McMorris and Dubois-Dalcq, 1988, Hu et al., 2012) and Neuregulins (Canoll et al., 1996, Ortega et al., 2012) are among some of these factors. Anyhow, *in vivo*, the production of myelin is upon axonal request and therefore of course much more complex and regulated by an orchestra of intrinsic and extrinsic signals. Before OPCs start to myelinate axons, they migrate and proliferate to their final point of destination. PDGF-AA is an essential mitogen produced by both neurons and astrocytes and regulates OPC proliferation and survival (Yeh et al., 1991, Mudhar et al., 1993). In PDGF-AA knockout mice, a severe hypomyelination occurs due to reduced OPCs (Pringle et al., 1989, Fruttiger et al., 1999). In addition to polypeptide growth factors, the thyroid hormones Triiodothyronin (T3) and Thyroxin (T4) are as well regulators of oligodendrocyte differentiation (Barres et al., 1994, Rodriguez-Pena, 1999). A delayed onset of myelination in hypothyroid rats (Balazs et al., 1969, Walters and Morell, 1981) and an accelerated myelination in hyperthyroid rats (Marta et al., 1998) emphasizes their role. The myelination process starts when several oligodendrocyte processes interact with the axonal membrane (Watkins et al., 2008). Indeed, many signals and molecular interactions regulate the onset of myelination, but how these processes are orchestrated is still elusive. Hence, besides the already described soluble molecules, also adhesive key players regulating the myelination process were discovered, for instance the axonal adhesive protein L1 and the extracellular matrix (ECM) molecule laminin-2 (Colognato et al., 2002). In general, the ECM and its secreted factors own an important role in the development of the CNS (Discher et al., 2009). Laminin-2 interferes with the lateral distribution of integrins. This allows for the integration of integrin and growth factor signalling to direct oligodendrocyte behaviour regarding survival and myelination (Baron et al., 2005, Baron and Hoekstra, 2010, Relucio et al., 2012). Integrins belong to the heterodimeric transmembrane receptor family and are often involved in cellular interactions with the ECM. In oligodendrocytes, of the known 20 integrin species

only a limited subset of the integrin receptors is expressed and associated in the regulation of one aspect of oligodendrocyte development (Benninger et al., 2006, Barros et al., 2009, Camara et al., 2009). The Tenascin-C dependent proliferation of OPCs for instance depends on $\alpha_v\beta_3$ integrin (Garcion et al., 2001). The related ECM glycoproteins Tenascin-C (Tnc) and Tenascin-R (Tnr) are synthesized by astroglia at early postnatal stages (Bartsch et al., 1992, Gotz et al., 1997) and are known to regulate OPC development. The loss of Tnc in Tnc-deficient mice causes severe effects on the development of oligodendrocytes regarding proliferation, migration and survival (Garcion et al., 2001, Garwood et al., 2004). Our group showed that both proteins inhibit the formation of myelin membranes and regulate antagonistically the expression of MBP. Tnc reduces MBP expression via Contactin-1 and with the Fyn and Akt pathway (Czopka et al., 2009, Czopka et al., 2010). Additionally, the expression of Sam68 (Src-associated substrate of mitosis of 68 kda) is downregulated in response to Tnc (Czopka et al., 2010). It was the first time that Sam68 was proposed to have a role in oligodendrocyte differentiation and this finding is in line with previous studies of our group showing a similar interplay of Sam68 and Tnc signalling in neural stem cells (Moritz et al., 2008b).

1.3. The STAR-Family proteins Sam68, Slm-1 and Slm-2

1.3.1. Functional motifs of STAR-Family proteins

Sam68, Slm-1 and Slm-2 are multifunctional members of the STAR (Signal transducer and Activator of RNA Metabolism)-family proteins. The structure of all seven STAR-family members is conserved from yeast to plants and mammals and in the case of Slm-1 and Slm-2 (sam-like mammalian protein 1 and 2) even declared by their names. Members of this protein family are characterised by a single heteronuclear ribonucleoprotein particle K (hnRNP K) domain (Vernet and Artzt, 1997). This KH domain is flanked by N-and C-terminal sequences, which are important for RNA binding (Chen et al., 1997, Lin et al., 1997). In turn the N- and C-terminal sequences are flanking the entire structural RNA-binding domain GRP33/SAM68/GLD-1 (GSG), containing about 200 amino acids (Burd and Dreyfuss, 1994). Additionally Sam68, Slm-1 and 2 contain several proline-rich sequences that are sites of protein-protein interactions with SH3 and WW domain-containing proteins

(Wong et al., 1992). Furthermore, they own arginine-glycine-rich regions methylated by protein arginine methytransferases (Burd and Dreyfuss, 1994). The tyrosine-rich C-terminus, as a target site of phosphorylation by tyrosine kinases and bound by SH2 domains, is underlining their multifunctional character (Wong et al., 1992). The amino acid sequences in human, mouse, rat and chicken are highly conserved within the functional domains (Lukong and Richard, 2003, Sanchez-Jimenez and Sanchez-Margalet, 2013).

1.3.2. Functional roles of Sam68 motifs

This thesis focuses on the function of Sam68. The human *Sam68* gene is located on chromosome1 p32 and contains 9 exons (Lukong and Richard, 2003). The first functions identified for Sam68 were the participation in cell cycle regulation and mitosis. It was the first substrate for Src in the cytoplasm during mitosis, explaining likewise its name. Misleading data suggested a relation of Sam68 and GAP associated protein p62, however later studies showed different roles for Sam68 and p62 during mitosis (Courtneidge and Fumagalli, 1994, Fumagalli et al., 1994, Lock et al., 1996). The human genome organisation (HUGO) renamed Sam68, Slm-1 and 2 as Khdrbs-1, 2 and 3 (kh Domain containing RNA binding signal transduction associated -1,-2,-3). Anyhow, the old names are more commonly used to prevent confusion. Sam68 regulates through its KH domain cell proliferation by promoting S phase entry in NIH3T3 cells (Barlat et al., 1997). The KH domain allows for the binding of distinct RNA sequences. Initially, Sam68 was shown to bind non-specifically to poly(U) and poly(A) RNA, and additionally to the high affinity binding sequences UAAA or UUAA *in vitro* (Taylor and Shalloway, 1994, Lin et al., 1997, Sanchez-Jimenez and Sanchez-Margalet, 2013). Further on, Sam68 was shown to bind some mRNA targets *in vivo*, for instance hnRNPA2/B1 and beta-actin mRNA (Itoh et al., 2002). Another interaction partner of Sam68 is hnRNPA1. Both proteins form a complex and modulate the alternative splicing of Bcl-x (Paronetto et al., 2007). In the last years many more functions were found and confirmed its multifunctional character. The argine-glycine-rich methylation sites (RGG boxes) for instance are important for the localisation of Sam68. Hypomethylated Sam68 is located in the cytoplasm, whereas methylated Sam68 is located in the nucleus (Cote et al., 2003). Later, also an involvement of Sam68 in cell growth, alternative splicing and in the export of unspliced viral RNAs was described.

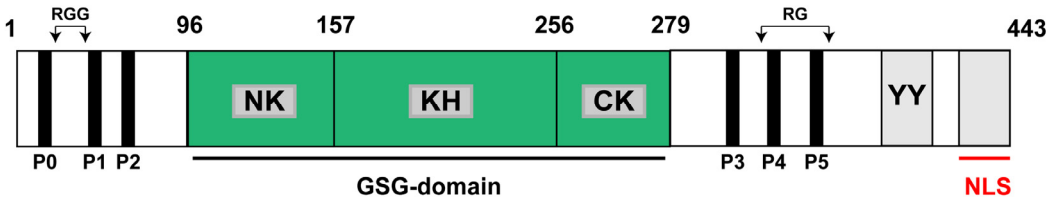

Figure 3. Schematic diagram illustrating the structural and functional domains of Sam68.

Sam68 consists of the KH-domain flanked by the N-and C-terminal segment, building together the GSG-domain responsible for RNA-binding activity. Furthermore, it contains six proline rich segments (P0-P5), RGG boxes, the C-terminal tyrosine-rich domain (YY) and the nuclear localisation signal (NLS).

1.3.3. Role of Sam68 during development

Beside its role in spermatogenesis, tumourigenesis and cell cycle regulation, recently explicit roles for Sam68 were described during CNS development. In P19 cells, Sam68 was described as a promoter of neuronal differentiation by identifying a set of alternative exons whose splicing is dependent on Sam68 (Chawla et al., 2009). An analysis of Sam68-null mice revealed clear motor coordination defects, demonstrating also *in vivo* the effects of Sam68 in CNS development. Although, regarding the severe effects of altered *Sam68* gene, these observed effects on the CNS in Sam68 deficient mice were rather light (Lukong and Richard, 2008, Sette et al., 2010). Sam68 -/- pups either directly die at birth or they live a normal life span. Strong effects of Sam68 ablation were observed regarding reproduction. Sam68 -/- females have defects of mammary gland and uterine development, whereas males are infertile (Richard et al., 2008). Besides the motor coordination defects, little is known about Sam68 effects on the CNS. Our group demonstrated a distinct role of Sam68 in neural stem cell development by its identification as a Tnc regulated target gene. An overexpression of Sam68 causes a clear reduction of NSC proliferation and furthermore an increase of the larger Tnc isoforms (Moritz et al., 2008a). Further studies of our group support these findings. An overexpression of Sam68 and Slm-1 increased NSC differentiation to a neuronal fate, accompanied with a reduction of neurosphere formation and an increased cell-cycle exit. Slm-2 showed opposing effects by promoting NSCs maintenance in a proliferative state. Those effects of all three STAR-family members were regulated by MAP kinase pathway. Overexpression of STAR-family proteins decreased ERK1/2 phosphorylation in response to

EGF, whereas increased Slm-2 level sustained MAP kinase signalling in response to FGF-2 (Bertram, 2013). Our identified role for Sam68 and Slm-1 in neuronal development is in line with the identification of both proteins as regulators of neuronal alternative splicing. A specific interaction of Sam68 and the activity-dependent biosynthesis of the elongation factor eEF1A was shown. The translation of eEF1A mRNA is strongly induced by neuronal depolarisation and correlates with enhanced association of Sam68 with polysomal mRNAs (Grange et al., 2009). A specific function of Sam68 and Slm-1 in neuronal alternative splicing clarifies the role of both proteins in neuronal development. Sam68 regulates the neuronal-activity dependent alternative splicing of Neurexin-1 in cooperation with Slm-1. In contrast, the alternative splicing of Neurexin-2 reporters is specifically regulated by SLM-1 (Iijima et al., 2011, Iijima et al., 2014). Furthermore, Sam68 was shown to regulate hippocampal synapse number by promoting the association of *actb* mRNA with synaptic polyribosomes (sites of local translation at synapses) (Klein et al., 2013).

As the effect of Sam68 in the CNS is not limited to neuronal cells, our group already showed a distinct regulation of OPC differentiation. A knockdown of endogenously expressed Sam68 in rat oligodendrocytes leads to a reduced MBP-level. Hence, Sam68 was identified as a promoter of oligodendrocyte maturation. The mechanism of this regulation is still elusive, but it was demonstrated, that the expression of Sam68 is Tnc dependent by repressing Sam68 levels in oligodendrocytes (Czopka et al., 2010). Additionally, only the overexpression of Sam68 in neural stem cells causes a higher amount of myelin-forming oligodendrocytes. The overexpression of Slm-1 and Slm-2 had no effect on the maturation state of oligodendrocytes (Bertram, 2013). Those observed effects of Sam68 on OPC differentiation are coherent, given that the isoforms QK-6 and QK-7 of the related STAR-family member *quaking* regulates oligodendrocyte maturation (Larocque et al., 2005). However, so far these are the only findings for Sam68 functioning in oligodendrocytes, giving the fundament for my thesis.

1.3.4. Role of Sam68 in alternative splicing

Alternative splicing describes the production of different RNAs from the same gene by the optional use of alternative splice sites within a pre-mRNA. It allows genes to encode for multiple protein isoforms, which can fulfil different biological functions (Maniatis and Tasic, 2002). The sequential assembly of the spliceosome, a multicomponent ribonucleoprotein

complex, onto the pre-mRNA leads to the removal of intron sequences. Its function is dependent on several splicing factors, binding additionally to this complex (Moore and Sharp, 1993). A study, revealing completely new insights into splicing events during cerebral cortex development and offering a splicing database was recently published. This transcriptome database enables the detection of alternative splicing events in each analysed cell type (e.g. neurons, astrocytes and oligodendrocytes) and demonstrated already how neurons and astrocytes differ in their ability to regulate glycolytic influx (Zhang et al., 2014). As described earlier, Sam68 is a known regulator of alternative splicing events in the CNS (Iijima et al., 2011). Sam68 was firstly described as an interaction partner of the tyrosine-phosphorylated nuclear protein YT521-B in a yeast two-hybrid screen. This interaction of both proteins was mediated through the glutamic acid/arginine-rich region of YT521-B and negatively regulated by tyrosine phosphorylation of Sam68 (Hartmann et al., 1999). Other studies confirmed the role of Sam68 in splicing events. Sam68 crosslinks to an intronic regulatory RNA-sequence of tropomyosin pre-mRNA (Grossman et al., 1998) and binds to the spliceosome-associated protein FBP21 (Bedford et al., 1997). A direct function of Sam68 in alternative splicing was shown by demonstrating a binding of Sam68 to the exon splice-regulatory elements of exon v5 of CD44. This in turn is regulated by the Ras signalling pathway. Higher Sam68 levels enhanced ERK-mediated inclusion of v5-exon sequence in mRNA (Matter et al., 2002). Besides ERK- dependent phosphorylation, Fyn-dependent tyrosin-phosphorylation of Sam68 was demonstrated as well to play a role in alternative splicing. Moreover, this study showed that a specific mutation in the RNA-binding domain affects *Bcl-x* splicing. This amino acid exchange of valine against phenylalanine at the position 276 (Sam68_V→F) hindered Sam68 to favour the selection of *Bcl-x* splice site. Furthermore, Sam68_V→F was unable to favour the expression of endogenous *Bcl-x* mRNA. As alternative splicing is regulated by several splicing regulators, in the regulation of *Bcl-x* splicing hnRNPA1 was identified as well as an interaction partner of Sam68. The last 93 amino acids of Sam68 (351-443) were identified as the hnRNPA1 binding site. Although a weak binding was also observed in the N-terminal (1-277) region indicating a weak interaction through a common RNA (Paronetto et al., 2007).

1.4. hnRNPA1

hnRNPA1 belongs to the A/B subfamily of ubiquitously expressed heterogeneous nuclear ribonucleoproteins. In general, the hnRNP family is composed of at least 20 members named from A through U with a molecular weight range from 34 kDa to 120 kDa (Pinol-Roma et al., 1988, Dreyfuss et al., 1993). As the name indicates, a key function is the complexing with heterogeneous nuclear RNA (hnRNA) and its processing into mature messenger RNA. In fact, it is one of the most abundant expressed nuclear proteins and plays a crucial role in the transcription, splicing, stability, export through nuclear pores and translation of cellular and viral transcripts (Jean-Philippe et al., 2013). Furthermore, besides its regulation of mRNA biogenesis, it owns functions in processing of microRNAs, telomere maintenance and the regulation of transcription factor activity (Jean-Philippe et al., 2013). The activation of hnRNPs is regulated by several posttranslational modifications, including phosphorylation, SUMOylation, ubiquitination and methylation. These modulations may alter hnRNP activity by controlling their localisation, RNA binding specifity and interaction with other cellular factors (Dreyfuss et al., 2002, Jean-Philippe et al., 2013). The complex formed by hnRNPAs and nascent transcripts is remodelled through the loss or acquisition of hnRNPs with other proteins and is termed "mRNP code" (Singh and Valcarcel, 2005). So far, only two isoforms of hnRNPA1 were identified, A1-B and A1-A. The main localisation is in the nucleus, but in response to specific stimuli it can relocate to the cytoplasm und shuttle between nucleus and cytoplasm. The direct interaction of the 38-amino acid long M9 nucleo-cytoplasmic shuttling sequence (Siomi and Dreyfuss, 1995) with two receptors of the karyopherin-β family (Transportin 1 and 2) mediates the nuclear import of hnRNPA1 (Pinol-Roma and Dreyfuss, 1992, Allemand et al., 2005). The major functions of hnRNPA1 depend on its ability to recognize distinct nucleic acid sequences. Two RNA-Recognition motifs (RRMs) are located on the N-terminus and are closely related to each other. The C-terminal region is characterised by a highly flexible glycine-rich composition (RGG-boxes) and has both, protein and RNA-binding properties. It is interspersed with aromatic acids and KH domains (Burd and Dreyfuss, 1994, He and Smith, 2009). The Gly-rich domain is required for the interaction with other hnRNPs and RNA-binding proteins (Cartegni et al., 1996). The RNA recognition motifs (RRMs) are the most common RBDs, about 90 amino acids-long and highly conserved (Dreyfuss et al., 1988). Besides its functions in RNA-binding, hnRNPA1 is also a known regulator of transcriptional events, although precise mechanisms of this regulation are unresolved. The association of hnRNPA1 with the promoters of genes coding

for the vitamin D receptor (Chen et al., 2003), γ-fibrinogen (Xia, 2005) and the thymidine kinase (Lau et al., 2000) induces for instance the transcriptional repression. Whereas the binding onto ApoE leads to an activation (Campillos et al., 2003, Jean-Philippe et al., 2013).

A key function of hnRNPA1 is the alternative splicing of nascent transcripts through the participation in all steps of spliceosome assembly, proofed by the assembly with the splicing factor U2AF. (Jurica et al., 2002, Zhou et al., 2002, Tavanez et al., 2012). Not only the splicing of pre-mRNA is regulated by hnRNPA1, it modulates the translation of fully processed mRNAs as well, for instance of *interleukin 2* (Henics et al., 1994).

Due to its multifunctional character mutated hnRNPA1 is involved in several severe human neurodegenerative diseases, for instance Alzheimer's disease (Berson et al., 2012), amyotrophic lateral sclerosis and multiple sclerosis (Bekenstein and Soreq, 2013). The mechanisms behind hnRNPA1 role in these diseases remain unclear. Only some regulatory pathways were identified, e.g. the interaction with the STAR-family protein Quaking. Quaking was shown to have an important role in myelin formation and contains a binding site for hnRNPA1. Quaking regulates the level of hnRNPA1 by stabilising its mRNA and hnRNPA1 in turn binds MAG pre-mRNA and modulates its alternative splicing (Zearfoss et al., 2011). As mentioned earlier, also Sam68 contains a binding site for hnRNPA1 and an interaction of both proteins in the regulation of *Bcl*-x splicing was demonstrated. Therefore, an interplay of both proteins in the regulation of myelin formation is most likely and was investigated in this thesis.

Aim of Study

During CNS development oligodendrocyte precursor cells (OPCs) generate oligodendrocytes in a controlled and regulated process through the activity of diverse intrinsic and extrinsic factors. The STAR-family protein Sam68 is among one of the intrinsic factors involved in oligodendrocyte differentiation. Our group already demonstrated an increasing Sam68- level during oligodendrocyte maturation and a promotion of MBP-expression. In further studies Sam68 was identified as a promoter of neural stem cell (NSC) differentiation. However, the mechanism(s) how Sam68 control neural stem cell and oligodendrocyte development in detail are still unresolved.

In regard to NSC development the first approach of this thesis is the determination of the cellular identity of cells expressing Sam68. Immunhistochemical investigations with characteristic stem cell markers will elucidate its expression profile. Further cell culture experiments allow for the identification of the fate of Sam68 expressing cells.

The main goal of this thesis is the investigation of the role of Sam68 during oligodendrogenesis. Therefore, I assess several Sam68 constructs, which contain mutations in the RNA-binding site or the nuclear localisation signal to characterize the relevant domains of Sam68 that control oligodendrocyte development by transfection of primary rat OPCs. Particularly, the effect on OPC maturation and MBP-expression is of special interest. Considering the interaction of Quaking I, a member of the STAR-family proteins, and hnRNPA1 during Myelin-associated glycoprotein splicing, raised the question of a similar interaction pathway of Sam68 and hnRNPA1 in regulating MBP-expression. hnRNPA1 is a well-known splicing regulator and modulates together with Sam68 the splicing of Bcl-x. Thus, besides the identification of the Sam68 domains, the role of hnNRNPA1 during oligodendrogenesis and a possible interaction with Sam68 will be investigated. To follow this aim a new protocol for the transfection of non-adherent OPCs is required, due to the sensitive properties of OPCs towards the electroporation process. This optimized protocol will be established and enable for the first time the high efficiency transfection of non-adherent OPCs.

2. Material

2.1. Equipment

2.1.1. Companies

American National Cam, Chicago, USA
AnalaR Normapur, VWR, Fontenais sous Bois, France
AppliChem GmbH, Darmstadt, Germany
Beckman Coulter, Inc. Fullerton CA, USA
BD Biosciences, New Jersey, USA
Biometra, Göttingen, Germany
Brand GmbH, Wertheim, Germany
Charles River, Sulzfeld, Germany
Dianova, Hamburg, Germany
Eppendorf AG, Hamburg, Germany
Fermentas, St. Leon-Rot, Germany
Greiner bio one, Frickenhausen, Germany
Heraeus, Hanau, Germany
Heidolph, Schwabach, Germany
Ibidi, Martinsried, Germany
Invitrogen, Karlsruhe, Germany
J.T. Baker, Deventer, Niederlande
Leica, Wetzlar, Germany
Lonza, Cologne, Germany
Menzel GmbH, Braunschweig, Germany
Merck, Darmstadt, Germany
Mettler Toledo, Gießen, Germany
Millipore, Eschborn, Germany
New England Biolabs, Frankfurt, Germany
Nunc, Wiesbaden, Germany
Preprotech, Rocky Hill, USA
Promega, Madison, USA
Qiagen, Hilden, Germany
Roche, Mannheim, Germany
Satorius, Göttingen, Germany
Seromed, Berlin, Germany
Starlab Learning Technologies, Inc., Massachusetts, USA
Sigma-Aldrich Chemie GmbH, München, Germany
The Baker Company, Sanford, USA
Thermo Fischer, Darmstadt, Germany
Zeiss, Jena, Germany

2.1.2. Chemicals

Acrylamide Merck
Agar Invitrogen
Agarose Applichem
Ampicillin Invitrogen
Aprotinin Sigma
APS J.T. Baker
B27 supplement Invitrogen
Bactotryptone BD
BSA Sigma
Bromine-phenol-blue Serva
$CaCl_2 \times 2\ H_2O$ Sigma
Coomassie blue Serva
L-Cystein Sigma
DMEM Sigma
DMSO Sigma
EDTA Merck
EGTA AppliChem
Ethanol Sigma
F12 Sigma
FCS Biochrom
FGF-2 PreProTech
Formaldehyde J.T. Baker
L-Glutamin Sigma
Glycerol J.T.Baker
Glycine Roth
Heparin sodium salt Sigma
HEPES Roth
Hoechst 33258 Sigma
Immumount Thermo-scientific
Kanamycin Invitrogen
KCl Sigma
KH_2PO_4 Applichem
Laminin Invitrogen
L15 Sigma
MEM Sigma
Methanol Sigma
$MgCl_2$ J.T. Baker
$MgSO_4 \times 7\ H_2O$ J.T. Baker
Milk powder Roth
N2 supplement Gibco
NaCl Sigma
Na-citrate AppliChem
Na-carbonate AppliChem
Na-deoxycholate AppliChem
$NaHCO_3$ AppliChem
$Na_2HPO_4 \times 2\ H_2O$ AppliChem
NaH_2PO_4 AppliChem
Paraformaldehyde J.T. Baker
Poly-D-Lysin Sigma
Polyornithin Sigma
Polyvinylalcohol Serva
PDGF PreProTech
PMSF Sigma
P/S Gibco
SDS Serva
Sucrose Roth
T3 Sigma-Aldrich
TEMED Roth
Tris Sigma
Triton X100 AppliChem
Trypsin-EDTA Invitrogen
Tween20 AppliChem
Yeast Extract Roth

2.1.3. Plastic Ware

5 ml tubes Greiner
15 ml tubes Greiner
50 ml tubes Greiner
100 mm petri dishes Sarstedt
96-well microtest plate Roth
6-well plates Greiner
35 mm culture dishes Nunc
60 mm culture dishes Nunc
100 mm culture dishes Nunc
4-well multiwell dishes Nunc
25 cm^2 culture flask Nunc
75 cm^2 culture flask Nunc
100 cm^2 culture flask Nunc
Serological pipettes Sarstedt

2.1. Antibodies

Table 1 Primary Antibodies

antigen	clone	produced in	iso-type	clonality	company	order nr	Dilution IF	Dilution WB
GAPDH	6C5	ms	IgG1		Acris	ACR001PT	-	1:2000
GFAP	G-A-5	ms	IgG1	monoclonal	Sigma	G 3893	1:500	-
GFP		goat	IgG	polyclonal	biomol (Rockland)	600-101-215	1:500	1:5000
GFP-FITC		goat			biomol (Rockland)	600-102-215	1:500	-
hnRNPA1		rb		polyclonal	Cell Signaling	#5380	1:50	1:1000
Hoechst 33258 bis-Benzimide					Sigma	B1155 25MG	1:100000	-
MBP (Isoform)		rb			Sigma	SAB2104171-50UG	1:100	1:500
MBP (myelin basic protein)		rb			Sigma	M3821	1:100	1:500
Nestin	rat-301	ms	IgG1	monoclonal	Millipore	MAB353	1:300	-
O4	O4	ms	IgM	monoclonal	Sigma	O7139	1:100	-
O4		ms	IgM		Sommer and Schachner, 1981		1:30	-
Olig2		rb	IgG	polyclonal	abcam	ab81093	1:200	-
Pax6		ms	IgG		Developmental Studies Hybridoma Bank (Stoykova et al)		1:100	-
PDGFR-a	C-20	rb	IgG	polyclonal	Santa Cruz	sc338	1:30	1:500
SAM68	EPR 3231	rb		monoclonal	Epitomics	2529-1	1:500	1:20000
SLM-1		goat		polyclonal	santa cruz	sc-9472	1:10	1:100
SLM-2		goat		polyclonal	santa cruz	sc-9475	1:10	1:100
α-Tubulin	DM1A	ms	IgG1	monoclonal	Sigma	T6199	-	1:10000
βIII-Tubulin	2G10	ms	IgG2a	monoclonal	Sigma	T8578	1:300	-

Table 2 Secondary Antibodies

Antibody	produced in	Species	Isotype	Company
α Rb	goat	Cy3	IgG (H+L)	Dianova
α Ms	goat	Cy3	IgG + IgM (H+L)	Dianova
α Ms	goat	HRP	IgG + IgM (H+L)	Dianova
α Ms	goat	Cy3	IgG (H+L)	Dianova
α Rb	goat	HRP	IgG (H+L)	Dianova
α Rb	goat	Cy2	IgG (H+L)	Dianova
α Ms	donkey	Cy2	IgM (µ-chain)	Dianova
α Rat	goat	Cy3	IgM (µ-chain)	Dianova
α Rat	goat	HRP	IgM (µ-chain)	Dianova
α Ms	sheep	Cy2	IgG (H+L)	Dianova
α Ms	goat	Cy5	IgM (µ-chain)	Dianova
α Goat	donkey	Cy3	IgG (H+L)	Dianova
α Rat	donkey	Cy3	IgG	Dianova
α Ms	donkey	Cy2	IgG	Dianova
α Goat	donkey	Cy2	IgG	Dianova
α Rb	donkey	Cy5	IgG (H+L)	Dianova
α Ms	donkey	Cy3	IgM (µ-chain)	Dianova
α Goat	donkey	HRP	IgG	Santa Cruz

2.1. siRNA

SignalSilence Control siRNA, Cell Signaling, #6201

SignalSilence hnRNPA1 siRNA, Cell Signaling, #7668

2.1. Oligonucleotide Primer

Table 3 Primer

Primer name	Sequence	Annealing
GAPDH for	5'-CAAGGTCATCCATGACAACTTTG-3‘	60°C
GAPDH rev	5'-GTCCACCACCCTGTTGCTGTAG-3'	60°C
GFP for	5‘-ATGGTGAGCAAGGGCGAGG-3‘	60°C
GFP rev	5‘-TTACTTGTACAGCTCGTCCATGCC-3‘	60°C
MBP for	5’-GGACTGCAGGAGTTCTCTGG-3’	60°C
MBP rev	5’-GTGCCAGTGTGGGTCTCTTT-3’	60°C
SLM1 for	5’-ATGGGAGAAGAGAAATACTTG-3’	60°C
SLM1 rev	5’-ATATCTACCATAGGGGTGCTC-3’	60°C
SLM2 for	5’-ATGGAGGAGAAGTACCTGC-3’	60°C
SLM2 rev	5’-GTATCTGCCATATGGCTGG-3’	60°C

2.1. Plasmids

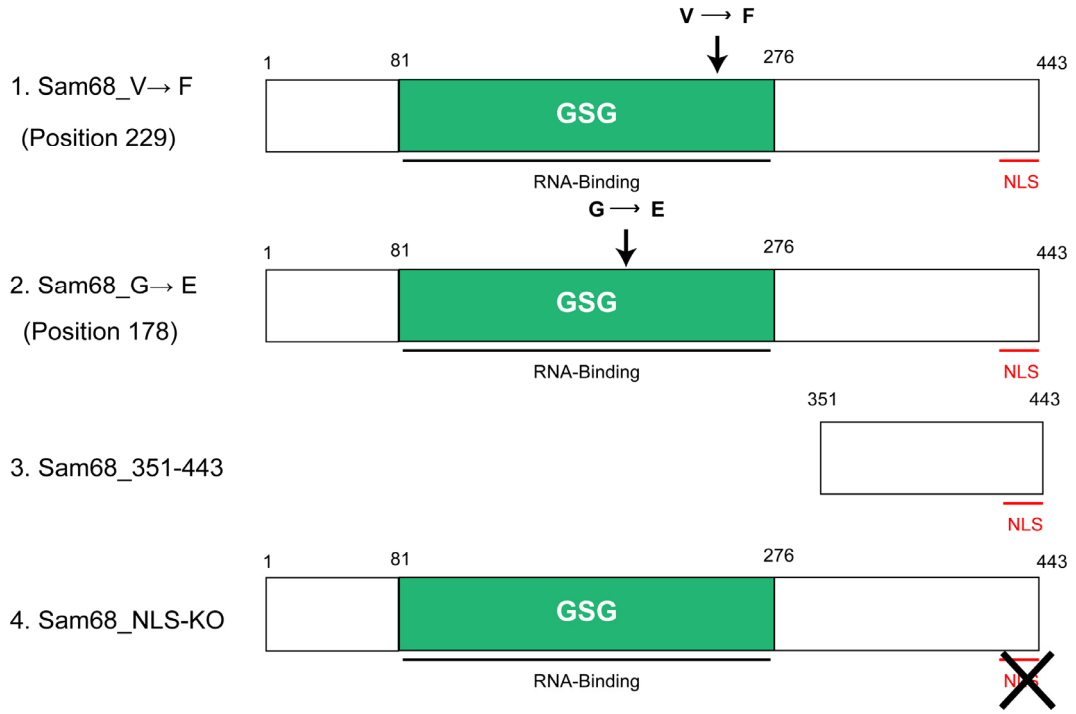

Figure 4. Schematic diagram illustrating the Sam68 constructs used in this thesis.

Constructs 1 (V→F) and 2 (G→E) contain an amino acid exchange in the RNA-binding domain, preventing RNA binding by steric interference and electrostatic repulsion. Construct 3 (351-443) is a truncated nuclear form of Sam68 containing the hnRNPA1 binding site but lacking the homodimerization domain and the RNA-binding domain, acting as a dominant negative control. Construct 4 (NLS-KO) contains an amino acid exchange in the NLS, inhibiting the transport of bound proteins and RNA into the nucleus.

All used plasmids were kindly provided by Claudio Settes' lab and are described subsequently (Paronetto et al., 2007, Pedrotti et al., 2010). All mutant forms of Sam68 were cloned into the pEGFP-C1 vector, whereas the wild type form of Sam68 was cloned into the pcDNA3 vector.

2.1. Kits

Nucleobond Xtra Maxi Machery-Nagel

First strand cDNA Synthesis Kit Thermo Scientific

QIAprep Spin Miniprep Qiagen

RNeasy Mini Qiagen

BCA Protein quantification Biorad

P3 Primary Cell 4D-Nucleofection Kit Lonza

2.6. Animals

For the experiments timed pregnancies of the inbred NMRI mice from Charles River and SD Rats from Janvier were used. The rats were kept in the local animal facility in a 12h light/dark cycle until the pups reached an age of P2.

2.2. Buffer

2.2.1. Cell Culture Media / Supplements

Mixed Glial Culture Medium (MGC)
DMEM
10% FCS
100 U/ml Penicillin
100 µg/ml Streptomycin

Oligodendrocyte Culture Medium, Chemically-Defined Medium (CDM)
DMEM
1% N2-Supplement
100 µg/ml BSA V
0,2 mg/ml L-Glutamin
100 U/ml Penicillin
100 µg/ml Streptomycin

Oligodendrocyte Proliferation Culture Medium (CDM_Prol.)
DMEM
1% N2-Supplement
100 µg/ml BSA V
0,2 mg/ml L-Glutamin
100 U/ml Penicillin
100 µg/ml Streptomycin
10 ng/ml FGF
500 mU/ml Heparin
10 ng/ml PDGF-AA

Neurosphere Medium
DMEM/F12 (1:1)
0,2 mg/ml L-Glutamin
2% (v/v) B27
100 U/ml Penicillin
100 µg/ml Streptomycin

Neurosphere Differentiation Medium
DMEM/F12 (1:1)
0,2 mg/ml L-Glutamin
2% (v/v) B27
100 U/ml Penicillin
100 µg/ml Streptomycin
1% FCS

Neurosphere Growth Medium
DMEM/F12 (1:1)
0,2 mg/ml L-Glutamin
2% (v/v) B27
100 U/ml Penicillin
100 µg/ml Streptomycin
10 ng/ml EGF
10 ng/ml FGF-2
500 mU/ml Heparin

HEK-Cell Medium
10% (v/v) FCS
DMEM
100 U/ml Penicillin
100 µg/ml Streptomycin

Oligodendrocyte Differentiation Culture Medium (CDM_Diff.)	**Ovomucoid**
DMEM	L15
1% N2-Supplement	1 mg/ml soybean trypsin inhibitor
100 µg/ml BSA V	50 µg/ml BSA V
0,2 mg/ml L-Glutamin	40 µg/ml DNaseI
100 U/ml Penicillin	
100 µg/ml Streptomycin	
1% FCS	
400 ng/ml T3	

2.2.2. Buffer for Immunocyto- and Immunohistochemistry

Citrate buffer	2 mM Citrate acid 8 mM Sodium citrate
KRH	125 mM NaCl 4.8 mM KCl 1.3 mM $CaCl_2$ 1.2 mM $MgSO_4$ 1.2 mM KH_2PO_4 5.6 mM D-glucose 25 mM HEPES
KRH/A	KRH containing 0.1% (v/w) BSA
PBS	137 mM NaCl 3.0 mM KCl 6.5 mM Na_2HPO_4 1.5 mM KH_2PO_4
PBS/A	PBS with 0.1% (w/v) BSA
PBT1	PBS with 1% BSA and 0.1% (v/v) Triton X 100
PBT01	PBS with 0,1% Triton X 100, 100 mM L-Lysine
PBT/ IM	PBS with 0.75% Triton, 10% Serum
PFA	4% PFA (w/v) in PBS, pH 7.4

2.2.3. Molecular Biology

LB-Medium	25 g LB-medium in 1L H_2O
LB-Medium with Agar	25 g LB-medium 12.5 g Agar dissolved in 1L H_2O
TAE	30 mM Tris 1 mM $Na_2EDTA \times H_2O$
Loading Buffer 6x	0.25 % Bromphenolblau, 40 % (w/v) Sucrose

2.2.4. Proteinbiochemistry

Blocking Solution	5% Milkpowder in TBST
Cell Lysis Buffer	50 mM Tris/HCL pH 7.5 150 mM Nacl 5 mM EDTA 5 mM EGTA 1%(v/v) Triton-X 100 0.1%(v/v) Na-deoxycholate 0.1%(v/v) SDS
SDS-Sample Buffer Laemmli 4x	0.5 M Tris-HCl, 10 % (w/v) SDS, 0.5 % (w/v) Bromphenolblue, Glycerol, H_2O; pH 8
SDS-Running buffer	25 mM Tris, 192 mM Glycin, 0.1 % (v/v) SDS
TBS	19 mM Tris-Cl, 137 mM NaCl; pH 7.4
TBST	TBS, 0.05 % (v/v) Tween 20
Transfer Buffer	25 mM Tris pH 8.2-8.4, 0.1% (v/v) SDS, 192 mM Glycin, 20% (v/v) Methanol

3. Methods

3.1. Cell culture

3.1. Cultivation of HEK293T Cells

HEK293T cells were routinely cultured on uncoated 10 cm culture dishes in HEK-medium at 37°C, 5% CO_2. When they reached confluence, they were passaged in a 1:20 dilution by a trypsin digestion.

3.1.1. Preparation and setting up mouse neural stem cell cultures

For setting up neural stem cell cultures E13.5 embryos were extracted from the uterus, after killing the mother animal by cervical dislocation. The embryos were decapitated and the forebrains were exposed. After separating the hemispheres, the meninges were removed and cortex and GE were separately collected in MEM containing microtubes. The tissue was digested for 20' in MEM containing 30 U/ml papain, 0.24 mg/ml L-cystein and 20 µg/ml DNaseI at 37°C in the waterbath. Before adding L-cystein and DNase, papain was preincubated for 10' in MEM at 37°C. The tissue was triturated to a homogenous solution and the digestion was stopped by addition of an equal volume of ovomucoid. The single cell suspension was afterwards pelleted (120xg for 5') and resuspended in neurosphere medium. For cultivation of free floating neurospheres 10 µg/ml FGF, 10 µg/ml EGF and 500 mU/ml heparin were added to the medium and 100,000 cells were plated in uncoated T25 culture flasks in 4ml medium. Cells were incubated at 37°C and 5% CO_2. For immunoblotting, neurospheres were spun down after 7 days of cultivation. For cell identity experiments, 20,000 cells were directly plated in neurosphere medium without growth factors. After 2h and 24h of cultivation cells, were fixed in 4% PFA followed by an immunocytochemical staining.

3.1.2. Isolation of Oligodendrocyte precursor cells

Rat pups from postnatal day 2 to 3 were decapitated and the forebrains were exposed. After separating the hemispheres, the meninges were removed and 4 cortices were collected in a microtube. The collected tissue was digested for 20′ in 2 ml 0.25% TE at 37°C in the waterbath. The digestion was stopped by the addition of 2 ml MGC medium containing 200 µg DNaseI. The mechanical destruction of cell formations performed by gentle trituration led to a homogenous single cell suspension. The solution was filled up to 10 ml with MGC medium followed by a centrifugation step for 5′ at 220xg. After withdrawal of the cell debris containing supernatant, the cell pellet was resuspended with 10 ml MGC medium and plated on 10 µg/ml PDL-coated T75 cell culture flasks. The flasks were placed in an incubator for 7 days at 37°C and 5% CO_2.

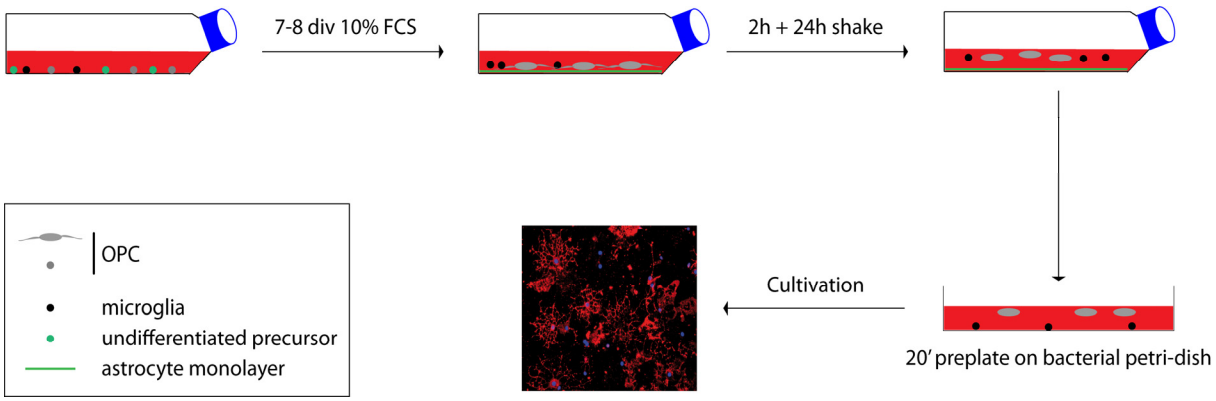

Figure 5. Isolation of oligodendrocyte precursor cells.

The cartoon illustrates the preparation of mixed glial cultures. Single cell suspension, obtained from postnatal rodent brains, is cultured for 7 days in the presence of 10% FCS. The separation of astrocytes, OPCs and microglia in two layers is exploited to remove the OPCs and the microglia from the bottom astrocyte layer by shaking on an orbital shaker overnight. The separation of microglia and OPCs was done by a pre-plating on a bacterial dish where microglia attach to the bottom and OPCs remain in the supernatant. The resulting cell suspension mainly consists of OPCs and immature oligodendrocytes, which can either be expanded in the presence of PDGF and FGF or differentiated by the addition of 1% FCS and T3.

After 7 days of cultivation a two layered cell culture developed, with an astrocyte/fibroblast layer on the bottom and OPCs and microglia attached on top (Figure 5). The first removal of microglia was performed by a 2h pre-shake at 220 rpm on an orbital shaker in the incubator. The removal of resulting microglia and the OPCs was performed by a 24h shake. Residual contaminating microglia cells were removed by pre-plating the supernatant on a bacterial petri-dish for 20′ at 37°C. The supernatant was transferred to a microtube and cells were

spun down for 5' at 220xg. The isolated OPCs were either expanded in CDM_Prol. with 10 ng/ml PDGF-AA, 10 ng/ml FGF-2 and 30 U/ml heparin, or they were cultured under differentiating conditions in CDM_Diff. without growth factors, but with 400 ng/ml T3 and 1% FCS.

3.1.3. Transfection of oligodendrocyte precursor cells

One aim of this thesis was the establishment of an innovative new transfection protocol enabling a high efficiency transfection of OPCs with the *4D Nucleofector of Lonza*. The detailed protocol of the establishing process is described in chapter 4.2. High efficiency Transfection of Oligodendrocyte Precursor Cells, whereas a short protocol is depicted and described in Figure 6.

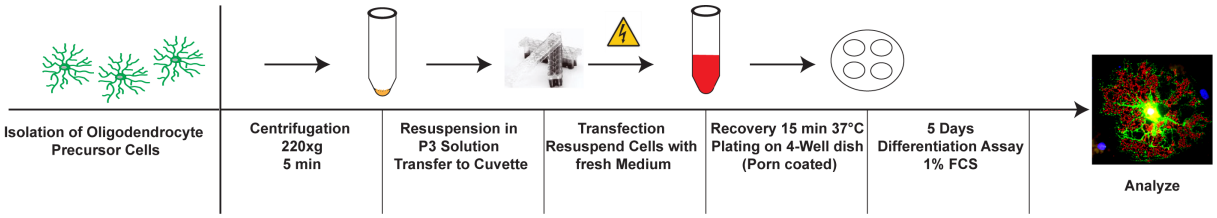

Figure 6. Transfection of oligodendrocyte precursor cells.

The scheme is illustrating the major steps of transfecting OPCs with the 4D Nucleofector of Lonza. First step in preparing the OPCs for the process of transfection is the centrifugation and the following determination of the cell number. 250,000 cells were collected in a fresh tube and spun down again. Afterwards, the cell pellet was resuspended with 20 µl of P3 solution containing 0.5 µg of plasmid (pEGFP-C1). Immediately, the resuspended cell solution was transferred to the transfection cuvette. Avoiding air bubbles, as it affects the electroporation of the cells, was very important. Several pulses were tested to identify an optimal ratio between viability and transfection. After transfection, fresh pre-warmed medium was added to the cells in the cuvette and the cell suspension was transferred to a clean tube. In the last step, cells were resuspended with medium covering the pellet and plated on PORN coated 4-well dishes. The cells were then cultured for 3-5 days in CDM_Diff. Afterwards, the transfection efficiency and morphology were analysed.

3.1.3.1. Transfection of OPCs with hnRNPA1 siRNA

The transfection with hnRNPA1_siRNA was performed with the protocol described previously (3.1.3. Transfection of oligodendrocyte precursor cells). OPCs were double transfected with 100 mM of SignalSilence hnRNPA1 siRNA and additionally with 0.5 µg pEGFP-C1 or the Sam68 plasmids (2.1. Plasmids). For the control situation 100 mM of SignalSilence control siRNA were double transfected with 0.5 µg pEGFP-C1. Cells were cultured for 5 days and subsequently used for immunocytochemically stainings or immunoblotting.

3.1.4. Detection of antigens in single cells and on tissue sections

3.1.4.1. Immunocytochemistry

For the detection of antigens in cultured cells, the medium was carefully removed and cells were washed with KRH/A. The incubation with the O4 antibody, used for a detection of the cell surface ceramide containing glycolipid sulfatide, was performed for 20′ in KRH/A buffer at RT. After washing twice with KRH buffer for removing unspecific bound antibody, cells were fixed for 10′ with PFA. Afterwards cells were washed and permeabilized with PBT/1 for 15′. The incubation with the primary antibody against intracellular epitopes also occurred in PBT/1 buffer for 30′. Again, the removal of unspecific bound antibody was done by two washes with PBS/A. The incubation with the appropriate secondary antibody was also done in PBS/A for 30′ at RT. The cells were mounted in PBS/Glycerin, after two final washing steps with PBS.

3.1.4.2. Immunohistochemistry

Brains from E13.5 mice were immersion fixed with 4% PFA. The fixation time depended on the intended antibody. For Pax6 staining, fixation durations of 2h were chosen, for all other antibodies the fixation occurred overnight at 4°C. Postnatal mice were perfused at the age of P10. After determining the body weight, the appropriate mixture of anaesthetics was

calculated (xylazine 10mg/kg and ketamin 200 mg/kg) and injected intraperitoneal. Once the mouse was anaesthetized, the limbs were fixed and the heart was uncovered by opening the rib cage. The perfusion needle was inserted into the left ventricle and subsequently the perfusion set up was opened allowing the 4% PFA to rinse through the vasculature. The rinsed blood escaped by a small incision in the atrium. After 6-8 minutes fixation, the brains were removed and washed in PBS. After fixation, they were cryoprotected in 30% sucrose for 24h at 4°C. Finally the brains were embedded in tissue freezing medium on dry ice and were stored at -20°C until the sectioning with the cryostat into 14-16 µm sections was performed. The slides were again stored at -20°C until their usage.

The cryosections were cooked for 5' in citrate buffer for improving the presentation of the antigens followed by 10' on ice. For removing the citrate buffer, the sections were washed with PBS. Depending on the intended antibody, different serums were used for blocking unspecific binding sites. The blocking was performed with 10% serum diluted in PBT/IM for 1h. The primary antibody was diluted in PBT/IM and incubated at 4°C overnight. After washing with PBS, the sections were incubated with the appropriate secondary antibody, diluted in PBS/A for 1h at RT. Finally, after three washing steps with PBS, the sections were mounted with glass coverslips in ImmuMount.

3.1.5. Image Acquisition and Statistical Analysis

For measuring the optical density of immunoblots and PCR images, the *ImageJ software* (http://imagej.nih.gov/ij/) was used. After converting the image to grayscale and inverting it, the bands of interest were surrounded with equally sized rectangles. The relative density of each band was calculated by Image J. The mean density of the loading control or the empty vector was set to 100% and the mean densities of the samples were calculated in relation to this control.

Analysis of cell size and cell proportion of single cell types was as well performed with the Image J software. For quantifying the proportion of immunopositive cells in relation to the total cell amount, the cell counting plug in was used. In order to measure the length of PDGFRα-positive OPCs, a line from the tip to the end of the cell was drawn. For measuring cell area, O4 or MBP positive cells were surrounded with freehand selection. Subsequently, the cell length and area was calculated with the ROI-Manager plug in. Only distinct

immunopositive and successfully transfected cells were analysed in at least 3 independent experiments. A minimum of 200 Hoechst positive- and 20 GFP-positive-cells was analysed for each antibody and experimental condition. Successfully transfected cells were identified either by a clear overexpression of the gene product or by GFP-stain.

Statistical significance was estimated using the two-tailed students test for the comparison of two data sets (4.1.2. Immunocytochemical analysis of Sam68 expression pattern). The analysis of variance (Anova) and the Tukey's multiple comparison test was used to analyse differences among group means after different treatments (4.3.1. Role of Sam68 domains in oligodendrocyte differentiation). The p-value is given as $^{*}P \leq 0.05$, $^{**}P \leq 0.01$ and $^{***}P \leq 0.001$ in the figures, text and/or figure legends. All data are expressed as mean $\pm$ SD.

3.2. Proteinbiochemistry

3.2.1. Cell Lysis and protein quantification

For protein lysis, cells were spun down and cell pellets were either directly lysed, or they were stored at -20°C until usage. Depending on the pellet size, the pellet was resuspended with 20-60 µl of protein lysis buffer containing 1% protease inhibitor. The cells were lysed for 30' on ice and subsequently centrifuged for 30' at 16,000 rpm at 4°C. The resulting supernatant was transferred to a clean microtube on ice.

Protein concentration was measured with the *BioRad quantification assay kit* according to the manufactures instructions.

3.2.2. SDS-PAGE

The separation of the before lysed proteins was performed with the *Mini-PROTEAN Tetra Cell System (Biorad)*, after heating the samples in SDS-buffer for 5' at 95°C. After loading the gels, the separation occurred by running the gels with a constant power of 200 V per gel for 35-45 '. The separation gels had a concentration of 3.75%, the gradient gels of 10%.

3.2.3. Immunoblotting

The transfer of the separated proteins on a with methanol activated PVDF membrane was performed with the *SD Semi-Dry Transfer Cell (Biorad)*. Three layers of Whatman paper, the PVDF membrane, the gel and again three layers of Whatman paper were layered from the anode to the cathode. The protein transfer occurred for 1.15h with approximately 1.5mA/cm^2. The membrane was blocked subsequently with 5% (w/v) low fat milk powder in TBST for 1h at RT. Primary antibodies were incubated overnight at 4°C. For removal of not bound antibody, the membrane was washed three times for at least 15'. Afterwards, the incubation with HRP-conjugated secondary antibody was done for 1h at RT. After three final washing steps (20' each), the membrane was incubated with the ECL reagent. Finally, X-ray films of different exposure times were developed in a developing machine.

3.3. Molecular Biology

3.3.1. RNA-Isolation and cDNA synthesis

From 2x10^5 oligodendrocytes, total RNA was isolated with the *RNeasy Mini Kit* from Qiagen including *QiaShredder* columns all according to manufacturer's instructions. RNA was eluted in a total volume of 30 µl. The transcription of cDNA from isolated RNA was performed subsequently with the *first strand cDNA synthesis kit* according to the manufacturer's instructions. Depending on the obtained RNA-concentration, the total reaction volume was changed, if neccessary to 30-40 µl, by adjusting the concentration of buffer, primers and dNTPs. The concentration of reverse transcriptase was kept constant.

3.3.2. Reverse Transcriptase polymerase chain reaction (RT-PCR)

PCR set up:

Template DNA	1 µl
Forward Primer (10pmol)	0.5 µl
Reverse Primer (10pmol)	0.5 µl
dNTPs (5nmol)	0.5 µl
10x Reaction Buffer	2.5 µl
Taq Polymerase	1 µl
H_2O	19 µl

PCR reaction

1. Denaturation	95°C	2′30′′	
2. Denaturation	95°C	30′′	
3. Annealing	60°C	30′′	
4. Elongation	72°C	1′05′′	Back to Step 2, 30 Cycles
5. Elongation	72°C	5′	

3.3.3. Isolation of plasmid DNA

Plasmid DNA was isolated from overnight bacterial cultures using the *QIA prep Spin* Miniprep Kit for 4 ml and the *Nucleobond Xtra Maxi* for 150 ml bacterial cultures. The isolation was performed according to the manufacturer's instructions, by binding of DNA to silica columns and subsequent washing steps. The DNA was finally eluted in H_2O and the concentration was determined via Nanodrop measurement.

4. Results

4.1. Identity of Sam68 expressing cells in the forebrain

4.1.1. Immunohistochemical analysis of Sam68 expression pattern

Our group identified Sam68 as a target and regulator of Tenascin C in the cortical niche (Moritz et al., 2008a). In ongoing studies, we examined the role of Sam68 and the related STAR-family proteins Slm-1, Slm-2 during forebrain development, beginning with an immunohistochemical analysis of their expression pattern in the mouse embryonic and postnatal brain (Bertram, 2013). Sam68 expression was observed throughout the whole CNS including hippocampus, striatum, olfactory bulb and cerebellum (Grange et al., 2004). We observed a widespread expression in the germinal layers of the dorsal forebrain as well as in the intermediate zone (IZ) and in the cortical plate (CP) of the developing cortex where early born neurons reside. Sam68 is also expressed throughout the LGE and MGE. Slm-1 and Slm-2 are both expressed in the cortical plate of the developing cortex and the GE, but only Slm-2 expression was detected in the ventricular zone (VZ) of the cortex and a strong expression was observed in the dorsolateral GE while Slm-1 was not detected in the VZ. The analysis of STAR-family members at P10 displayed parallels to embryonic expression. Sam68 is expressed throughout the 6 cortical layers with the strongest signal in cortical layer V (Bertram, 2013).

However, the cellular identity of cells in the embryonic and postnatal brain expressing STAR-family proteins is unknown. So far, using cell culture experiments, our group revealed that Sam68 and Slm-1 enhance neuronal differentiation of cortical NSCs and in turn reduce their proliferation ability (Bertram, 2013). For underlining this finding, the co-expression of Sam68 with the characteristic cortical neural stem markers (Pax6 and Nestin) and some of their derivative cell types, i.e. neurons (βIII-Tubulin) and astrocytes (GFAP) was analysed in immunohistochemical stainings on frontal sections of E13.5 and P10 mouse brains. E13.5 was chosen given that at this particular time the five fundamental zones (VZ, subventricular zone (SVZ), IZ, CP and marginal zone (MZ)) are developed and neurogenesis peaks (Bystron et al., 2008). At P10, the 6 cortical layers and other structures like the hippocampus are

completely established (Tole et al., 1997). With Pax6 as a marker for dividing neuroepithelial precursor and radial glia cells (Gotz et al., 1998), a clear co-expression with Sam68 was observed in the VZ of the cortex and the ONL of the eye. A co-expression was also recorded in the ganglion cell layer (GCL) of the eye, where postmitotic RGCs reside (Figure 7).

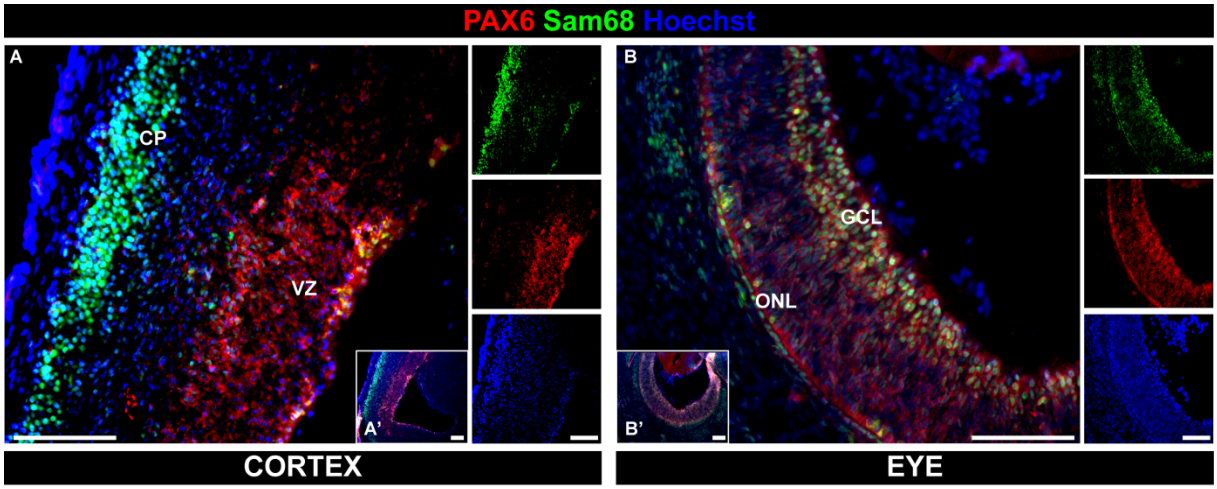

Figure 7. Co-expression of Sam68 and Pax6 in the eye and the cortex.

Depicted are photographs of immunhistochemical double-stainings of E13.5 frontal mouse brain cryosections labelled with Sam68 (green) and Pax6 (red) antibodies. For orientation, in (A') and (B') the whole brain and eye regions are shown. (A) A higher magnification illustrates the clear co-localisation of Sam68 and Pax6 in the VZ of the cortex and is confirmed by the depiction of the single channels. (B) A higher magnification of the retina in overlay and the illustration of the single channels demonstrates a co-expression of Sam68 and Pax6 in the ganglion cell layer (GCL). Note also few double positive cells in the outer nuclear layer (ONL). Nuclei are counterstained with Hoechst. Scale Bar 100 µm.

Also, with Nestin, a marker for neural stem cells (Lendahl et al., 1990), a co-expression with Sam68 was seen in the VZ of the cortex and in the subpallium (Figure 8).

So far, I demonstrated that Sam68 is expressed by neural stem cells and radial glia cells in the VZ of the cortex and the GCL of the eye. Furthermore, Sam68 is generally expressed by Nestin-positive neural stem cells in the VZ of the cortex and the hippocampal anlage. Next, coming back to the previous findings of Sam68 enhancing neuronal differentiation, a co-expression with characteristic markers for differentiating cells was analysed. βIII-Tubulin, a typical marker for young neurons was used for this purpose. Also, this immunohistochemical staining revealed a clear co-localization of both proteins in the cortical plate (Figure 9A) and the GCL of the eye (Figure 9B).

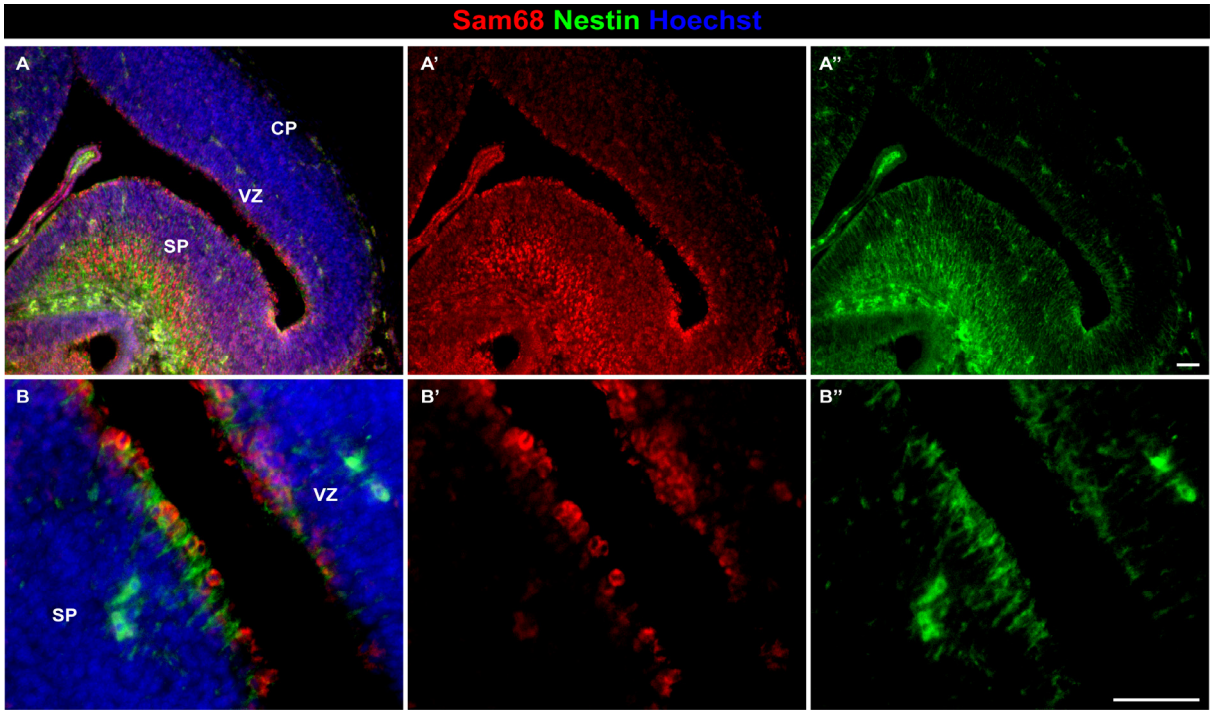

Figure 8. Co-expression of Sam68 and Nestin in the E13.5 mouse cortex.

Depicted are images of immunohistochemistry of frontal section through an E13.5 mouse brain stained with Sam68 (red) and Nestin (green) antibodies. (A) The illustration of the whole cortex with the cortical plate (CP) and subpallium (SP) (A-A'') demonstrates a strong co-expression of Sam68 and Nestin in the SP but also in the ventricular zone (VZ) of the cortex. A higher magnification and the illustration of the single channels clearly exhibits single cells co-expressing both proteins (B-B''). Nuclei are counterstained with Hoechst. Scale Bar 50 µm.

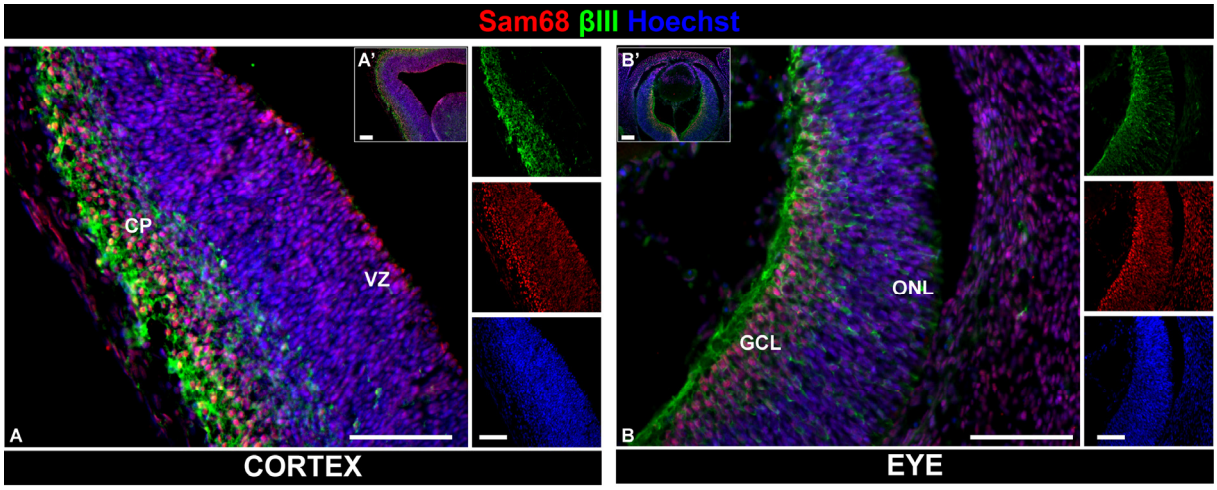

Figure 9. Co-expression of Sam68 and βIII-Tubulin in the cortex and the eye.

The immunhistochemical analysis of E13.5 mouse brains with antibodies against Sam68 and βIII-Tubulin revealed a clear co-expression of both proteins in the cortex and the eye. Brain and eye regions of interest are depicted for orientation in A' and B'. A higher magnification of the cortex and the illustration of the single channels demonstrates a clear co-expression in the cortical plate (CP). Also note a co-labelling of Sam68 and βIII-Tubulin expressing cells in the GCL (Ganglion cell Layer) and the ONL (Outer Nuclear Layer) of the retina, underlined by the exhibition of the single channels (A). Nuclei are counterstained with Hoechst. Scale Bar 100 µm. VZ (Ventricular Zone).

Furthermore, a co-localisation of Sam68 and GFAP, mainly expressed in basic fibrous astrocytes and in specialised astrocytes in layer 1 of the murine cerebral cortex (Garcia-Marques and Lopez-Mascaraque, 2013, Tabata, 2015), was investigated on P10 frontal cryosections, due to the later developmental appearance of astrocytes. Only in the SVZ, few astrocytes were found to be double-positive for both proteins, whereas cortical astrocytes did not express detectable levels of Sam68 (Figure 10).

Sam68 has a wide spread expression pattern in the CNS, with a stronger expression in the CP and the GCL of the eye. Indeed, as shown in this thesis, Sam68 is clearly co-expressed with the region specific progenitor markers Pax6 and Nestin as well as with βIII-Tubulin. This observation supports the hypothesis that Sam68 is expressed by precursor cells leaving the cell cycle with a neurogenic fate (Bertram, 2013).

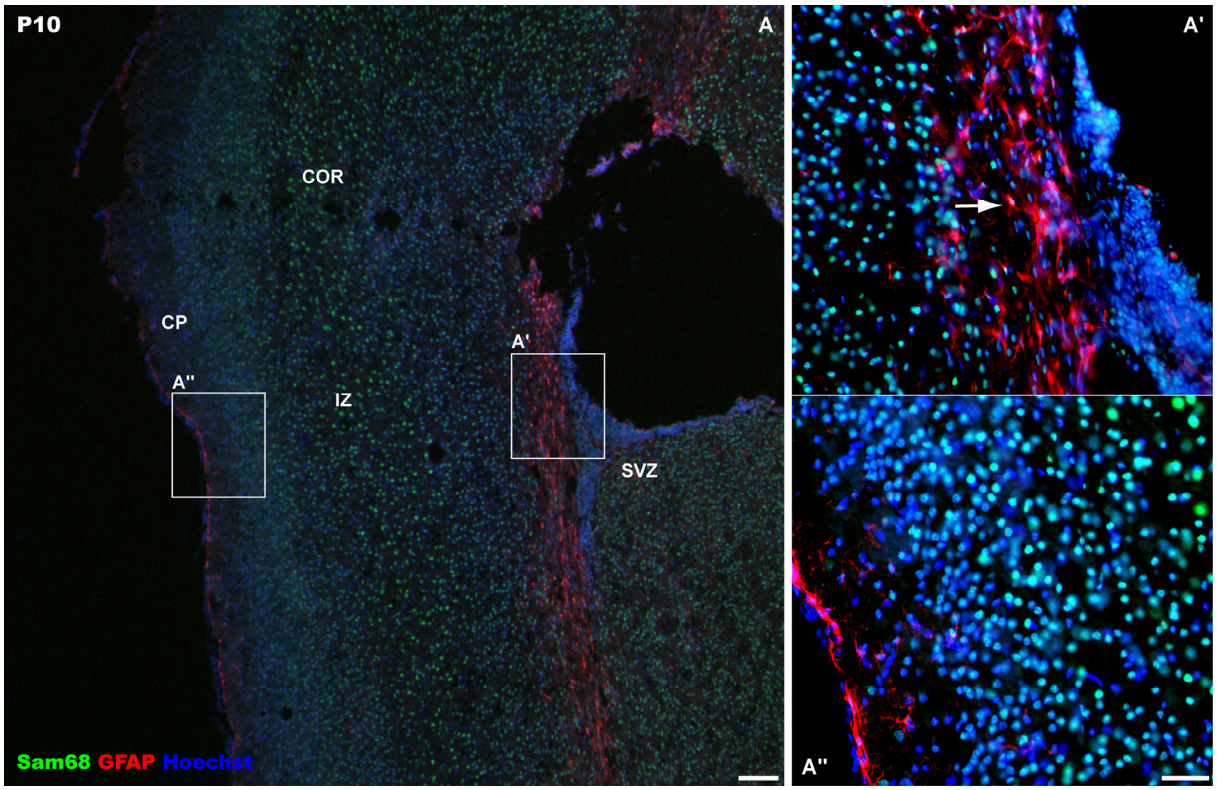

Figure 10. Sam68 and GFAP are co-expressed in the SVZ of P10 mouse brain.

Shown are immunohistochemical analysis of P10 mouse brain displaying a co-expression of Sam68 and GFAP in the subventricular zone (SVZ); clearly demonstrated in the magnification in A' (white arrow). Note that no cells in the cortical plate (CP) were identified co-expressing both proteins (A''). The overview in (A) revealed additionally a wide spread expression pattern of Sam68 in all cortical layers, but a stronger signal in the intermediate zone (IZ). Nuclei are counterstained with Hoechst. Scale Bar 50µm.

4.1.2. Immunocytochemical analysis of Sam68 expression pattern

The immunohistochemical analysis already revealed a co-expression of Sam68 with markers for neural stem cells and their progenies *in situ*. These stainings are in line with the previous findings of Sam68 acting as a promoter for neuronal differentiation. To get a deeper insight into the complex regulation mechanisms controlled by Sam68, a detailed investigation with cells isolated from E13.5 cortical and GE tissue was performed. These investigations were aiming at the identification of a time-dependent change in the expression pattern of Sam68 expressing cells and shall support the hypothesis of Sam68 promoting differentiation. After isolating and plating the cortical and GE derived cells, they were fixed after a culture duration of 2h and 24h. Indeed, a clear change in the expression pattern of Sam68-positive cells was noticed after 24h compared to the situation after 2h. The quantitative analysis revealed a distinct shift in the number of precursor cells towards differentiating cells. In cortical derived cells a decrease in the percentage of Pax6- and Sam68-double positive cells (from 54% to 39%) and a significant reduction of Nestin- and Sam68- double positive cells occurred (from 60% to 37%) (Figure 11 and Figure 13). In contrast, a significant increase of Sam68 expressing cells double positive either for βIII-Tubulin or GFAP was observed in cortical and GE-derived cells. The amount of cortical Sam68/βIII-Tubulin double positive cells increased from 43% to 63%, whereas the percentage of GE derived Sam68/βIII-Tubulin cells increased from 55% to 77% (Figure 12 and Figure 13).

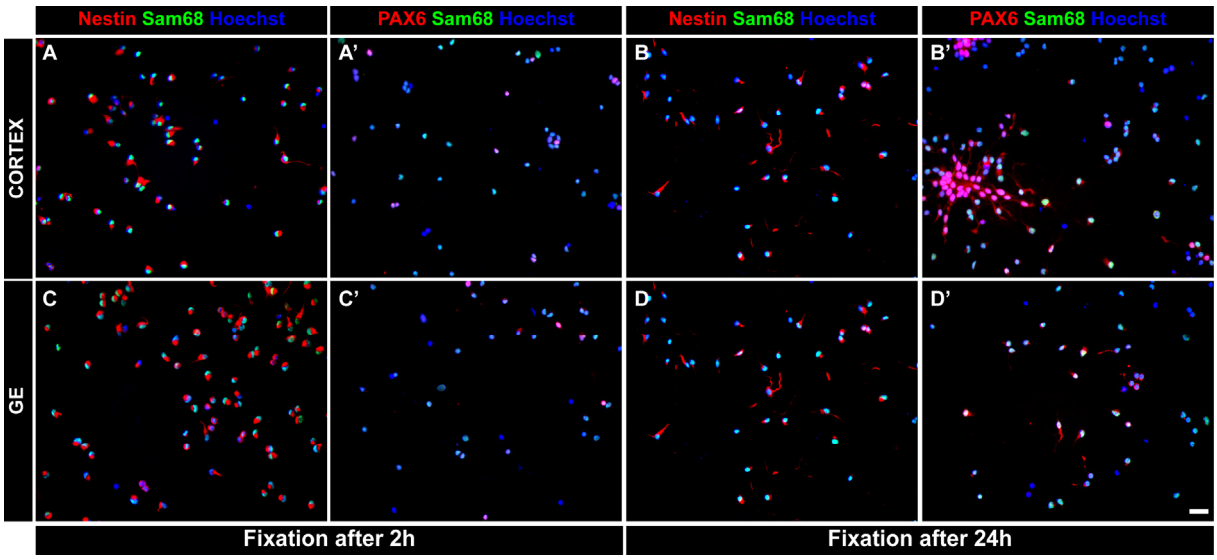

Figure 11. Co-expression of Sam68 with Pax6 and Nestin in neural stem cells

The photomicrographs show immunocytochemical stainings of neural stem cells (E13.5) isolated from cortical (A-B′) and GE (C-D′) tissue. The cells were fixed after 2h (A,A′ and C, C′) and 24h (B,B′ and D,D′) of cultivation. The double labelling with Pax6 and Nestin (both red) as markers for neural stem cells and radial glia cells revealed a co-expression with Sam68 (green) under all conditions. Cell nuclei are counterstained with Hoechst. Scale Bar: 50µm

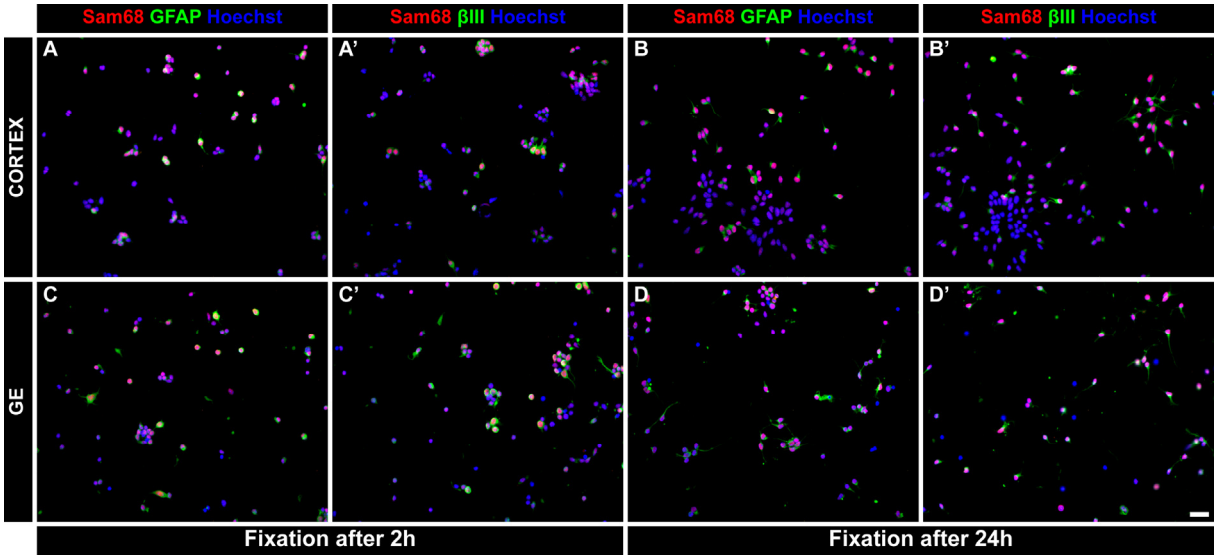

Figure 12. Co-expression of Sam68 with βIII-tubulin and GFAP in neural stem cells

Depicted are immunocytochemical stainings of neural stem cells (E13.5) isolated from cortical (A-B′) and GE (C-D′) tissue. After a culture duration of 2h (A,A′ and C,C′) and 24h (B,B′ and D, D′), the cells were fixed and analysed for a co-expression of Sam68 (red) and βIII-Tubulin or GFAP (both in green). Note that Sam68 is co-expressed with either βIII-Tubulin or GFAP under all conditions. Cell nuclei are counterstained with Hoechst. Scale Bar: 50 µm

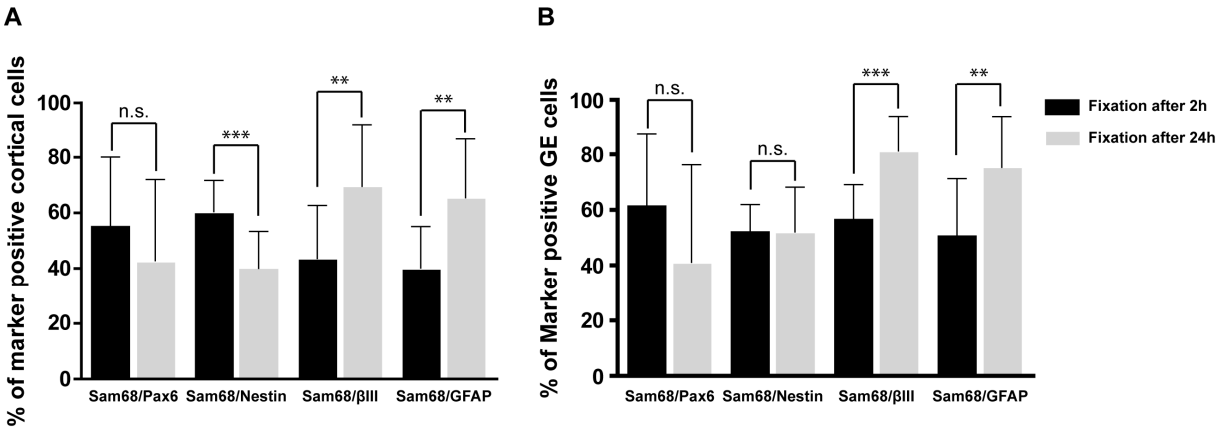

Figure 13. Quantification of neural stem cells co-expressing Sam68 and typical neural stem cell markers

Depicted are bar charts illustrating quantifications of immunocytochemical stainings (Figure 11 and Figure 12). Double positive cortical (A) and GE (B) derived cells were counted and expressed in relation to the total amount of Sam68-positive cells. Double labellings were performed with the characteristic neural stem cell markers Pax6 and Nestin for precursor cells and βIII-Tubulin and GFAP for young neurons and astrocytes.
Data are expressed as mean ± SD. (n=3, ** indicates $p \leq 0.01$, *** indicates $p < 0.001$, n.s. indicates not significant, Students t-test).

These findings confirm the results obtained with the imunnhistochemical stainings showing that Sam68 is not only expressed by neural stem cells and radial glia cells, but also by cells already determined to a neuronal or glial fate, which is true for the developing cortex and eye. Particularly, the quantitative analysis delineates the distinct time-dependent shift in the Sam68 expression pattern towards specific neuronal and glial cell markers and gives an overview of the percentage distribution of precursor cells in comparison to lineage determined cells. Given that Sam68 is present in neural stem and progenitor cells as well as in their postmitotic progenies raises the question what differences in Sam68 function might be on the molecular level. It can be assumed to be different in dividing versus postmitotic differentiating cells.

4.2. High efficiency Transfection of Oligodendrocyte Precursor Cells

Transfection is a widely used approach to assess the functional importance of proteins. Allowing for the overexpression or the knockdown of genes, selective information about the respective function can be obtained. The main goal of this thesis was to elucidate the role of Sam68 for OPC development, particularly with respect to their maturation behaviour. The transfection of OPCs with the earlier mentioned Sam68 plasmids (see 2.1. Plasmids) seemed to be a reasonable way to investigate in detail the function of Sam68 by analysing the importance of its single domains. Especially, given that our group recently established a new protocol for the high efficiency transfection of neural stem cells (Bertram et al., 2012). However, in particular rat OPCs turned out to be rather sensitive with respect to the transfection process. Although a transfection was feasible (Czopka et al., 2010), it was limited by the high amount of $5x10^6$ cells needed for each transfection and a considerable loss of OPCs caused by cell death during the procedure. To overcome these two disadvantages, I established a completely new protocol for the *4D-Nucleofector of Lonza*. In order to establish this protocol I used the pEGFP-C1 plasmid to transfect $2x10^5$ OPCs. This plasmid was chosen for the establishing process given that the Sam68 constructs were cloned into this vector and the design of the protocol therefore incorporates my specific experimental conditions. Due to the low yield isolation of OPCs, 16-well Nucleocuvette Strips (20 µl) were used for the optimisation phase, as they allow for the transfection of lower cell numbers ranging between $2x10^5$-$5x10^5$ cells. During the establishing procedure, the best transfection results were obtained with an amount of 2-$5x10^5$. Several cell numbers were tested, ranging between 2.5 to $9x10^5$ (Table 4). The first step was a pulse screen in which 26 different pulses were tested. Initially, the cell viability was selected as the most critical parameter for the evaluation of the tested pulses. The first tested pulses showed a comparatively low viability and the surviving cells failed to differentiate into oligodendrocytes (Figure 14). Therefore, a meaningful quantification of the transfection efficiency was impossible. In contrast, weak pulses led to high cell viability, but produced at the same time only a low transfection efficiency. Finding a pulse striking a balance between these two aspects was the next step. Based on these results, the collaborating company *Lonza* provided more pulses, whereupon the viability increased dramatically (Figure 15A). Among many different pulses tested, the pulse protocol CA-138 produced the highest level of viable cell numbers, with a 90 ± 21 % (n=10 ± SD) of cells surviving post transfection and allowed for a quantification of the transfection efficiency.

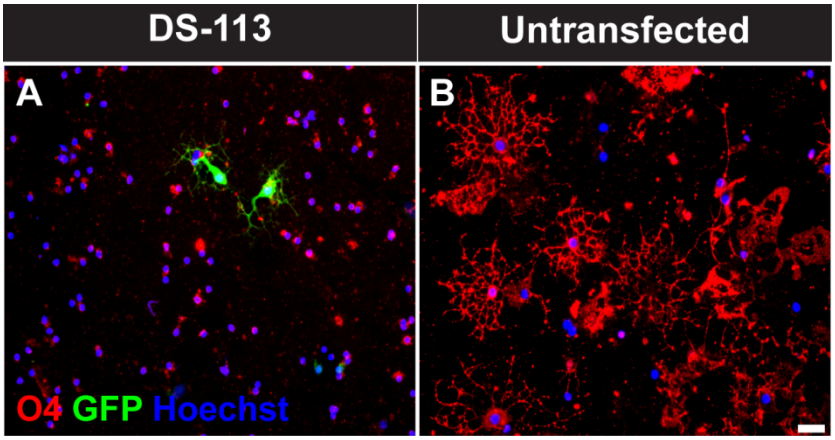

Figure 14. Transfection result with suboptimal pulse protocol DS-113.

Photomicrographs of immuncytochemical stainings of transfected OPCs with *P3 solution* and DS-113 cultured for 3d are shown in (A). EGFP is visualised with the fluorochrome Cy2 (green). O4 labels immature oligodendrocytes and is visualised with Cy3 (red). Cell nuclei are Hoechst-stained. For pointing out the suboptimal transfection conditions, untransfected OPCs are depicted as well (B). Scale Bar: 30µm.

The latter was determined by counting the number of O4- and EGFP-positive immature oligodendrocytes as determined by double-immunocytolabelings. By comparing CA-138 with five other pulses with reasonable cell survival rates, CA-138 resulted in 17±7% (n=10, ± SD) successfully transfected oligodendrocytes, which was the best obtained transfection rate (Figure 15B). Beside the identification of the optimal pulse protocol, culture conditions and transfection parameters before, during and post-transfection were improved as well. An overview about the changed parameters is given in Table 4. Transfected OPCs developed best on PORN coated 4-well dishes after a short recovery time of 15 min, extended recovery periods from 30 min to overnight recovery did not improve the cell survival rate. Furthermore, regarding transfection efficiency and viability, the direct plating of the transfected cells in P3 solution and CDM was more effective than the foregoing removal of P3 solution. The comparison of P1 and P3 solution revealed high cell mortality with P1 solution, indicating that P3 solution is ideal for the transfection of OPCs. Determining an optimal plasmid concentration emerged as another crucial parameter. Low concentrations caused less transfected cells, whereas high amounts increased cell mortality. By testing different plasmid concentrations (Table 4), 0.5 µg plasmid afforded the best balance between transfection efficiency and cell survival. Next, it appeared necessary to show that this transfection protocol also allows for the differentiation and characteristic maturation of cultured OPCs.

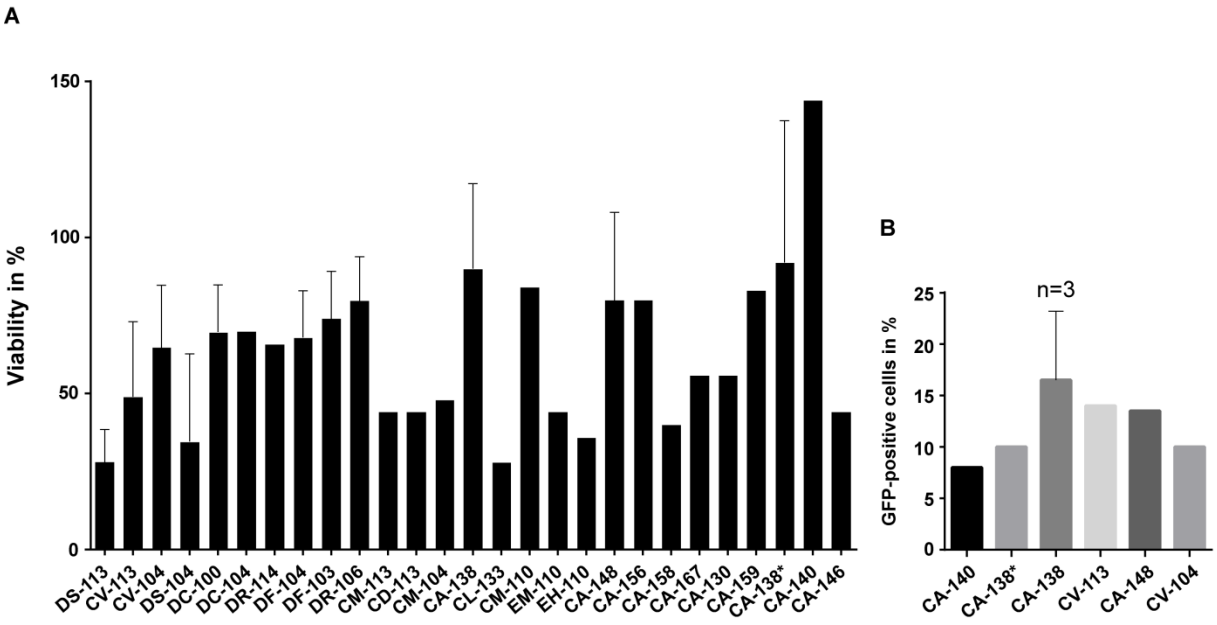

Figure 15. CA-138 displayed the best balance of viability and transfection efficiency

Depicted are bar charts delineating the quantification of the viability (A) and the transfection efficiency (B) after the pulse screening. OPCs were transfected with 0.5µg pEGFP-C1 (exception: CA-138* with 1µg pEGFP-C1) using 26 different programs. OPC viability was determined directly after transfection. Using a set of pre-selected pulses, the transfection efficiency was determined 24h after transfection by counting EGFP and O4 double - positive cells. Data are expressed as mean ± SD. Bars with SD represent at least 3-10 independent experiments. Those without error bars were performed once or twice, due to an extremely low viability. Counting low cell numbers with the Neubauer cell chamber (around 250,000 cells) can cause variation, explaining viability rates above 100%.

Table 4 Transfection parameters changed during the establishing process

Pre-Transfection	Transfection	Post-Transfection
Coating of 4-Well dishes (poly-L-ornithine, poly-D-lysine, pre-incubation with medium) **Centrifugation steps** (duration, RPM) **Amount of cells per transfection** ($2.5\text{-}9\times10^5$ cells)	**Solutions** (P1, P3) **Amount of plasmid** (0.1 µg, 0.25 µg, 0.5 µg, 1 µg) **Different plasmids** (pmaxGFP,pEGFP-C1, pEGFP-N1) **26 pulses tested**	**Recovery steps** (e.g. recovery over night, or for max. 30 min at 37°C after transfection) **Start of cell culture** (either direct plating of cells with transfection solution, or previous resuspension of cells in fresh medium) **Amount of plated cells** ($2\text{-}5\times10^4$ cells/Well)

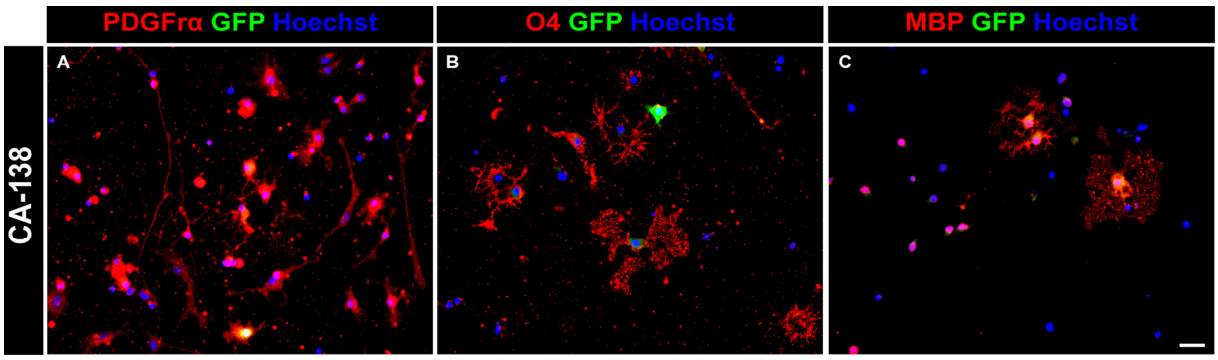

Figure 16. Transfected OPCs perform a normal morphological maturation

Shown are immunocytochemical stainings of OPCs 48h after transfection with the program CA-138. In the above photomicrographs, the signal of the transfected EGFP-positive cells is intensified with the fluorochrome Cy2 (green). A co-labeling of the transfected oligodendrocytes with the characteristic oligodendrocyte lineage markers revealed a regular maturation; (A) Co-staining against PDGFRα (red) a marker for OPCs, (B) against O4 (red), labelling immature oligodendrocytes and (C) against MBP (Cy3, red), which becomes expressed in mature oligodendrocytes. Cell nuclei are Hoechst-stained. Scale Bar: 30µm.

Since the morphological maturation of OPCs along the lineage toward mature oligodendrocytes is characterised by the expression of specific proteins (Zhang, 2001), I performed double-immunostainings against EGFP and defined lineage markers of OPCs, which were allowed to differentiate for 48h after the nucleofection with pulse CA-138. Under these conditions a normal pattern of differentiation and maturation was observed. I recorded transfected OPCs identified by the expression of the PDGFRα, O4 and mature oligodendrocytes expressing MBP (Figure 16).

Taken together it was clearly shown that the transfection of non-adherent OPCs is now reproducibly possible with a high viability, normal differentiation and an acceptable transfection efficiency of up to 25%. In combination with the huge advantage that a low cell number of only $2x10^5$ is needed for the single electroporation process, no further improvements were attempted. This improved electroporation protocol now allows to elucidate the role of Sam68 for oligodendrocyte development.

4.3. Functional Analysis of Sam68 during Oligodendrocyte Development

4.3.1. Role of Sam68 domains in oligodendrocyte differentiation

Oligodendrocytes are essential for the myelination of axons in the central nervous system. During development, oligodendrocyte precursor cells generate oligodendrocytes in a controlled and regulated process through the activity of diverse intrinsic and extrinsic factors. The members of the STAR-family proteins are among the intrinsic factors involved in oligodendrocyte differentiation (Czopka 2009, Bertram 2013). Due to the multifunctional character of Sam68 and its related family members Slm-1 and Slm-2, further studies were done, in which Sam68 and Slm-1 were identified as promoters of neural stem cell differentiation. Both proteins promote the differentiation of neural stem cells into a neuronal fate, but also enhance oligodendrocyte maturation (Bertram, 2013). However, the detailed mechanism(s) of how Sam68 controls oligodendrocyte development are still unknown. Therefore, I assess several Sam68 plasmids which contain mutations in the RNA-binding site or the nuclear localisation signal to characterise the Sam68 domains relevant for controlling oligodendrocyte development, by transfection of isolated OPCs (Figure 4).

The Sam68_V→F and Sam68_G→E plasmids carry point mutations caused by amino acid exchanges (valine against phenylalanine and glycine against glutamic acid) in the RNA-binding domain, ultimately hindering the RNA-binding by steric and electrostatic repulsion. The third construct, Sam68_351-443, is a truncated version of the protein, lacking the homodimerisation domain but still containing the hnRNPA1 binding site and the C-terminal tyrosine rich domain. Tyrosine residues are potential sites of phosphorylation and it is known that Sam68 is tyrosine phosphorylated by numerous soluble tyrosine kinases (Fusaki et al., 1997, Derry et al., 2000). The fourth construct, Sam68_NLS-KO, carries a mutation in the NLS-Region. This mutation is caused by an amino acid exchange at positions 436 and 442, preventing its transport to the nucleus and therefore suppressing all Sam68 functions in the nucleus, i.e. its role in splicing (Paronetto et al., 2007). With this construct, the role of the nuclear localisation signal for the differentiation of oligodendrocytes can be elucidated.

The newly established protocol for the transfection of OPCs allowed for a detailed analysis of Sam68 functions in OPCs. After electroporating OPCs with the Sam68 constructs, cells were cultured for 5d under differentiating conditions and were fixed subsequently.

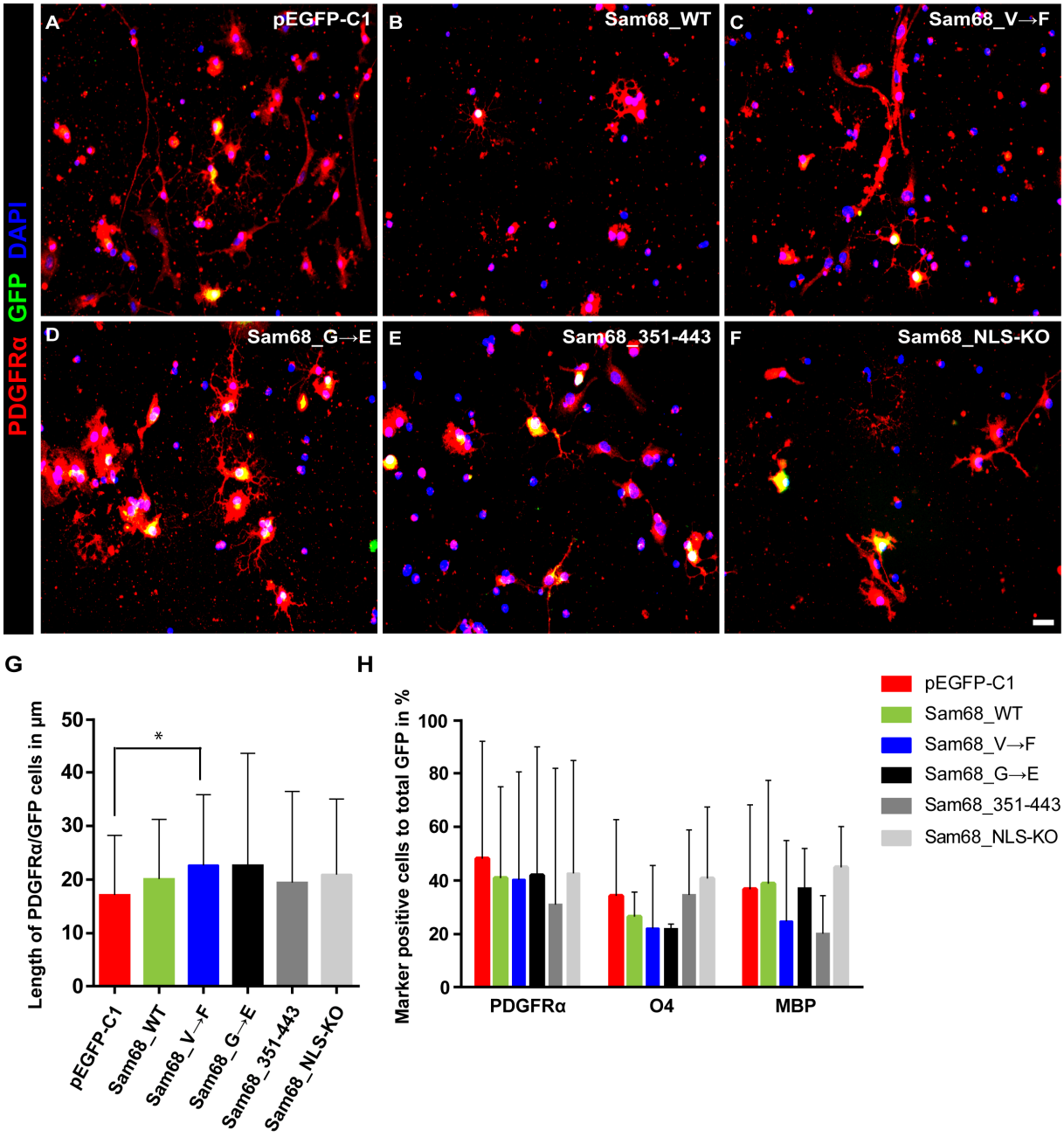

Figure 17. PDGFRα-positive OPCs transfected with Sam68_V→F are significantly elongated, whereas no significant differences were observed in the proportion of transfected marker positive oligodendrocytes.

Isolated OPCs from P2 rat cortices were transfected with the denoted Sam68 constructs and cultured for 5d. In comparison to the control (pEGFP-C1), the immunocytochemical staining with PDGFRα (red) and GFP (green) exhibited significantly elongated cells after a transfection with Sam68_V→F (A,C and G). (G) Bar chart plotting the cell length of transfected PDGFRα-positive cells. The quantification of transfected lineage marker positive cells (PDGFRα, O4 and MBP) in relation to the total GFP-cell amount revealed no significant differences in the proportion of immature and mature oligodendrocytes (H). Cell nuclei are Hoechst-stained. Scale Bar: 50 µm. Data are expressed as mean ± SD, n=3 (Oneway Anova followed by Tukey's multiple comparison test).

The differentiation of oligodendrocytes from their progenitors follows a stepwise morphological transition. This morphological change is accompanied by the sequential expression of molecular markers, which consequently permits for a stepwise analysis of the differentiation process (Figure 2) (Zhang, 2001). Therefore, the transfected cells were immunocytochemically stained with PDGFRα for OPCs, O4 for immature and MBP for mature oligodendrocytes. At first, the number of transfected marker positive cells was analysed in relation to the total amount of GFP-positive cells and compared to the control situation (pEGFP-C1). No significant differences were observed regarding the relative numbers of PDGFRα, O4 or MBP positive cells in comparison to the control situation (pEGFP-C1), although a reduction of O4-positive cells transfected with Sam68_WT, Sam68_V→F and Sam68_G→E was noticed. In addition, a multiple comparison of all conditions with each other did not reveal any significant differences (Figure 17H). While counting the cells, morphological differences regarding the cell size of PDGFRα-, O4- and MBP - positive oligodendrocytes were noticed. The expression of myelin components and the formation of myelin membranes are the two properties defining differentiated oligodendrocytes from their specified precursors, which possess a bipolar morphology. Immature oligodendrocytes are characterised by complex branching, whereas mature cells develop large myelin membranes (Zhang, 2001). Therefore, in a further consideration, the cell morphologic maturation was investigated in detail by measuring the length of PDGFRα-positive cells and the cell area of O4 and MBP-positive oligodendrocytes. Indeed, compared to the control (pEGFP-C1), a significant extension of OPCs transfected with Sam68_V→F was recognized (Figure 17 C, G). PDGFRα-positive OPCs transfected with Sam68_G→E were elongated as well, although this effect was not significant (Figure 17 D, G). Distinct differences were also observed, considering the area of transfected O4-positive cells. In comparison to the control (pEGFP-C1) OPCs transfected with Sam68_WT and Sam68_V→F had a significantly larger surface (Figure 18 I). This effect emerged in all OPCs that were transfected with one of the constructs, albeit only the size difference between the control vector transfected with the Sam68_WT construct or the above mentioned vector was significant (Figure 18 I).

Hence, the results of this cell size measurement were categorized in 8 steps ranging between 0-10000 μm^2. This categorisation delineated that cells transfected with Sam68_WT had the highest percentage (20%) of O4-positive cells larger than 10000 μm^2. Cells transfected with pEGFP-C1 exhibited by far the highest percentage (20%) of small cells, in fact between 0 - 1000 μm^2 (Figure 18 G and H).

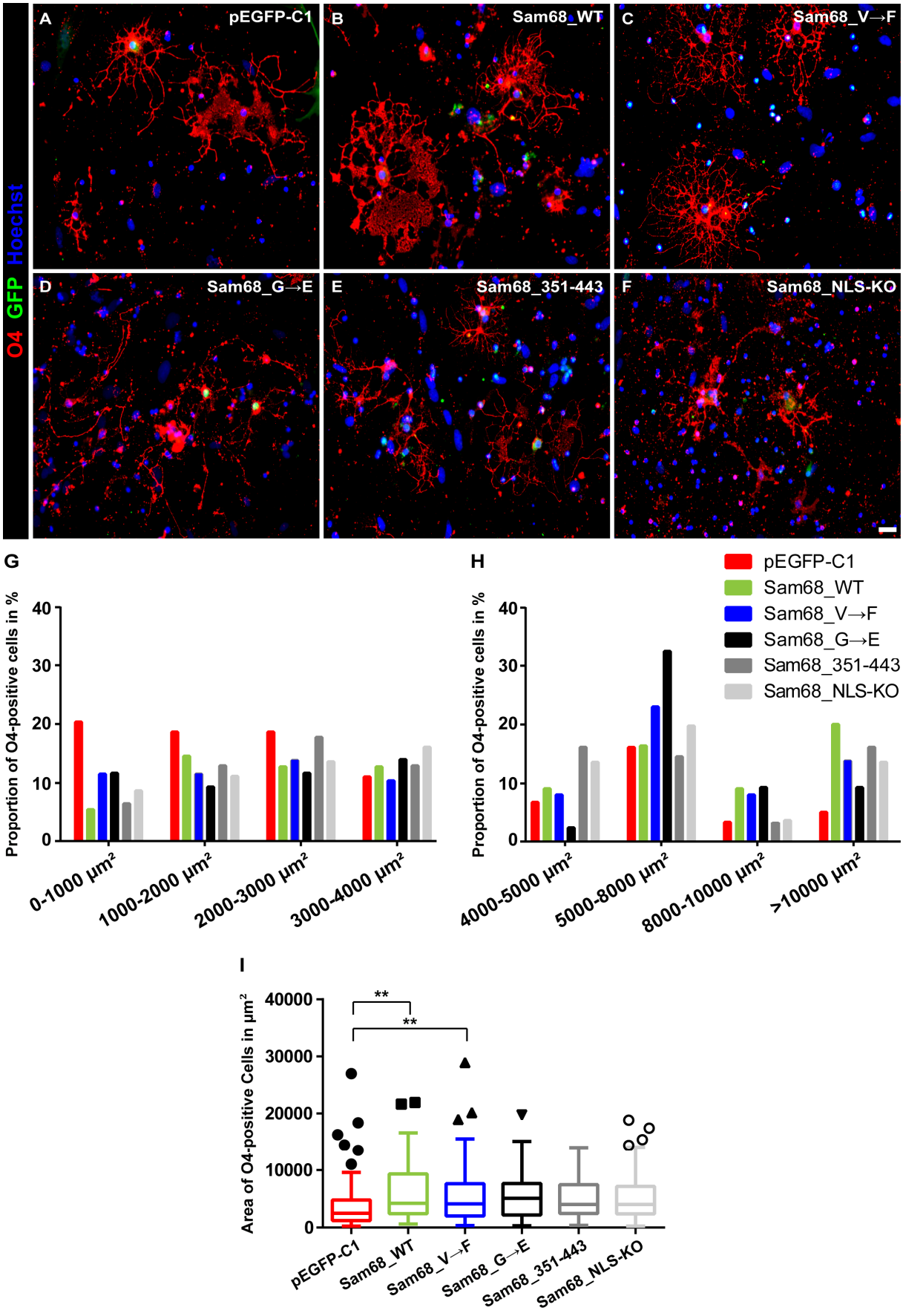
A
pEGFP-C1
B
Sam68_WT
C
Sam68_V→F
D
Sam68_G→E
E
Sam68_351-443
F
Sam68_NLS-KO
O4 GFP Hoechst
G
Proportion of O4-positive cells in %
0-1000 µm²
1000-2000 µm²
2000-3000 µm²
3000-4000 µm²
H
pEGFP-C1
Sam68_WT
Sam68_V→F
Sam68_G→E
Sam68_351-443
Sam68_NLS-KO
4000-5000 µm²
5000-8000 µm²
8000-10000 µm²
>10000 µm²
I
Area of O4-positive Cells in µm²
**
**

Figure 18. O4 - positive cells transfected with Sam68_WT and Sam68_V→F exhibited a significantly larger surface.

(A-F) The photomicrographs show immunocytochemical stainings of isolated OPCs from P2 rat cortices transfected with the denoted Sam68 constructs and cultured for 5d. This immunocytochemical analysis with O4 (red) and GFP (green) revealed differences in the size of cells, depending on the transfected plasmid. OPCs transfected with Sam68_WT and Sam68_V→F were significantly larger than the control situation transfected with pEGFP-C1; clearly demonstrated in the box plot (I). A detailed percentage subdivision of the cell sizes is shown in the graphs (G) and (H), with a range from 0- 4000 μm^2 (G) and 4000 to < 10000 μm^2 in (H). Cell nuclei are Hoechst-stained. Scale Bar: 50µm. Data are expressed as mean ± SD $^{*}p<0.05$,** $p<0.01$, n=3 (Oneway Anova followed by Tukey's multiple comparison test).

Significant differences were also observed regarding the morphology of MBP-positive cells. The area of cells transfected with Sam68_WT was significantly larger in comparison to Sam68_351-443 and Sam68_NLS-KO. In general, cells transfected with Sam68_351-443 and Sam68_NLS-KO had the smallest surface in comparison to all other conditions (Figure 19I). Interestingly, while the surface of O4-positive cells transfected with Sam68_V→F was comparable to the size of O4-positive cells transfected with Sam68_WT, MBP-positive cells transfected with Sam68_V→F appeared smaller in comparison to Sam68_WT (Figure 19I). Additionally, analysis of Sam68_V→F transfected OPCs revealed with 41% a high proportion of small cells (0-1000 μm^2). Oppositely, by far the highest percentage of large cells (<10000 μm^2) was noticed when cells were transfected with Sam68_WT (17%). Cells transfected with Sam68_351-443 showed the highest proportion (47%) of small cells (0-1000 μm^2) followed by cells transfected with Sam68_NLS-KO (39%). Underlining these findings, no cells larger than 10000 μm^2 where observed when the cells were transfected with Sam68_NLS-KO and only 2% of the cells transfected with Sam68_351-443 emerged larger than 10000 μm^2 (Figure 19 G,H). Regarding the morphology of MBP-positive cells transfected with Sam68_V→F in comparison to Sam68_WT a smaller surface was noticed, but these cells also exhibited a more mature stadium. More oligodendrocytes transfected with Sam68_V→F (<17%) formed myelin membranes in comparison to Sam68_WT (<11%). This revealed a detailed analysis of the morphologic maturity by categorising the oligodendrocytes in four categories according to the complexity of their branches and membrane formation (Figure 20). In Figure 20 (A) the criteria of categorisation are specified by examples. This analysis supports findings described above. Cells transfected with Sam68_351-443 and Sam68_NLS-KO exhibited less mature oligodendrocytes of category 3+4 in comparison to all other conditions and in particular to Sam68_WT (Figure 20 B). A bar chart showing separately the oligodendrocytes of category 4 illustrates the severe effect of Sam68_NLS-KO on membrane formation.

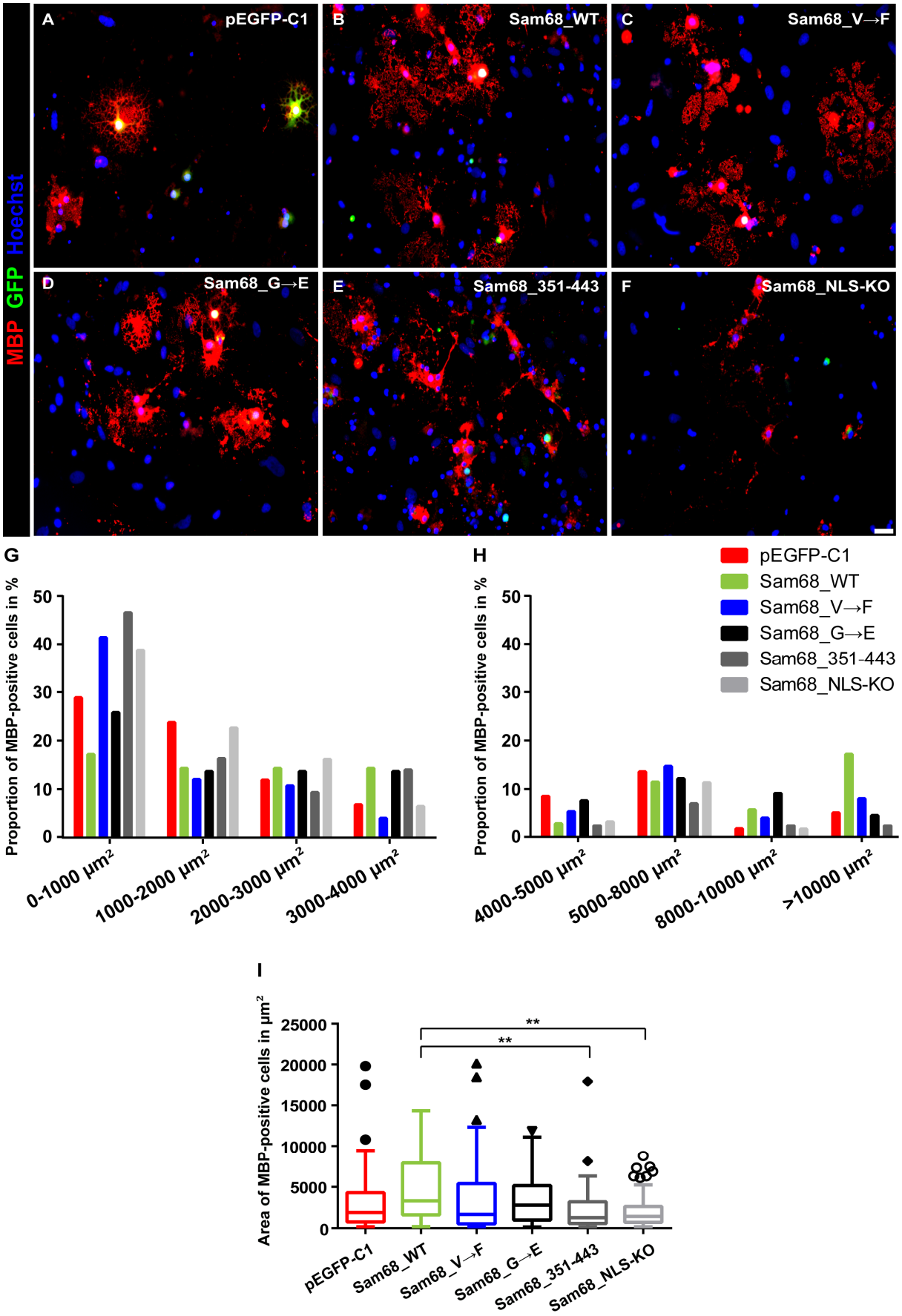
A
pEGFP-C1
B
Sam68_WT
C
Sam68_V→F
D
Sam68_G→E
E
Sam68_351-443
F
Sam68_NLS-KO
MBP GFP Hoechst
G
Proportion of MBP-positive cells in %
0-1000 µm²
1000-2000 µm²
2000-3000 µm²
3000-4000 µm²
H
pEGFP-C1
Sam68_WT
Sam68_V→F
Sam68_G→E
Sam68_351-443
Sam68_NLS-KO
4000-5000 µm²
5000-8000 µm²
8000-10000 µm²
>10000 µm²
I
Area of MBP-positive cells in µm²
**
**
pEGFP-C1
Sam68_WT
Sam68_V→F
Sam68_G→E
Sam68_351-443
Sam68_NLS-KO

Figure 19. MBP-positive cells transfected with Sam68_351-443 and Sam68_NLS-KO display a significantly smaller surface in comparison to Sam68_WT overexpression.

Shown are immunocytochemical stainings of transfected OPCs (with denoted Sam68 constructs) obtained from P2 rat cortices after a culture duration of 5d. These immunocytochemical stainings with MBP (red) and GFP (green) revealed significant differences in the surface of the cells, depending on the transfected plasmid. The box plot delineates that OPCs transfected with Sam68_WT were significantly larger in comparison to OPCs transfected with Sam68_351-443 and Sam68_NLS-KO (I). OPCs transfected with Sam68_351-443 and Sam68_NLS-KO showed the smallest size in comparison to all other conditions. A detailed percentage subdivision of the cell area is shown in the graphs (G) and (H), with a range from 0- 4000 µm² (G) and 4000 to < 10000 µm² in (H). Cell nuclei are Hoechst-stained. Scale Bar: 50µm. Data are expressed as mean ± SD $^{*}p<0.05$,** $p<0.01$, n=4 (Oneway Anova followed by Tukey's multiple comparison test).

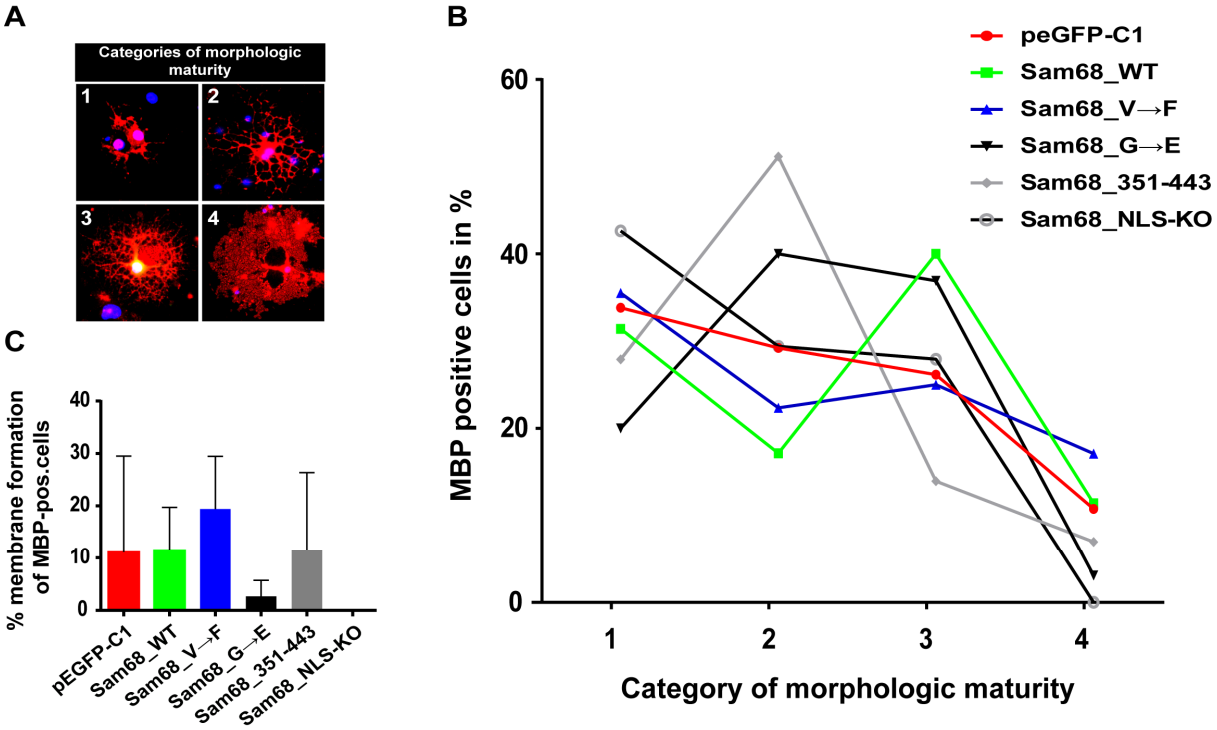

Figure 20. Sam68_NLS-KO prevents myelin sheet formation

(A) This panel illustrates the classification of oligodendrocytes according to their morphological appearance by showing immunofluorescence images of MBP-positive (red) cells at different maturation states, which are divided into four different categories (from 1: immature to 4: mature).
The graph describes the proportion of transfected MBP-positive cells and reveals no myelin sheet forming oligodendrocytes under the condition of Sam68_NLS-KO and an decrease of maturation under the condition of Sam68_351-443. Additionally, the graph shows most mature oligodendrocytes (categorie 3+4) under the condition of Sam68_WT (B). The percentage of myelin forming oligodendrocytes of category 4 is additionally depicted in a bar chart (C). Data are expressed as mean ±SD, n=4 (Oneway Anova followed by Tukey's multiple comparison test).

No membrane formation occurred when cells were transfected with this construct. Only few membrane forming cells were counted when the cells were transfected with Sam68_G→E (>3%). Additionally, it illustrates that most membrane forming oligodendrocytes appear, when cells were transfected with Sam68_V→F (Figure 20 C). This impression is supported by western blot analysis, demonstrating a higher amount of MBP in comparison to Sam68_WT transfected OPCs. Moreover, in comparison to Sam68_351-443 and Sam68_G→E, a significantly higher amount of MBP was noted (Figure 21A and B).

The western blot analysis supported the results of the immunocytochemical investigations, delineating a higher MBP level in cells transfected with the Sam68_WT overexpression plasmid in comparison to the control (pEGFP-C1). A higher MBP-level of Sam68_WT construct, Sam68_V→F and pEGFP-C1 in comparison to Sam68_G→E, Sam68_351-443 and Sam68_NLS-KO is additionally supporting the above findings of an impaired myelin sheet formation. In contrast, RT-PCR-analysis with MBP-primers binding in the 3'UTR recognizing all MBP-isoforms, revealed on mRNA-level a higher MBP-mRNA-level in the presence of overexpressed Sam68_G→E, Sam68_351-443 and Sam68_NLS-KO in comparison to Sam68_V→F and pEGFP-C1. Surprisingly, also in presence of overexpressed Sam68_WT a higher MBP-mRNA level was observed, similar to high amounts of Sam68_351-443 (Figure 21C and D).

Altogether one can summarize that overexpression of Sam68 in oligodendrocytes significantly accelerates their maturation and increases their size. Therefore, Sam68 is critical for oligodendrocyte development. In order to fulfil its function for OPC development, Sam68 relies on its RNA-binding properties. OPCs overexpressing Sam68 with a dysfunctional mRNA binding domain or an absent NLS are neither able to promote OPC size expansion nor their maturation.

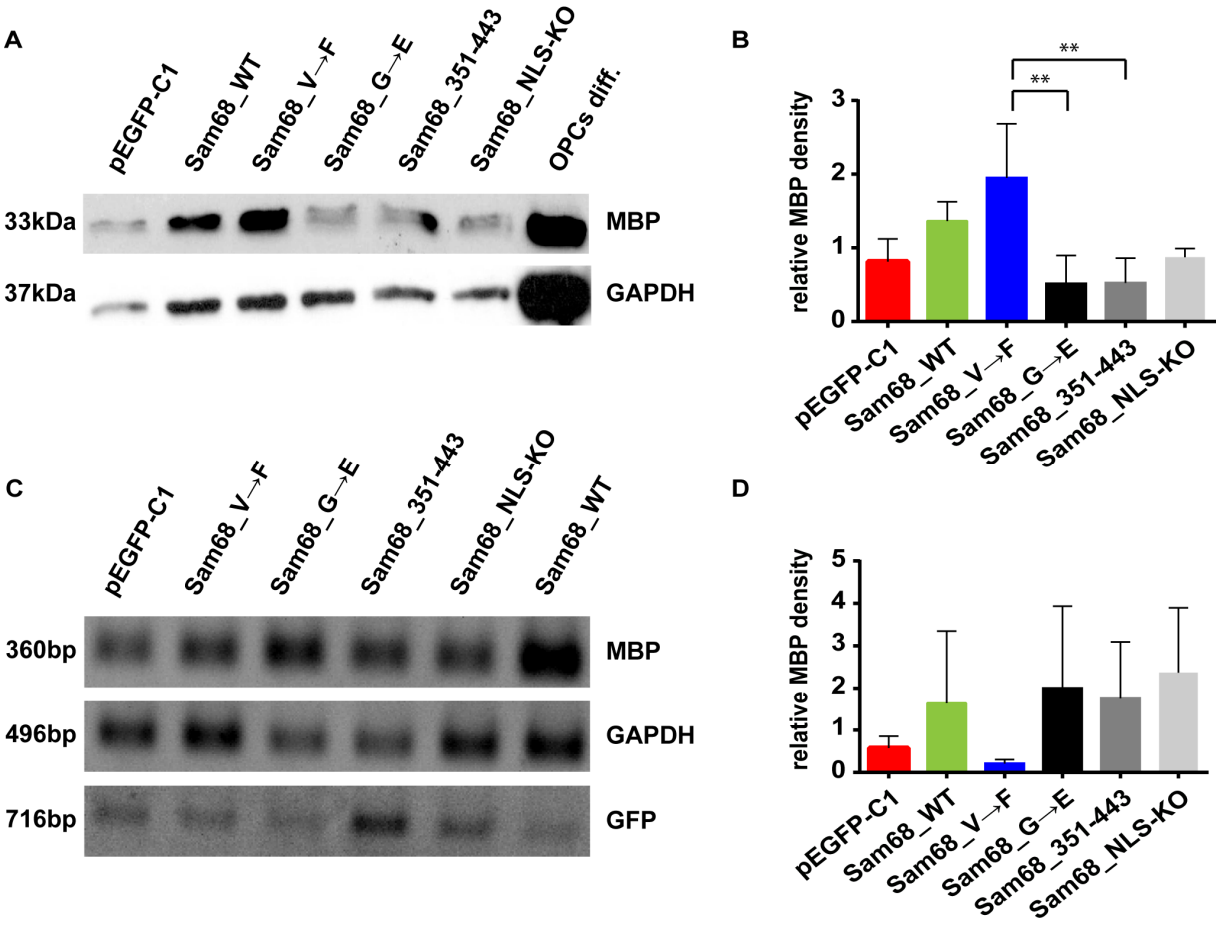

Figure 21. Transfection with Sam68_V→F significantly increased MBP-protein level and reduced MBP-mRNA level

(A) The radiograph shows a western blot analysis of protein lysates obtained from OPCs transfected with the denoted Sam68 constructs. Untransfected OPCs (OPCs diff.) cultured for 5 d and the empty vector (pEGFP-C1) served as controls. (B) This bar chart demonstrates the quantitative analysis of the western blot signals (expressed in arbitrary units) normalised to the associated GAPDH signals illustrating the significant decrease in the MBP density of Sam68_G→E and Sam68_351-443 in comparison to Sam68_V→F. Data are expressed as mean ± SD $^{*}p<0.05$,** $p<0.01$, $^{***}p<0.001$, n=3 (Oneway Anova followed by Tukey's multiple comparison test).
(C) This image shows an RT-PCR-analysis of cDNA synthesized from mRNA isolated of transfected OPCs. It demonstrates differences on MBP-mRNA level depending on the transfected Sam68-plasmid. The successful transfection of OPCs is demonstrated with GFP-primers. (D) The bar chart demonstrates the quantitative analysis of the MBP signal normalised to the GAPDH loading control and reveals a decrease of the relative MBP-mRNA-level under the condition of pEGFP-C1 and Sam68_V→F. n=2

4.3.2. Interplay of hnRNPA1 and Sam68 during OPC differentiation

I already demonstrated a functional importance of the RNA binding site and the nuclear localisation signal for cell growth, myelin sheet formation and MBP-expression. Next, I wanted to decipher a possible mechanism how this influence on oligodendrocyte differentiation may be regulated. Sam68 is supposed to be a regulator of MBP splicing (Czopka, 2009) and it contains a binding site for hnRNPA1, a member of the hnRNP-family. Besides Sam68, also hnRNPA1 is a known repressor of alternative splicing, by regulating a set of transcripts and exons in oligodendrocytes important for the formation of myelin sheets. In detail, Quaking binds hnRNPA1 mRNA through its 3'UTR and enhances its stability. hnRNPA1 itself co-regulates *MAG* exon 12 alternative splicing (Zearfoss et al., 2011). Both, Sam68 and Quaking belong to the highly conserved STAR-family proteins, thus a comparable interplay of Sam68 and hnRNPA1 is conceivable. Furthermore, the controlling of alternative splicing of Bcl-x by Sam68 and hnRNPA1 (Paronetto et al., 2007) supported the idea that hnRNPA1 could be a possible interaction partner of Sam68 during oligodendrocyte development. Most likely, Sam68 controls hnRNPA1 mRNA abundance and the translational efficiency. Furthermore, the binding of hnRNPA1 by Sam68 may repress the alternative splicing and the translation of MBP-mRNA.

To test this hypothesis, the experiments described in this chapter elucidate whether there is a general role for hnRNPA1 in the differentiation of oligodendrocytes. In a first approach, hnRNPA1 was knocked down in OPCs using hnRNPA1_siRNA. A possible interplay of Sam68 and hnRNPA1 was investigated by double-transfections with the previously used Sam68 constructs and hnRNPA1_siRNA. The transfections were performed with the earlier described transfection protocol (4.2. High efficiency Transfection of Oligodendrocyte Precursor Cells). The analysis of immunocytochemical stainings exposed effects on the morphology, whereas the influence on MBP-expression was discovered by western blot analysis.

At first, the functionality of hnRNPA1_siRNA was tested by its transfection in OPCs. After culturing the cells for 5 days under differentiating conditions, the successful knockdown was determined by western blot analysis (Figure 22A and B). Additionally, the transfection with hnRNPA1_siRNA in combination with a Sam68 overexpression was performed to elucidate the collective effect on hnRNPA1 expression. Interestingly, after the double transfection the

amount of hnRNPA1 protein was even lower compared to the simple knockdown with hnRNPA1_siRNA. Especially in comparison to not transfected oligodendrocytes, the effect is severe (Figure 22A and B).

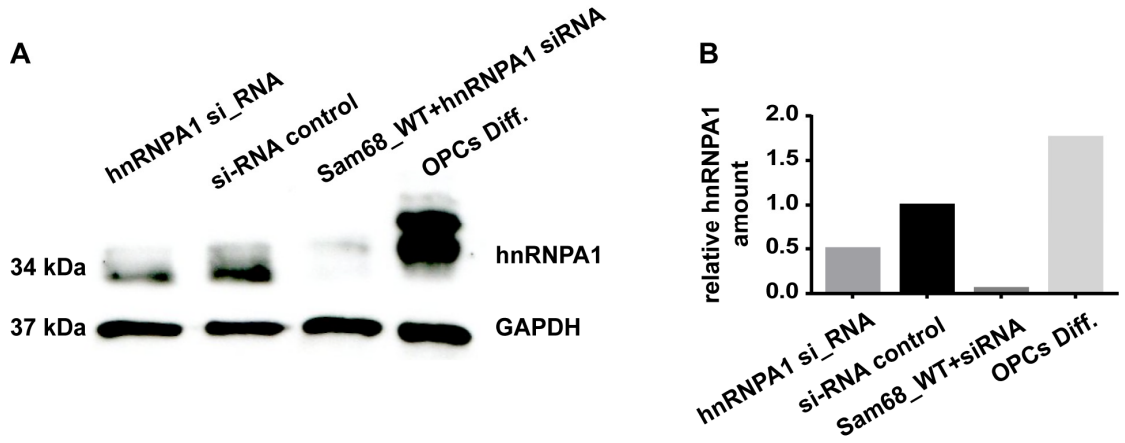

Figure 22. Immunoblotting confirms the successful knockdown of hnRNPA1 in OPCs.

(A) The radiograph depicts a western blot analysis of protein lysates derived from P2 rat OPCs transfected with hnRNPA1_siRNA alone, or in combination with the Sam68_WT overexpression vector. The transfection with a nontargeting siRNA and untransfected OPCs (OPC Diff.) served as controls. (B) The bar chart shows the quantification of the western blot signals from one experiment. The relative density of a protein band within each sample was normalized to the intensity of the associated GAPDH protein signal and is expressed in arbitrary units. The quantification illustrates the successful knock-down of the hnRNPA1 protein in OPCs transfected with the respective siRNA. Note that the parallel overexpression of Sam68_WT causes an even more pronounced reduction in hnRNPA1 levels compared to the control.

Thus, hnRNPA1 knockdown with hnRNPA1_siRNA is intensified through the forced expression of Sam68. This result provided strong evidence for a possible interplay between those two proteins in oligodendrocytes. A regulation of MBP-expression through both proteins appeared to be possible. Therefore, to answer this issue OPCs were double-transfected with hnRNPA1_siRNA and the Sam68 constructs: Sam68_V→F, Sam68_351-443 and Sam68_NLS-KO, respectively. The reason for using these constructs based upon the fact that they executed the most severe effects on oligodendrocyte differentiation. Particularly, the possible effects on OPC maturation and MBP-expression were of interest.

Therefore, after the transfection, the morphology of immature and mature oligodendrocytes was analysed by immunocytochemical stainings with the earlier introduced oligodendrocyte lineage markers PDGFRα, O4 and MBP (Figure 2) (Zhang, 2001). The measurements of cell size revealed that O4-positive cells transfected with control siRNA (Figure 23A, G) exhibited the smallest surface compared to all other conditions, whereas OPCs double transfected with hnRNPA1_siRNA and either Sam68_351-443 (Figure 23C and G) or Sam68_NLS-KO (Figure

23 F and G) showed the largest surface. Cells double transfected with hnRNPA1_siRNA (Figure 23D and G) and Sam68_WT (Figure 23B and G), revealed a size of about 16000-19000 µm². This was comparable to cells double transfected with hnRNPA1_siRNA and Sam68_V→F (Figure 23D, E and G). Regarding the morphology of MBP positive cells no distinct differences regarding the cell size were observed. OPCs double transfected with hnRNPA1_siRNA and Sam68V→F had the smallest surface. All other conditions showed a comparable cell size (Figure 23A'-F' and H).

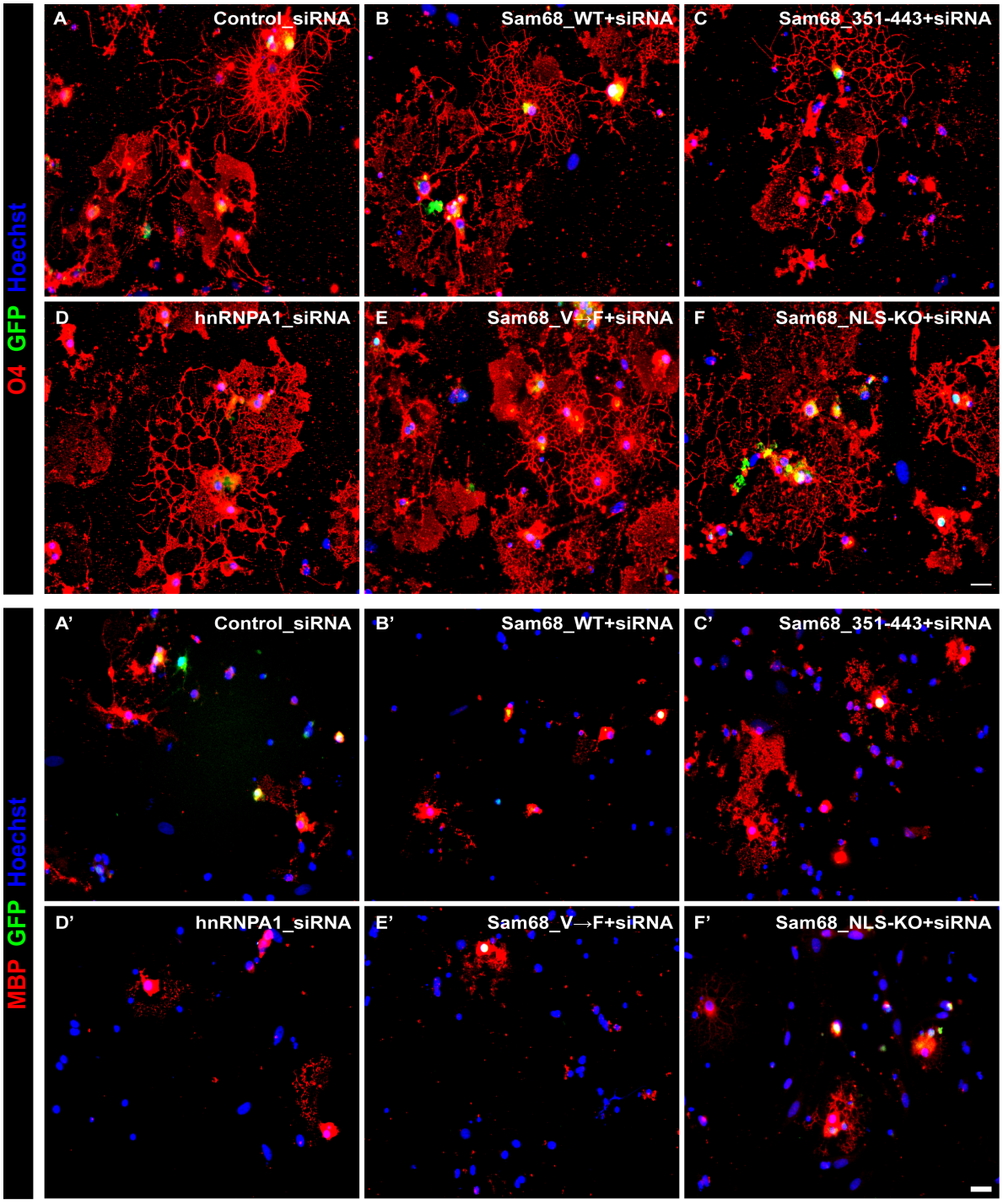
A
Control_siRNA
B
Sam68_WT+siRNA
C
Sam68_351-443+siRNA
D
hnRNPA1_siRNA
E
Sam68_V→F+siRNA
F
Sam68_NLS-KO+siRNA
O4 GFP Hoechst
A'
Control_siRNA
B'
Sam68_WT+siRNA
C'
Sam68_351-443+siRNA
D'
hnRNPA1_siRNA
E'
Sam68_V→F+siRNA
F'
Sam68_NLS-KO+siRNA
MBP GFP Hoechst

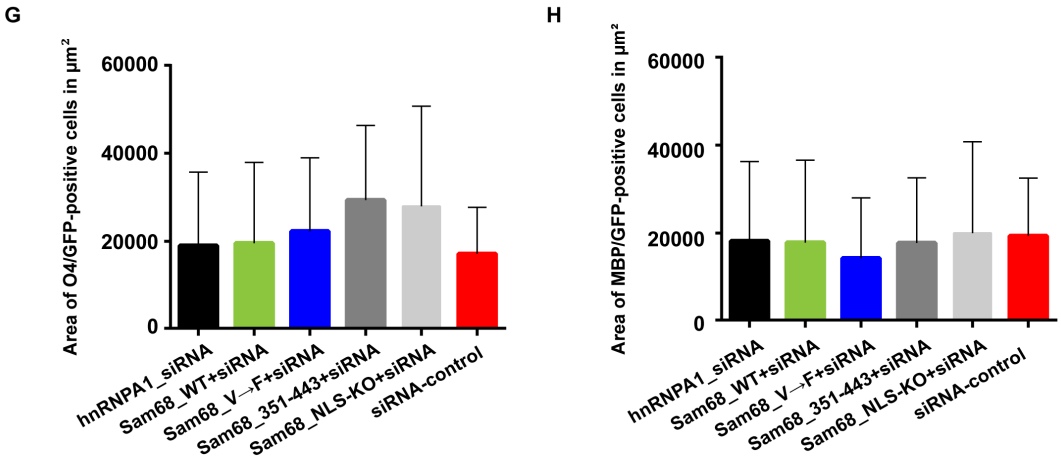
G
Area of O4/GFP-positive cells in µm²
60000
40000
20000
0
hnRNPA1_siRNA
Sam68_WT+siRNA
Sam68_V→F+siRNA
Sam68_351-443+siRNA
Sam68_NLS-KO+siRNA
siRNA-control
H
Area of MBP/GFP-positive cells in µm²
60000
40000
20000
0
hnRNPA1_siRNA
Sam68_WT+siRNA
Sam68_V→F+siRNA
Sam68_351-443+siRNA
Sam68_NLS-KO+siRNA
siRNA-control

Figure 23. hnRNPA1 knockdown in combination with either Sam68_351-443 or Sam68_NLS-KO transfection increases the surface of O4-positive cells

Depicted are immunocytochemical stainings of transfected OPCs obtained from P2-3 rat pups and cultured for 5d. The transfection was performed with non-targeting siRNA serving as control (A and A'), and hnRNPA1_siRNA (D and D'). To investigate a possible interaction of Sam68 and hnRNPA1 double-transfections were performed with the above introduced Sam68 plasmids, and hnRNPA1_siRNA (Figure 4). A morphologic analysis of the cell size revealed an enlargement of O4-positve cells double-transfected with Sam68_351-443 or Sam68_NLS-KO (C, F) and is demonstrated in the bar chart (G). The quantitative analysis of MBP-positive cells revealed no severe differences (H). n=2, Data are expressed as mean ± SD. Scale Bar: 50µm

In order to discover a possible influence on the morphologic maturity, the transfected oligodendrocytes were categorized in four categories according to the complexity of their branches and membrane formation. The procedure was performed as described previously (Figure 20A). This morphologic analysis exposed distinct differences in the amount of category 3 oligodendrocytes, characterising cells with complex branches and partially formed membranes. A six fold lower amount of category 3 oligodendrocytes was noticed when OPCs were double transfected with Sam68_V→F and hnRNPA1_siRNA in comparison to cells only transfected with hnRNPA1_siRNA. In addition, OPCs double transfected with Sam68_V→F and hnRNPA1_siRNA exhibited by far the highest percentage of category 1 oligodendrocytes, characterised by poorly branched processes. No severe differences were noticed when OPCs were double transfected with hnRNPA1_siRNA and each Sam68_WT, Sam68_351-443 or Sam68_NLS-KO (Figure 24 A-B). Most category 4 oligodendrocytes, which are characterised by prominent membrane formation, were recorded in the control situation. A bar chart plotting only the amount of category 4 oligodendrocytes illustrates this observation (Figure 24 B). Surprisingly, the second highest percentage of category 4 oligodendrocytes was detected when cells were double-transfected with Sam68_V→F and hnRNPA1_siRNA, although a 1.5 fold decrease in comparison to the control situation was noticed.

Taken together, the knockdown of hnRNPA1 and the overexpression with the mutant Sam68 forms revealed an influence on the cell size of oligodendrocytes. Next, it appeared necessary to study an effect of hnRNPA1 knockdown on MBP-expression. The overexpression with the mutated Sam68 constructs described in the previous chapter demonstrated their severe influence on MBP-expression. Here, western blot analysis examined, whether these constructs evoke an effect on MBP-expression in combination with a simultaneous hnRNPA1 knockdown.

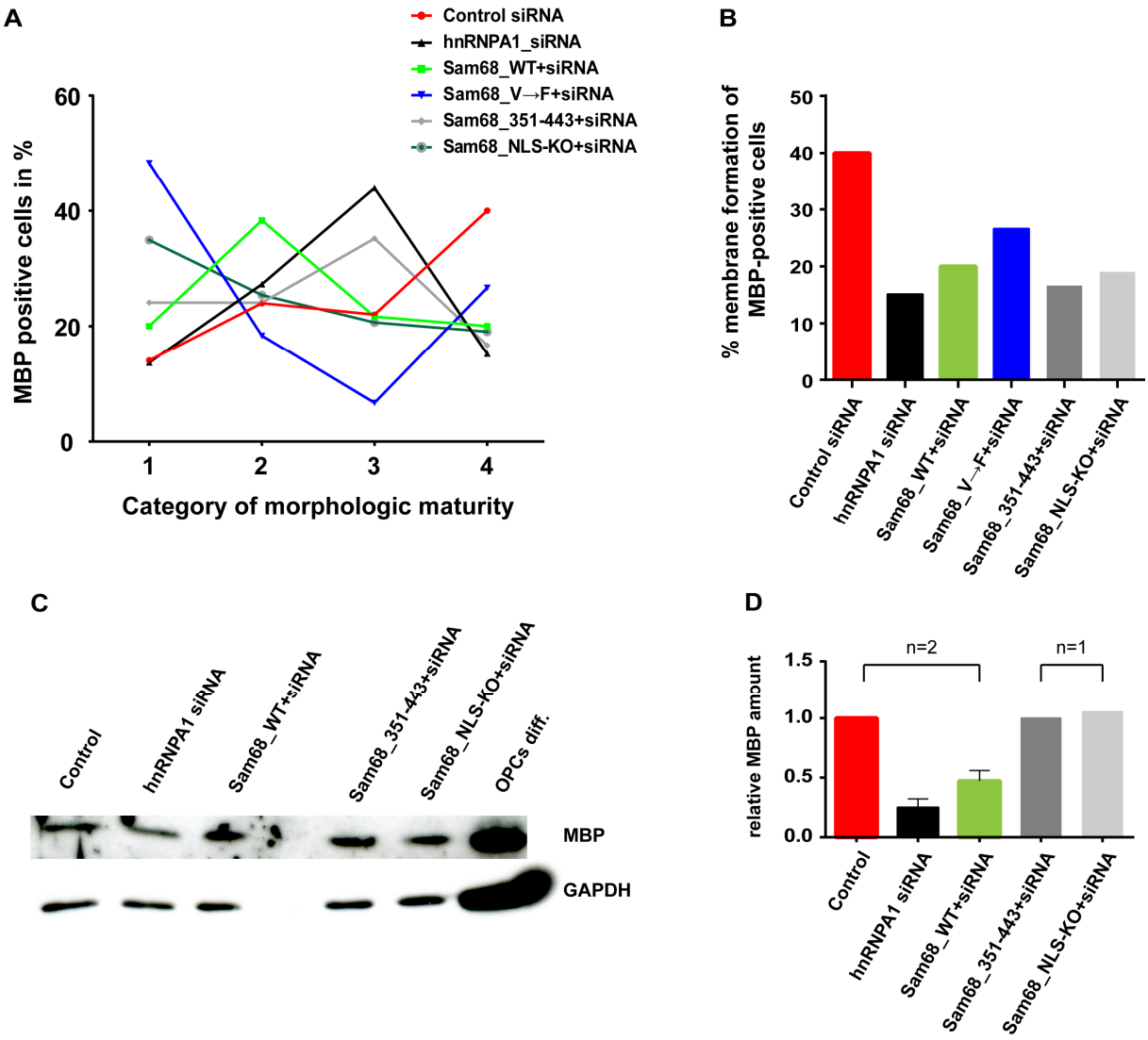

Figure 24. Sam68 and hnRNPA1 regulate myelin sheet formation and MBP expression

This panel illustrates a cell morphologic investigation of the cell maturity (A, B) and western transfer analysis (C, D) of OPCs transfected with the hnRNPA1_siRNA alone or in combination with the denoted Sam68 constructs in comparison to non-targeting si_RNA serving as control.
(A) The graph illustrates the proportion of transfected MBP-positive cells regarding their morphologic maturity (from 1:immature, to 4: mature), carried out as described previously (Figure 20 A). The proportion of only myelin forming oligodendrocytes of category 4 is additionally depicted in a bar chart, clarifying the decrease of membrane formation under all transfected conditions in comparison to the control situation (nontargeting siRNA) (B). n=2
The western transfer analysis (C) and the associated quantitative analysis (D) revealed a decrease of MBP-expression after transfecting the cells with hnRNPA1_siRNA alone and in combination with the Sam68_WT overexpression vector. Oppositely, the hnRNPA1_siRNA double-transfection with Sam68_351-443 or Sam68_NLS-KO showed an increase of relative MBP level in comparison to hnRNPA1_siRNA. These results demonstrate the collective role of Sam68 and hnRNPA1 in the regulation of myelin sheet formation and MBP-expression. The relative density of a protein band within each sample is normalised to the intensity of the associated GAPDH protein band and is expressed in arbitrary units.

For this purpose, the protein lysates of OPCs transfected with hnRNPA1_siRNA and Sam68_WT, Sam68_351-443 or Sam68_NLS-KO, respectively, were analysed via immunoblotting. A distinct decrease of MBP expression in comparison to the control situation was recorded when OPCs were only transfected with hnRNPA1_si-RNA. A similar effect was observed when OPCs were double-transfected with Sam68_WT and hnRNPA1_siRNA. The MBP amount of OPCs double-transfected with hnRNPA1_siRNA and either Sam68_351-443 or Sam68_NLS-KO was comparable to the control situation. So far, the data exhibited that hnRNPA1 knockdown has no severe effect regarding the cell size of oligodendrocytes, but it decreases MBP-expression. Hence, a collective effect of an overexpression with the Sam68 constructs and the hnRNPA1 knockdown was observed on cell growth and MBP-expression, respectively.

Taking in consideration the severe effects of the previously performed transfection experiments with the Sam68 constructs, it seemed reasonable to oppose the earlier obtained data of single transfected OPCs to the here described hnRNPA1_siRNA double transfections. For this purpose, the cell size of double-transfected MBP-positive cells was categorized in 8 steps from 0-10000 μm^2 as described previously. Then, the cell size of single transfected OPCs (Figure 19 G, H) was opposed to OPCs additionally transfected with hnRNPA1_siRNA.

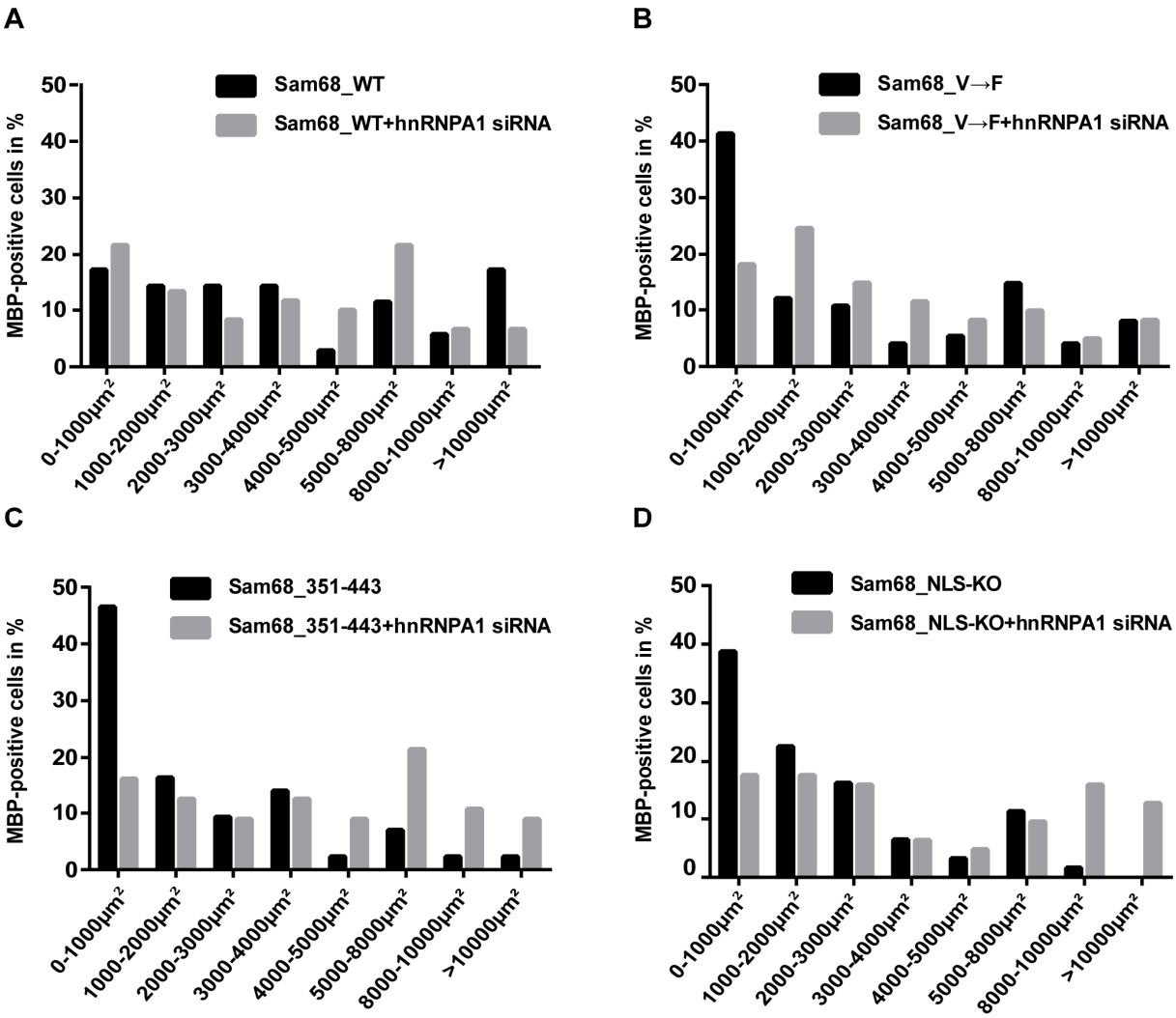

Figure 25. Cell size comparison of MBP-positive OPCs single and double transfected with Sam68 plasmids and hnRNPA1 siRNA.

The depicted graphs compare the earlier described results from OPC transfections with the Sam68 plasmids alone to the hnRNPA1 double-transfection results obtained in this chapter. The cell size is categorized in 8 Steps from 0 to >10000 µm². This juxtaposition points out the severe enlargement of oligodendrocytes double-transfected with hnRNPA1_siRNA and each of the plasmids Sam68_351-443 or Sam68_NLS-KO in comparison to OPCs transfected with Sam68_351-443 (C) and Sam68_NLS-KO (D) alone. The comparison of the size of MBP-positive cells of Sam68_WT and Sam68_V→F single transfected OPCs and double transfection with additional hnRNPA1_siRNA did not reveal distinct differences (A and B).

This juxtaposition showed a severe difference comparing OPCs single transfected with Sam68_351-443 and Sam68_NLS-KO in comparison to double transfections of both constructs with hnRNPA1_siRNA. In both conditions a distinct increase of the cell size was noticed when OPCs were additionally transfected with hnRNPA1_siRNA (Figure 25 C and D). The double transfected OPCs (Sam68_351-443 and hnRNPA1_siRNA) showed a 4-5 fold increase in the percentage of cells larger than 4000 μm^2 compared to OPCs only transfected with Sam68_351-443 (Figure 25 C). Comparing OPCs transfected with the Sam68_NLS-KO plasmid to the combined transfection with hnRNPA1_siRNA exhibited an even more drastic effect. A 7-12 fold increase in the percentage of cells larger than 8000 μm^2 was noticed when cells were double transfected with hnRNPA1_siRNA in comparison to the single transfection condition with Sam68_NLS-KO alone (Figure 25D). The comparison of OPCs transfected with the Sam68_WT overexpression plasmid and double transfected cells (Sam68_WT and hnRNPA1_siRNA) showed a 2.5 fold decrease of cells larger than 10000 μm^2 when hnRNPA1_siRNA was added. The juxtaposition of OPCs transfected with the Sam68_V→F construct and the combined transfection with hnRNPA1_siRNA revealed the most striking differences regarding cells with a surface of 0-1000 μm^2. The single transfection with Sam68_V→F showed a 2.3 fold increase in comparison to double transfected OPCs (Sam68_V→F and hnRNPA1_siRNA).

Taken together, the data clearly demonstrate a role of hnRNPA1 in MBP expression and during OPC differentiation. Although the data must be validated by repeated measurements, they exposed a role of hnRNPA1 and an additional interplay of Sam68 and hnRNPA1 in regulating MBP expression. The functional mechanism of both proteins is contrary, as Sam68 enhances and hnRNPA1 represses MBP expression. The RNA-binding properties and the NLS-region of Sam68 were necessary for this combined regulation shown by the accelerated MBP–level after an overexpression with the mutated Sam68 forms and hnRNPA1_siRNA.

5. Discussion

The results presented in this thesis can be subdivided into three major parts. In the first part I analysed the identity of Sam68 expressing cells *in vitro* and *in vivo*. Here, I could demonstrate that albeit Sam68 is continuously expressed in NSCs as well as in its progeny during lineage progression, more Sam68-positive cells co-express differentiation markers. This indicates that Sam68 is upregulated during differentiation process of NSCs.

The second part describes a successfully established method for the transfection of primary rat OPCs. This new protocol allows for the high efficiency transfection of non-adherent primary rat OPCs and provides big advantages especially with respect to the low-yield and time-consuming isolation of primary rat OPCs.

This method represents the basis for the main part of this work which displays the functional analysis of Sam68 during oligodendrocyte development. Due to the multifunctional character of Sam68 given through several functional domains of this protein, an intensive study revealed a strong influence on oligodendrocyte maturation and identified the responsible domains. The RNA-binding domain and the NLS-sequence were demonstrated to be functional relevant for MBP expression and myelin sheet formation. Furthermore, I identified an interaction between the well-studied splicing regulator hnRNPA1 and Sam68. Sam68 regulates hnRNPA1 expression and both proteins regulate commonly the expression of MBP.

Taken together, I studied the role of Sam68 in NSCs and oligodendrocytes and its functional role during oligodendrocyte maturation. Based on this new knowledge, a molecular model displaying the influence of Sam68 and hnRNPA1 on regulation of oligodendrocyte lineage progression was developed.

5.1. Cellular identity of Sam68 expressing cells

A widespread expression pattern of Sam68 in the embryonic and postnatal brain was recently identified (Bertram, 2013). However, the identity and the fate of cells expressing Sam68 remained elusive. In this thesis, co-labellings with characteristic stem cell markers via immunhistochemistry and time-dependent cell culture experiments following the fate of Sam68 expressing cells closed this missing knowledge.

I demonstrated that Sam68 is expressed by Nestin and Pax6-positive neuroepithelial and radial glial cells. Based upon earlier studies of our group, Sam68 was expected to be expressed by cells with a neurogenic fate (Bertram, 2013). This hypothesis was supported, since Sam68 colocolizes with the early neuron marker βIII-Tubulin not only in the VZ of the cortex but also in the GCL of the eye. Both are regions in which young neurons reside at E13.5 (Sharma and Netland, 2007, Paridaen and Huttner, 2014). Furthermore, Sam68 is expressed by postnatal GFAP-positive astrocytes in the SVZ. Although these immunohistochemical stainings revealed only few double positive cells, it is the first time that an expression of Sam68 by astrocytes was demonstrated. This co-expression was not surprising, due to studies delineating an expression of Sam68 by the astroglial cell line U87 (Li et al., 2002). As mentioned above, Sam68 was suggested to be expressed by precursor cells which are about to leave the cell cycle to differentiate into neurons. In order to support this hypothesis, cell culture experiments with cortical and GE derived cells were performed. Here, the immunocytochemical analysis of the cultivated cells at different culture times allowed to follow the cell fate of Sam68 expressing cells.

The hypothesis of Sam68-positive progenitor cells leaving the cell cycle to differentiate into neurons or astrocyte was confirmed with these experiments. The quantitative analysis of marker positive cell numbers in relation to the total amount of Sam68-positve cells revealed a significant change in the expression pattern. As expected, a clear reduction of Sam68-positive cells co-expressing either Pax6 or Nestin ocurred in cortex derived cells with progressing culture time. In turn, the significant increase of Sam68-positive cells co-labelled either with βIII-Tubulin or GFAP illustrates the shift towards differentiating cells. The local precursor cells in the cortex divide from E9 onward partly asymmetrically and differentiate into neurons at first and later to glia cells. Therefore the observed shift is in harmony with current knowledge. Also in GE derived cells the reduction of Sam68 and Pax6 double-positive cells and, on the other hand, the significant increase in the cell number of Sam68 and βIII-Tubulin

or GFAP double-positive cells after 24h, support the above mentioned hypothesis. The primary role of the GE is the production of several cell types migrating to their final point of destination, either to the bulbus olfactorius or to the cortex (Corbin and Butt, 2011). The major function of the MGE for instance is the production of neurons and glia of the basal ganglia and it generates a subpopulation of cortical neurons, namely the stellate-shaped GABA+ neurons. This population migrates after their appearance in the MGE towards the cerebral cortex (Corbin et al., 2001, Nakajima, 2007). In the LGE, Pax6 is important for the pallial/subpallial boundary formation (Carney et al., 2009, Cocas et al., 2011) and is therefore expressed only by few dorsal cells. Due to the fact, that the whole GE tissue was dissected, the counted Sam68/Pax6-positive cells were presumably from the dorsal part. The relation of Nestin and Sam68 double-positive cells remained similar after 24h. This could be explained by slowly dividing embryonic neural progenitors in the GE, indicating Nestin enhancer and promoter activity, which maintain their undifferentiated state at E13.5 and later become adult NSCs of the subependymal zone (SEZ) (Furutachi et al., 2015). A simple way to confirm this hypothesis is to co-label GE cells isolated from the *Rosa-rtTA;TRE-mCMV-H2B-GFP;Nestin-NLS-mCherry* mice used by the Furutachi lab. With these mice, an activity of the Nestin enhancer and promoter in slowly dividing NSCs can be identified, and an expression of Sam68 in these cells would be easy to discover. Another population of Nestin-positive cells residing in the GE migrating towards the cortex are OPCs (Gallo and Armstrong, 1995). The ventral most-precursors are produced from about E12.5, whereas the production of lateral ganglionic eminence precursor starts two days later (Spassky et al., 1998, Richardson et al., 2006). Thus, considering the early time-point of analysis, an amount of Nestin-positive precursor cells maintaining their undifferentiated state was not surprising.

Taken together, these experiments demonstrate a clear shift of Sam68 expressing cells towards differentiating cells and confirm the hypothesis that Sam68 is expressed by progenitor cells differentiating to their derivative cell types. Despite these findings, there are also strong evidences that Sam68 becomes expressed by a subpopulation of slowly dividing neural progenitors which maintain their undifferentiated state and compose a population of adult NSC of the SEZ, although this hypothesis needs to be verified.

5.2. High efficiency transfection of primary rat OPCs

The transfection of cells, regardless of which type, is a widely used approach to gain information about gene functioning. Allowing for the overexpression or knockdown of genes, selective information about respective gene functioning can be obtained. In particular, primary rat OPCs turned out to be even more sensitive with regard to the transfection process than NSCs. Although the Nucleofector Technology made the transfection of OPCs feasible (Czopka et al., 2010) it was limited by the high amount of $5x10^6$ cells needed for each transfection and a considerable loss of OPCs caused by cell death during the procedure.

The protocol established in this thesis enables for the first time the high efficiency transfection of non-adherent primary rat OPCs. During the intensive and complex establishing process several parameters were tested and improved. The first aim was to find a pulse protocol striking a balance between viability and transfection efficiency. The principal of electroporation is a short electrical pulse leading to DNA intake by the cell. The common opinion about how electroporation works is that the given electric pulse leads to nm-scale water-filled pores in the cell membrane allowing thereupon for the intake of foreign DNA (Neumann et al., 1982, Weaver, 1995, Joshi and Schoenbach, 2000). Due to the intern business secret of Lonza, the composition of the P3-solution and the voltage and duration of the provided pulse protocols were unknown. Therefore, the identification of the optimal pulse protocol resulted from the collaboration with the company. The first provided pulses were affecting the cells too strong leading to cell death. The electrical intensity of those pulses was presumably too high causing oversized waterfilled pores, which could not be recovered by the cells. In general, weak pulses led to high viability but low transfection efficiency, whereas strong pulses led to high transfection efficiency but to a low viability. As a result of a large and complex screening, the pulse protocol CA-138 was demonstrated to enable reproducibly the transfection of non-adherent OPCs with a high viability and an acceptable transfection efficiency of up to 25%. Despite the pulse screen, also various cell culture parameters were improved. For instance, different amounts of cells transfected and plated were tested considering that cell-cell interaction are crucial for the survival of cells. Based upon the knowledge that cell death can be induced by neighbouring cells (Brancolini et al., 1997), an optimal number of cells for the transfection ($2\text{-}5x10^5$cells) and seeding ($4x10^4$ cells/well) was determined. Additionally, it was demonstrated, that the transfected OPCs pass through the characteristic morphological maturation. Since the morphological

maturation of OPCs along the lineage towards mature oligodendrocytes is characterised by the expression of the specific proteins PDGFRα, O4 and MBP (Zhang, 2001) double-immunolabelings against GFP and one of the mentioned markers proved a normal differentiation pattern of transfected OPCs. In combination with the huge advantage that a low cell number of only $2x10^5$ cells is needed for the single electroporation process no further improvements were attempted. This established protocol provided a very good basis for the investigations regarding the main approach of this thesis which was the identification of the role and the function of Sam68 during oligdendrogenesis.

5.3. Role of Sam68 and hnRNPA1 during oligodendrocyte development

Sam68 was already identified as a regulator of oligodendrocyte differentiation by promoting OPC maturation (Czopka et al., 2010). The results presented in this thesis provide completely new insights into the role of Sam68 during oligodendrogenesis. Furthermore, these functions were linked to specific Sam68 domains by transfecting OPCs with several mutated Sam68 constructs. The knockdown of hnRNPA1 revealed a new interaction partner of Sam68 in the regulation of oligodendrocyte maturation and MBP-expression.

I identified for the first time the Sam68 domains involved in the regulation of cell growth and myelin sheet formation. In addition, the earlier mentioned effect of Sam68 on MBP-expression was confirmed in this thesis and connected to its RNA-binding domain and the NLS-sequence. In detail, the overexpression with the Sam68_WT construct enlarged significantly the surface of O4-positive cells in comparison to the control situation. None of the mutations in the specific Sam68 domains hindered the surface enlargement remarkably; in all transfected conditions the O4-positive cells were larger in comparison to the control. This is also true for the length of PDGFRα-positive cells. The overexpression with all constructs led to an elongation of the cells.

The process of oligodendrocyte cell growth is regulated by growth factors. Therefore an interaction or regulatory influence of Sam68 might be possible. The morphological transformation from a bipolar progenitor to a multi branched pre-oligodendrocyte is accompanied with the blockage of the intracellular signalling pathways from the PDGFRα to the nucleus (Hart et al., 1989). At the O4-positive stage, OPCs lose their mitogenic responsiveness to PDGF (Baumann and Pham-Dinh, 2001) and with ongoing morphologic

maturation PDGF receptors disappear (Ellison and de Vellis, 1994). Thus, Sam68 might be involved in the blockage of this signalling cascade, most likely by acting as an adapter protein. Quantifying the distribution of PDGFRα-positive cells did not reveal relevant differences. This result was not surprising, considering that the maturation is not related to the loss of PDGFRα (Hart et al., 1989), but to the blockage of the intracellular signalling cascade. Therefore, the length of PDGRα-positive OPCs was measured, given that with the onset of morphologic maturation bipolar OPCs undergo a transformation and enlarge in their size (Nawaz et al., 2015). In this thesis, the analysed PDGFRα-positive cells already exhibited multiple thin processes and were cultured under differentiating conditions, indicating that they already exit the bipolar migration stadium (Gao et al., 1998). Thus, the measured length of PDGFRα-positive cells was taken as an indicator for maturation. A possible influence of Sam68 on OPC migration could be elucidated with live imaging analysis under proliferative conditions. A promotive, RNA-binding-independent function of Sam68 on migration and polarized movements in OPCs would be expected, due to studies revealing this effect in Sam68-deficient fibroblasts (Huot et al., 2009).

However, an elongation of PDGFRα-positive OPCs was recorded, after the transfection with all mutant Sam68 constructs, respectively. Under the condition of Sam68_V→F, this elongation was even significantly. This mutant form of Sam68 carries a point mutation in the RNA-binding domain at position 229, disturbing its RNA-binding ability (to poly-A motifs) but still homodimerizes with endogenous Sam68 (Pedrotti et al., 2010). Claudio Settes lab demonstrated that Sam68_V→F was partially defective in binding *Bcl-x* mRNA and furthermore it affected *Bcl-x* alternative splicing. Moreover, this mutant form is localized to discrete nuclear foci, which are different from the regions where splicing factors like SC35 and ASF/SF2 accumulate. This localisation is similar to that observed, when Sam68_WT was co-expressed with Fyn-kinase (Paronetto et al., 2007). Thus, the overexpression with this mutant form has a dominant negative effect on Sam68 function and allows elucidating if the binding and alternative splicing of putative mRNA binding partners of Sam68 and its location within the nucleus is necessary for its function in oligodendrocyte development. A comparable elongation of PDGFRα-cells, although not significant, was also recorded with the mutant form Sam68_G→E. It carries as well a mutation in the RNA-binding domain, abolishing its binding to UAAA motifs. In contrast to Sam68_V→F, this mutant form exhibited after overexpression a diffuse localisation in the nucleus of P19 cells, similar to that of wild-type Sam68 (Chawla et al., 2009).

In regard to the elongation of PDGFRα-positive cells, the effects of Sam68_V→F and Sam68_G→E overexpression can be neglected due to the fact that all of the mutant Sam68 forms caused an elongation of PDGFRα-positive cells indicating that neither the defective RNA-binding domain, nor the mutated nuclear localisation signal seem to disturb the function of the still endogenously expressed Sam68. This provides strong evidence for a function of Sam68 as an adapter molecule in cell growth and in PDGFRα signalling. PDGF receptors are tyrosine kinases which phosphorylate both themselves and other target proteins (Schlessinger, 2000). Sam68 contains several tyrosine residues in the C-terminus, which are potential sites of phosphorylation (Wong et al., 1992) and it was demonstrated to be tyrosine-phosphorylated by numerous cell surface receptors (Lukong and Richard, 2003). This tyrosine phosphorylation decreases the RNA-binding ability of Sam68 and enhances its interaction with signalling proteins (Wang et al., 1995, Chen et al., 1997), supporting the hypothesis of its function as an adapter molecule. Hence, a phosphorylation by PDGFRα appears to be possible. The tyrosine phosphorylation of Sam68 enables the association with several SH2 domain proteins including src family kinases and PLC-γ1 (Richard et al., 1995), both known to bind to the phosphorylated PDGFRα-receptor (Ralston and Bishop, 1985, Coughlin et al., 1989). The binding of Sam68, either directly to the PDGFRα, or indirectly as an adapter protein may interrupt this signalling cascade. The binding of Sam68 with SH3 domains for instance negatively regulates its RNA-binding ability (Najib et al., 2005), providing a possible interaction mechanism by interrupting the alternative splicing of mRNAs necessary for the PDGF-signalling cascade.

Imaginable is a signalling cascade already identified for Sam68 and the insulin receptor (IR), which is also a receptor tyrosine kinase. The activation of the IR stimulates Sam68 phosphorylation and promotes its association with p85-PI3K. IGF-I (Insulin like growth factor I) is a crucial growth factor which was shown to increase proliferation, inhibit apoptosis, and promote differentiation of oligodendrocytes (McMorris and Dubois-Dalcq, 1988, Freude et al., 2008). Transgenic mice overexpressing IGFBP-1 exhibit a reduction of myelinated axons and a decreased myelin sheath thickness (Carson et al., 1993, Ye et al., 2002). An interaction of Sam68 and IRS1 (Insulin receptor substrate 1) was already demonstrated in rat adipocytes, CHO- and hepatoma cells. The activation of the IR stimulates tyrosine-phosphorylation of Sam68 and its relocation from the nucleus to different insulin signalling complexes in the cytoplasm, such as Grb2-SOS (Najib and Sanchez-Margalet, 2002), Ras-GAP (Guitard et al., 1998) and IRS1/PI3K (Sanchez-Margalet and Najib, 1999). Furthermore, in CHO cells, an overexpression of IR leads to an increased Sam68

expression and relocated Sam68 to the cytoplasm (Sanchez-Margalet and Najib, 2001). The interaction of IRS-1 and Sam68 was mapped to proline-rich regions in the N-and C-terminus (Quintana-Portillo et al., 2012). The truncated form of Sam68 (Sam68_351-443) lacks the N-terminal proline rich sequence. Nonetheless, the cell growth of PDGFRα- or O4-positve cells was not impaired, indicating that the N-terminus is not required for the role of Sam68 in cell growth. The fact that none of the mutated Sam68 forms caused an impaired cell growth strongly suggests that the C-terminal proline rich sequence (P3, P4 and P5) is important for the role of Sam68 in cell growth. Moreover, these results support the hypothesis that Sam68 functions as an adapter protein in cell growth. P3 and P4 interact with the SH3-domain of PLC-γ-1 and with p85 PI3K (Lukong and Richard, 2003), suggesting a possible interaction mechanism of Sam68 and IR in oligodendrocyte cell growth. Thus, an interaction of Sam68 and IGF-1 was already demonstrated, as well as a role of IGF-1 in oligodendrocyte development. But so far, a common interaction of IGF-1 and Sam68 in oligodendrocytes was not shown, although it seems probable and might be the most likely mechanism for Sam68 regulation on oligodendrocyte cell growth. Due to the fact, that IGF-1 is a crucial factor in chemically defined media and that its depletion causes oligodendrocyte cell death (Barres et al., 1992), made an ease testing of IGF-1 and Sam68 interaction by simple IGF-1 depletion impossible.

Sam68 executes multiple functions within the cell, thus besides the regulation of growth factor pathways, one can also speculate about a regulation of the cytoskeletal redistribution during oligodendrocyte cell growth. A direct connection between Sam68 and the cytoskeletal component β-actin was already demonstrated in dendritic spine formation. Sam68-KO mice have reduced levels of β-actin mRNA associated with synaptic polysomes and decreased levels of synaptic β-actin protein. This indicates that Sam68 promotes the translation of *actb* mRNA at synapses (Klein et al., 2013). In oligodendrocytes, the redistribution of F-actin is the driving force in myelin wrapping (Nawaz et al., 2015). A similar regulatory influence during oligodendrocyte growth is possible and could explain the increased cell size of O4-positive oligodendrocytes when cells are transfected with Sam68_WT and Sam68_V→F.

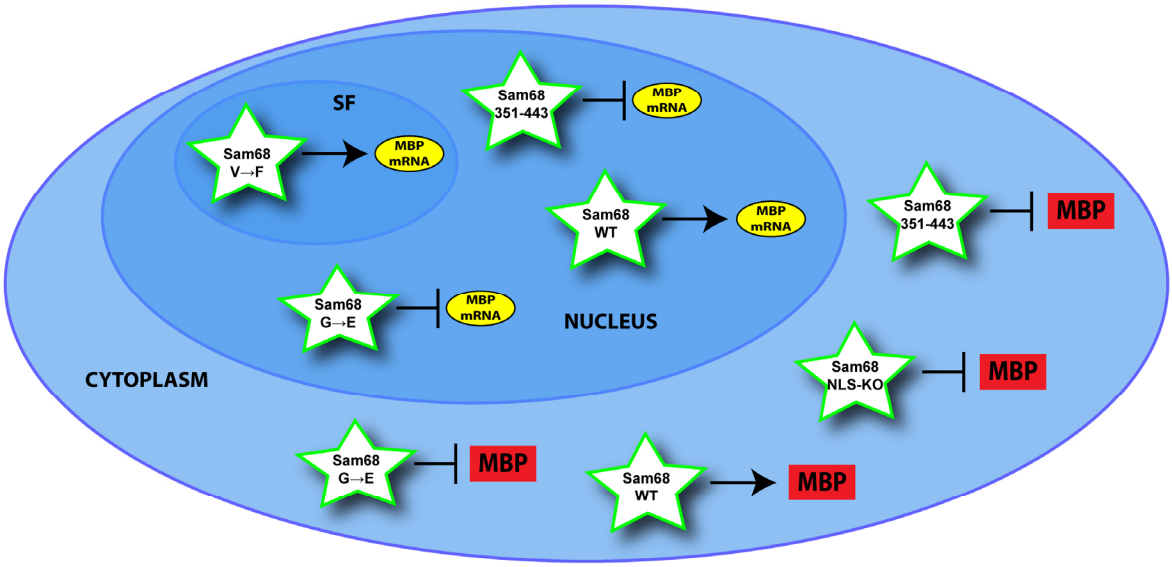

Figure 26. Influence of Sam68 constructs on MBP-expression.

The scheme pictures an oligodendrocyte and summarizes the effects of the overexpression of different Sam68 variants (green stars) on *MBP* mRNA splicing (yellow circle) and MBP-expression (red boxes). Inhibitory cues are illustrated with bars, whereas arrows delineate promotive functions. The specific mutations cause different localisations of the mutated Sam68 forms within the cell. Sam68_WT, Sam68_G→E and Sam68_351-443 are located diffuse in the nucleoplasm, whereas Sam68_V→F was reported to accumulate in discrete subnuclear foci (SF). Due to its mutated NLS-sequence, Sam68_NLS-KO is located in the cytoplasm, unable to enter the nucleus. Note that the overexpression with Sam68_WT and Sam68_V→F resulted in an increased MBP-expression. In contrast, the forced expression of Sam68_G→E, Sam68_351-443 and Sam68_NLS-KO decreased the MBP-level.

Despite the severe effects in cell growth, Sam68 has an influential role in oligodendrocyte differentiation accompanied with the regulation of MBP-expression. Our group already demonstrated that Sam68 is expressed within all stages of oligodendrocyte development and total Sam68 levels increase with ongoing oligodendrocyte differentiation. With respect to MBP-expression, Tim Czopka proposed a possible mechanism for the regulation by Sam68. In this model, Tnc binds to Cntn1 within lipid rafts of oligodendrocyte membrane. The resulting complex increases the phosphorylation of the regulatory tyrosine 531 of Fyn causing reduced Fyn activity and impairs the phosphorylation of Akt. Tnc, impaired Fyn and/or Akt activation results in inhibited Sam68 expression. In addition, a direct promotion of MBP-expression by Sam68 was demonstrated (Czopka et al., 2010). The effect on MBP-expression was confirmed in this thesis and furthermore the UAAA-binding motif within the RNA-binding domain and the localisation within the nucleus appear to be crucial for this effect. This revealed the comparison of the overexpression with the two Sam68 forms mutated in the RNA-binding domain. The overexpression with the Sam68_V→F mutant

increased the MBP-level significantly compared to Sam68_G→E. Moreover, an increased mRNA-level detected by RT-PCR analysis after Sam68_G→E overexpression provides evidence for a disruption of the *MBP*-mRNA translation. In contrast, the overexpression with Sam68_V→F caused an increased MBP-expression and a decrease of the mRNA–level, indicating a forced *MBP*-mRNA translation. A reduced MBP-level in presence of the truncated Sam68_351-443, lacking the RNA-binding domain, supports once more the importance of the RNA-binding during this process. Furthermore, the reduced MBP-level after overexpression with the mutant NLS-sequence form (Sam68_NLS-KO) indicates the importance of the transport and/or localisation of Sam68 during MBP-expression. My studies provide strong evidence for a role of Sam68 in splicing and transport of *MBP*-mRNA. Moreover, the reduced MBP-level after overexpression with the Sam68_NLS-KO mutant form suggests an additional cytoplasmic function in the translation process of *MBP*-mRNA. The transport of possible co-factors important for the splicing of MBP in the nucleus might be affected through the dominant negative effect resulting from the Sam68_NLS-KO overexpression.

The promotive effect of Sam68_V→F on MBP-expression is also reflected in the maturation behaviour of oligodendrocytes. Most myelin sheet forming cells were recorded in this condition. This supports once more, that for the splicing and translation of the MBP-isoform recognized by the here used antibody, the UAAA-motif within the RNA-binding domain is necessary. The overexpression with Sam68_G→E reduced drastically myelin sheet formation. Moreover, in the presence of overexpressed Sam68_NLS-KO, myelin sheets were absent, which reflects once more the negative effect of both mutant forms on MBP-expression.

Figure 26 summarizes the effects of the Sam68 constructs on MBP-expression. These results provide evidence for a role of Sam68 in the translational regulation of MBP, which is in line with previous findings of Tim Czopka demonstrating a binding of *MBP* mRNA by Sam68. Several *MBP* mRNAs originate from a single gene by alternative splicing of the primary transcript (de Ferra et al., 1985, Boggs, 2006). The antibody used in this thesis recognizes several MBP-isoforms, which were indeed detected after the transfection of OPCs with the Sam68 constructs. The 33 kDa isoform was chosen for further analysis and the determination of MBP-level, due to a prominent signal in the western blot analysis. Despite the knowledge about its existence (Ulmer and Braun, 1986) its role in OL and myelin formation remains elusive. My data also suggest a role for Sam68 in *MBP* splicing similar to the mechanism by

which Quaking I regulates *MAG* mRNA splicing. The cytoplasmic isoform QKI-6 regulates the alternative splicing of *MAG* mRNA in CNS myelination through the translational suppression of the well-known splicing inhibitor hnRNPA1. Thus, I investigated a possible role of hnRNPA1 in MBP-expression and furthermore, a possible interaction of Sam68 and hnRNPA1. Indeed, also Sam68 seems to suppress directly or indirectly the expression of hnRNPA1. The knockdown of hnRNPA1 by siRNA was enhanced through the additional transfection with the Sam68_WT construct. Further PCR-analysis would be needed to test the effect on hnRNPA1 mRNA level, and in addition sucrose gradient fractionation could assess the translation efficiency of endogenous hnRNPA1 mRNAs after Sam68 overexpression by determining their ability to carry translating polyribosomes. hnRNPA1 often binds exon splicing silencers near the target exon hindering the access of the splicing machinery (Kashima et al., 2007), thus an inhibitory effect on MBP-expression was expected. My studies revealed a role of hnRNPA1 in MBP-expression, but other than expected, its function seems to be supportive. The knockdown of hnRNPA1 caused a severe reduction of the MBP-protein level in comparison to the control. This effect was slightly rescued by the additional overexpression of Sam68_WT, indicating an interplay of both proteins in the regulation of MBP-expression. A complete rescue of the MBP-level was obtained with the overexpression of the mutated Sam68 forms, Sam68_NLS-KO, lacking the NLS-sequence and the truncated form (Sam68_351-443). This truncated form lacks the RNA-binding and the homodimerization domain and was furthermore demonstrated to interfere with the association of hnRNPA1 and Sam68 (Pedrotti et al., 2010). Thus, since it still contains the hnRNPA1 binding domain, it presumably binds hnRNPA1, hindering a binding to endogenous Sam68. This dominant negative effect would also explain the rescue of the MBP-level after Sam68_NLS-KO overexpression and furthermore indicates that the binding of hnRNPA1 occurs in the cytoplasm due to the mutated NLS-sequence. These results strongly support the hypothesis of an interaction between both proteins in regulating MBP-expression. Most likely, Sam68 negatively regulates the alternative splicing and/or the shuttling of *hnRNPA1* mRNA from the nucleus to the cytoplasm. Moreover a complex of hnRNPA1 and Sam68 seem to negatively regulate MBP-expression.These experiments need to be repeated and supported by further studies. Nevertheless, based on the current data, the presented mechanism (Figure 27) from splicing to *MBP* mRNA translation is quite possible. After the alternative splicing of the primary transcript, the mRNAs of the different MBP-isoforms are transported to several compartments of the cell. The 14 and 18.5 kDa isoforms are located at the plasma membrane, whereas the exon-II-containing isoforms 17 and 21.5

kDa are distributed diffusely in the cytoplasm and in the nucleus (Pedraza et al., 1997). *MBP* mRNA is known to be transported into the branches of oligodendrocytes (Trapp et al., 1987, Ainger et al., 1993). The regulatory mechanisms behind the spatial control of MBP translation within the branches are rarely understood. Within the 3'UTR of the MBP mRNA novel regions were identified being responsible for the regulation of its translation. It was shown that the mRNA-binding proteins hnRNP-A2, hnRNP-K and hnRNP-E1 possess distinct functions in regulating localized MBP protein synthesis (Torvund-Jensen et al., 2014). hnRNPA1 and Sam68 are well-known regulators of mRNA transport and translation (Lukong and Richard, 2003, Jean-Philippe et al., 2013). Thus, they may also play a role in the transport mechanism of *MBP* mRNA into the nucleus and/or directly to the branches for a local translation in polysomes.

Taken together, Sam68 promotes cell growth of PDGFRα-and O4-positive cells, most likely by acting as an adapter molecule. Its function in mature oligodendrocytes was demonstrated to be different. Sam68 promotes the expression of MBP and myelin sheet formation. The NLS-sequence and the RNA-binding domain were identified to be crucial for this function. In addition, hnRNPA1 was identified as a factor regulating together with Sam68 the expression of MBP. Sam68 suppresses the expression of hnRNPA1. This suppression seems to be dependent on the NLS-sequence and the RNA-binding domain of Sam68. This provides evidence for an impaired splicing ability of hnRNPA1 pre-mRNA, regulated by Sam68. Thus, Sam68 negatively regulates hnRNPA1 expression, and furthermore hnRNPA1 appears to be an important co-factor in regulating MBP-expression. The alternative splicing of Bcl-x is modulated by Sam68 and hnRNPA1 in which both proteins form a complex (Paronetto et al., 2007). A similar mechanism might regulate the alternative splicing of MBP. Both proteins, Sam68 and hnRNPA1 are very multifunctional and display lots of regulative roles within the cell. Thus, it remains open, how exactly Sam68 and hnRNPA1 regulate *MBP* mRNA metabolism, although this thesis provides a completely new possible interaction mechanism.

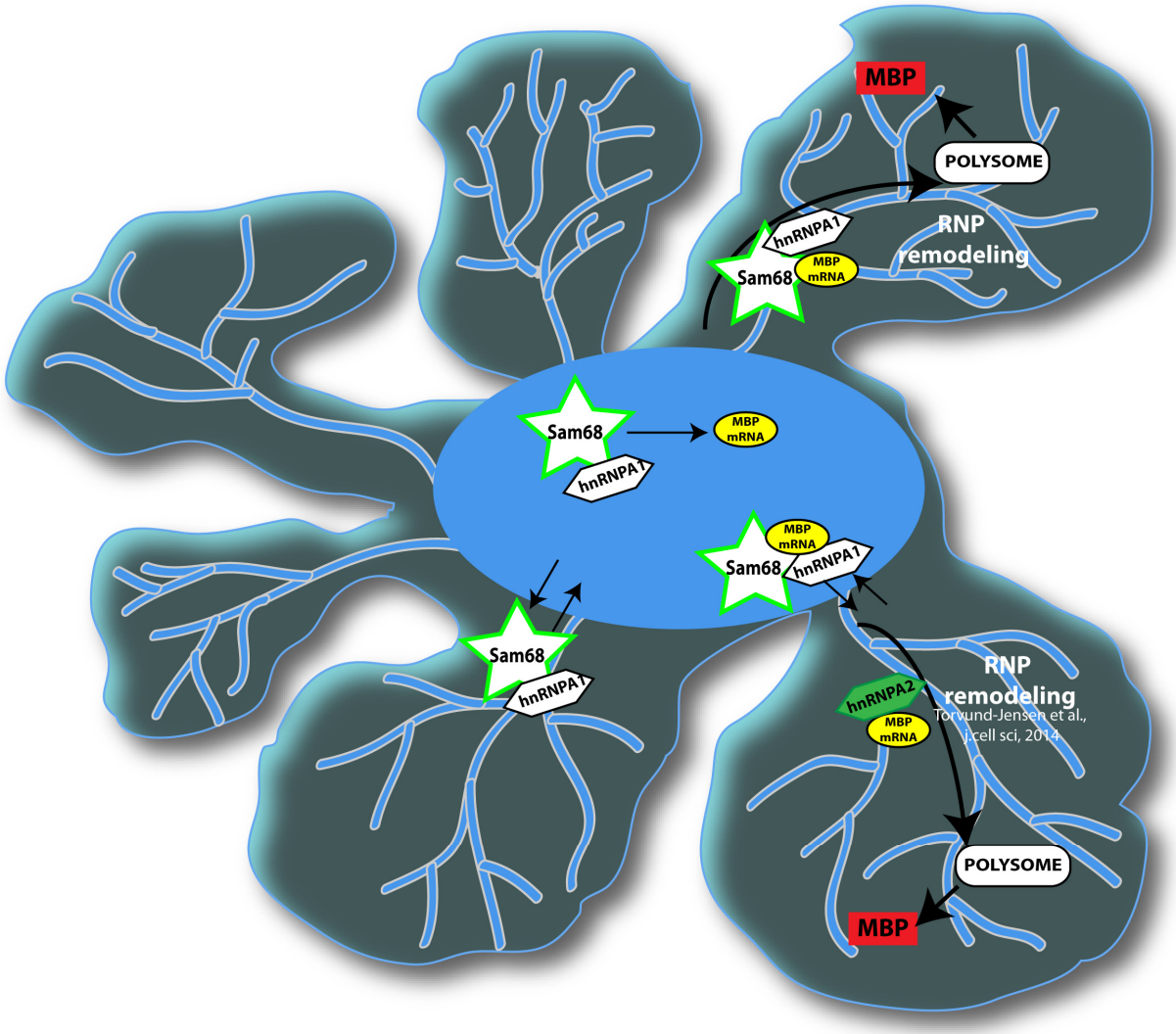

Figure 27. Proposed model for the regulation of MBP-expression through Sam68 and hnRNPA1.

Depicted is a schematic drawing of a mature oligodendrocyte, illustrating a possible interaction of Sam68 and hnRNPA1 in controlling the expression of MBP. Sam68 and hnRNPA1 may regulate the alternative splicing of MBP pre-mRNA and initiate its transport through the nuclear pore. Either the MBP-mRNA is released for the hnRNPA2 regulated transport to the branches or a further role in the mechanisms of transport/or translation of MBP-transcripts is imaginable. Several mechanisms are also possible regarding the regulation of hnRNPA1 expression through Sam68. Likely is the regulation of the transport of hnRNPA1 through the nuclear pore and/or the alternative splicing.

In conclusion, the experiments presented in this thesis exhibit completely new insights into the role of Sam68 during CNS and particularly oligodendrocyte development and contribute well to already existing knowledge. Nonetheless, further studies for instance with the Sam68-KO mouse could help to elucidate remaining issues. In utero electroporation or simple cell transfection experiments for instance could demonstrate the importance of the

single domains of Sam68 after overexpression of the denoted Sam68 constructs without the endogenously expressed Sam68. With regard to oligodendrocyte development, further studies with the Sam68-KO mouse would be needed to confirm the interplay between Sam68 and hnRNPA1. This interaction is of special interest with respect to the inflammatory autoimmune disease multiple sclerosis. Oligodendrocytes are affected by this disease leading to a demyelination of axons (Macchi et al., 2015), but so far, the mechanisms causing this malfunction are poorly understood. Some studies provided already evidence for a role of hnRNPA1 in this disease by identifying antibodies against it in cerebrospinal fluid of MS patients (Bekenstein and Soreq, 2013). Hence, the understanding of the complex mechanism between Sam68 and hnRNPA1 will also help to increase the knowledge about this disease.

6. References

Bertram, 2013:

http://www-brs.ub.ruhr-uni-bochum.de/netahtml/HSS/Diss/BertramBettinaEmily/

Czopka, 2010:

http://www-brs.ub.ruhr-uni-bochum.de/netahtml/HSS/Diss/CzopkaTim/

Aggarwal S, Snaidero N, Pahler G, Frey S, Sanchez P, Zweckstetter M, Janshoff A, Schneider A, Weil MT, Schaap IA, Gorlich D, Simons M (2013) Myelin membrane assembly is driven by a phase transition of myelin basic proteins into a cohesive protein meshwork. PLoS biology 11:e1001577.

Ainger K, Avossa D, Diana AS, Barry C, Barbarese E, Carson JH (1997) Transport and localization elements in myelin basic protein mRNA. The Journal of cell biology 138:1077-1087.

Ainger K, Avossa D, Morgan F, Hill SJ, Barry C, Barbarese E, Carson JH (1993) Transport and localization of exogenous myelin basic protein mRNA microinjected into oligodendrocytes. The Journal of cell biology 123:431-441.

Allemand E, Guil S, Myers M, Moscat J, Caceres JF, Krainer AR (2005) Regulation of heterogenous nuclear ribonucleoprotein A1 transport by phosphorylation in cells stressed by osmotic shock. Proceedings of the National Academy of Sciences of the United States of America 102:3605-3610.

Bakhti M, Snaidero N, Schneider D, Aggarwal S, Mobius W, Janshoff A, Eckhardt M, Nave KA, Simons M (2013) Loss of electrostatic cell-surface repulsion mediates myelin membrane adhesion and compaction in the central nervous system. Proceedings of the National Academy of Sciences of the United States of America 110:3143-3148.

Balazs R, Brooksbank BW, Davison AN, Richter D, Wilson DA (1969) The effect of thyroid deficiency on myelination in the rat brain. J Physiol 201:28P-29P.

Barbarese E, Pfeiffer SE (1981) Developmental regulation of myelin basic protein in dispersed cultures. Proceedings of the National Academy of Sciences of the United States of America 78:1953-1957.

Barlat I, Maurier F, Duchesne M, Guitard E, Tocque B, Schweighoffer F (1997) A role for Sam68 in cell cycle progression antagonized by a spliced variant within the KH domain. The Journal of biological chemistry 272:3129-3132.

Baron W, Colognato H, ffrench-Constant C (2005) Integrin-growth factor interactions as regulators of oligodendroglial development and function. Glia 49:467-479.

Baron W, Hoekstra D (2010) On the biogenesis of myelin membranes: sorting, trafficking and cell polarity. FEBS Lett 584:1760-1770.

Barres BA, Hart IK, Coles HS, Burne JF, Voyvodic JT, Richardson WD, Raff MC (1992) Cell death in the oligodendrocyte lineage. J Neurobiol 23:1221-1230.

Barres BA, Lazar MA, Raff MC (1994) A novel role for thyroid hormone, glucocorticoids and

retinoic acid in timing oligodendrocyte development. Development 120:1097-1108.
Barros CS, Nguyen T, Spencer KS, Nishiyama A, Colognato H, Muller U (2009) Beta1 integrins are required for normal CNS myelination and promote AKT-dependent myelin outgrowth. Development 136:2717-2724.
Bartsch S, Bartsch U, Dorries U, Faissner A, Weller A, Ekblom P, Schachner M (1992) Expression of tenascin in the developing and adult cerebellar cortex. The Journal of neuroscience : the official journal of the Society for Neuroscience 12:736-749.
Baumann N, Pham-Dinh D (2001) Biology of oligodendrocyte and myelin in the mammalian central nervous system. Physiol Rev 81:871-927.
Bedford MT, Chan DC, Leder P (1997) FBP WW domains and the Abl SH3 domain bind to a specific class of proline-rich ligands. The EMBO journal 16:2376-2383.
Bekenstein U, Soreq H (2013) Heterogeneous nuclear ribonucleoprotein A1 in health and neurodegenerative disease: from structural insights to post-transcriptional regulatory roles. Molecular and cellular neurosciences 56:436-446.
Benninger Y, Colognato H, Thurnherr T, Franklin RJ, Leone DP, Atanasoski S, Nave KA, Ffrench-Constant C, Suter U, Relvas JB (2006) Beta1-integrin signaling mediates premyelinating oligodendrocyte survival but is not required for CNS myelination and remyelination. The Journal of neuroscience : the official journal of the Society for Neuroscience 26:7665-7673.
Bergles DE, Roberts JD, Somogyi P, Jahr CE (2000) Glutamatergic synapses on oligodendrocyte precursor cells in the hippocampus. Nature 405:187-191.
Berson A, Barbash S, Shaltiel G, Goll Y, Hanin G, Greenberg DS, Ketzef M, Becker AJ, Friedman A, Soreq H (2012) Cholinergic-associated loss of hnRNP-A/B in Alzheimer's disease impairs cortical splicing and cognitive function in mice. EMBO Mol Med 4:730-742.
Bertram B, Wiese S, von Holst A (2012) High-efficiency transfection and survival rates of embryonic and adult mouse neural stem cells achieved by electroporation. J Neurosci Methods 209:420-427.
Boggs JM (2006) Myelin basic protein: a multifunctional protein. Cell Mol Life Sci 63:1945-1961.
Bogler O, Wren D, Barnett SC, Land H, Noble M (1990) Cooperation between two growth factors promotes extended self-renewal and inhibits differentiation of oligodendrocyte-type-2 astrocyte (O-2A) progenitor cells. Proceedings of the National Academy of Sciences of the United States of America 87:6368-6372.
Brancolini C, Lazarevic D, Rodriguez J, Schneider C (1997) Dismantling cell-cell contacts during apoptosis is coupled to a caspase-dependent proteolytic cleavage of beta-catenin. The Journal of cell biology 139:759-771.
Bunge RP (1968) Glial cells and the central myelin sheath. Physiol Rev 48:197-251.
Burd CG, Dreyfuss G (1994) Conserved structures and diversity of functions of RNA-binding proteins. Science 265:615-621.
Butt AM, Hamilton N, Hubbard P, Pugh M, Ibrahim M (2005) Synantocytes: the fifth element. J Anat 207:695-706.
Bystron I, Blakemore C, Rakic P (2008) Development of the human cerebral cortex: Boulder Committee revisited. Nature reviews Neuroscience 9:110-122.
Camara J, Wang Z, Nunes-Fonseca C, Friedman HC, Grove M, Sherman DL, Komiyama NH, Grant SG, Brophy PJ, Peterson A, ffrench-Constant C (2009) Integrin-mediated axoglial interactions initiate myelination in the central nervous system. The Journal of cell biology 185:699-712.
Campagnoni AT, Pribyl TM, Campagnoni CW, Kampf K, Amur-Umarjee S, Landry CF, Handley VW, Newman SL, Garbay B, Kitamura K (1993) Structure and developmental regulation of Golli-mbp, a 105-kilobase gene that encompasses the

myelin basic protein gene and is expressed in cells in the oligodendrocyte lineage in the brain. The Journal of biological chemistry 268:4930-4938.

Campillos M, Lamas JR, Garcia MA, Bullido MJ, Valdivieso F, Vazquez J (2003) Specific interaction of heterogeneous nuclear ribonucleoprotein A1 with the -219T allelic form modulates APOE promoter activity. Nucleic Acids Res 31:3063-3070.

Canoll PD, Petanceska S, Schlessinger J, Musacchio JM (1996) Three forms of RPTP-beta are differentially expressed during gliogenesis in the developing rat brain and during glial cell differentiation in culture. Journal of neuroscience research 44:199-215.

Carney RS, Cocas LA, Hirata T, Mansfield K, Corbin JG (2009) Differential regulation of telencephalic pallial-subpallial boundary patterning by Pax6 and Gsh2. Cereb Cortex 19:745-759.

Carson MJ, Behringer RR, Brinster RL, McMorris FA (1993) Insulin-like growth factor I increases brain growth and central nervous system myelination in transgenic mice. Neuron 10:729-740.

Cartegni L, Maconi M, Morandi E, Cobianchi F, Riva S, Biamonti G (1996) hnRNP A1 selectively interacts through its Gly-rich domain with different RNA-binding proteins. J Mol Biol 259:337-348.

Chawla G, Lin CH, Han A, Shiue L, Ares M, Jr., Black DL (2009) Sam68 regulates a set of alternatively spliced exons during neurogenesis. Molecular and cellular biology 29:201-213.

Chen H, Hewison M, Hu B, Adams JS (2003) Heterogeneous nuclear ribonucleoprotein (hnRNP) binding to hormone response elements: a cause of vitamin D resistance. Proceedings of the National Academy of Sciences of the United States of America 100:6109-6114.

Chen T, Damaj BB, Herrera C, Lasko P, Richard S (1997) Self-association of the single-KH-domain family members Sam68, GRP33, GLD-1, and Qk1: role of the KH domain. Molecular and cellular biology 17:5707-5718.

Chen YJ, Zhang JX, Shen L, Qi Q, Cheng XX, Zhong ZR, Jiang ZQ, Wang R, Lu HZ, Hu JG (2015) Schwann cells induce Proliferation and Migration of Oligodendrocyte Precursor Cells Through Secretion of PDGF-AA and FGF-2. J Mol Neurosci.

Cocas LA, Georgala PA, Mangin JM, Clegg JM, Kessaris N, Haydar TF, Gallo V, Price DJ, Corbin JG (2011) Pax6 is required at the telencephalic pallial-subpallial boundary for the generation of neuronal diversity in the postnatal limbic system. The Journal of neuroscience : the official journal of the Society for Neuroscience 31:5313-5324.

Colman DR, Kreibich G, Sabatini DD (1983) Biosynthesis of myelin-specific proteins. Methods in enzymology 96:378-385.

Colognato H, Baron W, Avellana-Adalid V, Relvas JB, Baron-Van Evercooren A, Georges-Labouesse E, ffrench-Constant C (2002) CNS integrins switch growth factor signalling to promote target-dependent survival. Nat Cell Biol 4:833-841.

Corbin JG, Butt SJ (2011) Developmental mechanisms for the generation of telencephalic interneurons. Dev Neurobiol 71:710-732.

Corbin JG, Nery S, Fishell G (2001) Telencephalic cells take a tangent: non-radial migration in the mammalian forebrain. Nat Neurosci 4 Suppl:1177-1182.

Cote J, Boisvert FM, Boulanger MC, Bedford MT, Richard S (2003) Sam68 RNA binding protein is an in vivo substrate for protein arginine N-methyltransferase 1. Mol Biol Cell 14:274-287.

Coughlin SR, Escobedo JA, Williams LT (1989) Role of phosphatidylinositol kinase in PDGF receptor signal transduction. Science 243:1191-1194.

Courtneidge SA, Fumagalli S (1994) A mitotic function for Src? Trends Cell Biol 4:345-347.

Czopka T, Ffrench-Constant C, Lyons DA (2013) Individual oligodendrocytes have only a few hours in which to generate new myelin sheaths in vivo. Dev Cell 25:599-609.

Czopka T, Lyons DA (2011) Dissecting mechanisms of myelinated axon formation using zebrafish. Methods Cell Biol 105:25-62.

Czopka T, von Holst A, ffrench-Constant C, Faissner A (2010) Regulatory mechanisms that mediate tenascin C-dependent inhibition of oligodendrocyte precursor differentiation. The Journal of neuroscience : the official journal of the Society for Neuroscience 30:12310-12322.

Czopka T, Von Holst A, Schmidt G, Ffrench-Constant C, Faissner A (2009) Tenascin C and tenascin R similarly prevent the formation of myelin membranes in a RhoA-dependent manner, but antagonistically regulate the expression of myelin basic protein via a separate pathway. Glia 57:1790-1801.

de Ferra F, Engh H, Hudson L, Kamholz J, Puckett C, Molineaux S, Lazzarini RA (1985) Alternative splicing accounts for the four forms of myelin basic protein. Cell 43:721-727.

Derry JJ, Richard S, Valderrama Carvajal H, Ye X, Vasioukhin V, Cochrane AW, Chen T, Tyner AL (2000) Sik (BRK) phosphorylates Sam68 in the nucleus and negatively regulates its RNA binding ability. Molecular and cellular biology 20:6114-6126.

Dimou L, Gotz M (2014) Glial cells as progenitors and stem cells: new roles in the healthy and diseased brain. Physiol Rev 94:709-737.

Discher DE, Mooney DJ, Zandstra PW (2009) Growth factors, matrices, and forces combine and control stem cells. Science 324:1673-1677.

Dreyfuss G, Kim VN, Kataoka N (2002) Messenger-RNA-binding proteins and the messages they carry. Nat Rev Mol Cell Biol 3:195-205.

Dreyfuss G, Matunis MJ, Pinol-Roma S, Burd CG (1993) hnRNP proteins and the biogenesis of mRNA. Annu Rev Biochem 62:289-321.

Dreyfuss G, Philipson L, Mattaj IW (1988) Ribonucleoprotein particles in cellular processes. The Journal of cell biology 106:1419-1425.

Durand B, Gao FB, Raff M (1997) Accumulation of the cyclin-dependent kinase inhibitor p27/Kip1 and the timing of oligodendrocyte differentiation. The EMBO journal 16:306-317.

Eisenbarth GS, Walsh FS, Nirenberg M (1979) Monoclonal antibody to a plasma membrane antigen of neurons. Proceedings of the National Academy of Sciences of the United States of America 76:4913-4917.

Ellison JA, de Vellis J (1994) Platelet-derived growth factor receptor is expressed by cells in the early oligodendrocyte lineage. Journal of neuroscience research 37:116-128.

Emery B (2010) Regulation of oligodendrocyte differentiation and myelination. Science 330:779-782.

Freude S, Leeser U, Muller M, Hettich MM, Udelhoven M, Schilbach K, Tobe K, Kadowaki T, Kohler C, Schroder H, Krone W, Bruning JC, Schubert M (2008) IRS-2 branch of IGF-1 receptor signaling is essential for appropriate timing of myelination. J Neurochem 107:907-917.

Fruhbeis C, Frohlich D, Kuo WP, Amphornrat J, Thilemann S, Saab AS, Kirchhoff F, Mobius W, Goebbels S, Nave KA, Schneider A, Simons M, Klugmann M, Trotter J, Kramer-Albers EM (2013) Neurotransmitter-triggered transfer of exosomes mediates oligodendrocyte-neuron communication. PLoS biology 11:e1001604.

Fruttiger M, Karlsson L, Hall AC, Abramsson A, Calver AR, Bostrom H, Willetts K, Bertold CH, Heath JK, Betsholtz C, Richardson WD (1999) Defective oligodendrocyte development and severe hypomyelination in PDGF-A knockout mice. Development 126:457-467.

Fumagalli S, Totty NF, Hsuan JJ, Courtneidge SA (1994) A target for Src in mitosis. Nature 368:871-874.

Furutachi S, Miya H, Watanabe T, Kawai H, Yamasaki N, Harada Y, Imayoshi I, Nelson M,

Nakayama KI, Hirabayashi Y, Gotoh Y (2015) Slowly dividing neural progenitors are an embryonic origin of adult neural stem cells. Nat Neurosci 18:657-665.

Fusaki N, Iwamatsu A, Iwashima M, Fujisawa J (1997) Interaction between Sam68 and Src family tyrosine kinases, Fyn and Lck, in T cell receptor signaling. The Journal of biological chemistry 272:6214-6219.

Gallo V, Armstrong RC (1995) Developmental and growth factor-induced regulation of nestin in oligodendrocyte lineage cells. The Journal of neuroscience : the official journal of the Society for Neuroscience 15:394-406.

Gao FB, Apperly J, Raff M (1998) Cell-intrinsic timers and thyroid hormone regulate the probability of cell-cycle withdrawal and differentiation of oligodendrocyte precursor cells. Dev Biol 197:54-66.

Garcia-Marques J, Lopez-Mascaraque L (2013) Clonal identity determines astrocyte cortical heterogeneity. Cereb Cortex 23:1463-1472.

Garcion E, Faissner A, ffrench-Constant C (2001) Knockout mice reveal a contribution of the extracellular matrix molecule tenascin-C to neural precursor proliferation and migration. Development 128:2485-2496.

Garwood J, Garcion E, Dobbertin A, Heck N, Calco V, ffrench-Constant C, Faissner A (2004) The extracellular matrix glycoprotein Tenascin-C is expressed by oligodendrocyte precursor cells and required for the regulation of maturation rate, survival and responsiveness to platelet-derived growth factor. Eur J Neurosci 20:2524-2540.

Givogri MI, Bongarzone ER, Schonmann V, Campagnoni AT (2001) Expression and regulation of golli products of myelin basic protein gene during in vitro development of oligodendrocytes. Journal of neuroscience research 66:679-690.

Gotz M, Bolz J, Joester A, Faissner A (1997) Tenascin-C synthesis and influence on axonal growth during rat cortical development. Eur J Neurosci 9:496-506.

Gotz M, Stoykova A, Gruss P (1998) Pax6 controls radial glia differentiation in the cerebral cortex. Neuron 21:1031-1044.

Grange J, Belly A, Dupas S, Trembleau A, Sadoul R, Goldberg Y (2009) Specific interaction between Sam68 and neuronal mRNAs: implication for the activity-dependent biosynthesis of elongation factor eEF1A. Journal of neuroscience research 87:12-25.

Grange J, Boyer V, Fabian-Fine R, Fredj NB, Sadoul R, Goldberg Y (2004) Somatodendritic localization and mRNA association of the splicing regulatory protein Sam68 in the hippocampus and cortex. Journal of neuroscience research 75:654-666.

Grigoryan T, Birchmeier W (2015) Molecular signaling mechanisms of axon-glia communication in the peripheral nervous system. Bioessays 37:502-513.

Grossman JS, Meyer MI, Wang YC, Mulligan GJ, Kobayashi R, Helfman DM (1998) The use of antibodies to the polypyrimidine tract binding protein (PTB) to analyze the protein components that assemble on alternatively spliced pre-mRNAs that use distant branch points. RNA 4:613-625.

Guitard E, Barlat I, Maurier F, Schweighoffer F, Tocque B (1998) Sam68 is a Ras-GAP-associated protein in mitosis. Biochemical and biophysical research communications 245:562-566.

Hardy RJ, Friedrich VL, Jr. (1996) Progressive remodeling of the oligodendrocyte process arbor during myelinogenesis. Dev Neurosci 18:243-254.

Hart IK, Richardson WD, Bolsover SR, Raff MC (1989) PDGF and intracellular signaling in the timing of oligodendrocyte differentiation. The Journal of cell biology 109:3411-3417.

Hartmann AM, Nayler O, Schwaiger FW, Obermeier A, Stamm S (1999) The interaction and colocalization of Sam68 with the splicing-associated factor YT521-B in nuclear dots is regulated by the Src family kinase p59(fyn). Mol Biol Cell 10:3909-3926.

He Y, Smith R (2009) Nuclear functions of heterogeneous nuclear ribonucleoproteins A/B.

Cell Mol Life Sci 66:1239-1256.
Hemmati-Brivanlou A, Kelly OG, Melton DA (1994) Follistatin, an antagonist of activin, is expressed in the Spemann organizer and displays direct neuralizing activity. Cell 77:283-295.
Henics T, Sanfridson A, Hamilton BJ, Nagy E, Rigby WF (1994) Enhanced stability of interleukin-2 mRNA in MLA 144 cells. Possible role of cytoplasmic AU-rich sequence-binding proteins. The Journal of biological chemistry 269:5377-5383.
Hildebrand C, Remahl S, Persson H, Bjartmar C (1993) Myelinated nerve fibres in the CNS. Prog Neurobiol 40:319-384.
Hockfield S, McKay RD (1985) Identification of major cell classes in the developing mammalian nervous system. The Journal of neuroscience : the official journal of the Society for Neuroscience 5:3310-3328.
Hsieh YW, Yang XJ (2009) Dynamic Pax6 expression during the neurogenic cell cycle influences proliferation and cell fate choices of retinal progenitors. Neural Dev 4:32.
Hu Q, Lee SY, O'Kusky JR, Ye P (2012) Signalling through the type 1 insulin-like growth factor receptor (IGF1R) interacts with canonical Wnt signalling to promote neural proliferation in developing brain. ASN Neuro 4.
Huot ME, Brown CM, Lamarche-Vane N, Richard S (2009) An adaptor role for cytoplasmic Sam68 in modulating Src activity during cell polarization. Molecular and cellular biology 29:1933-1943.
Iijima T, Iijima Y, Witte H, Scheiffele P (2014) Neuronal cell type-specific alternative splicing is regulated by the KH domain protein SLM1. The Journal of cell biology 204:331-342.
Iijima T, Wu K, Witte H, Hanno-Iijima Y, Glatter T, Richard S, Scheiffele P (2011) SAM68 regulates neuronal activity-dependent alternative splicing of neurexin-1. Cell 147:1601-1614.
Itoh M, Haga I, Li QH, Fujisawa J (2002) Identification of cellular mRNA targets for RNA-binding protein Sam68. Nucleic Acids Res 30:5452-5464.
Jean-Philippe J, Paz S, Caputi M (2013) hnRNP A1: the Swiss army knife of gene expression. Int J Mol Sci 14:18999-19024.
Joshi RP, Schoenbach KH (2000) Electroporation dynamics in biological cells subjected to ultrafast electrical pulses: a numerical simulation study. Phys Rev E Stat Phys Plasmas Fluids Relat Interdiscip Topics 62:1025-1033.
Jurica MS, Licklider LJ, Gygi SR, Grigorieff N, Moore MJ (2002) Purification and characterization of native spliceosomes suitable for three-dimensional structural analysis. RNA 8:426-439.
Kashima T, Rao N, David CJ, Manley JL (2007) hnRNP A1 functions with specificity in repression of SMN2 exon 7 splicing. Hum Mol Genet 16:3149-3159.
Kessaris N, Fogarty M, Iannarelli P, Grist M, Wegner M, Richardson WD (2006) Competing waves of oligodendrocytes in the forebrain and postnatal elimination of an embryonic lineage. Nat Neurosci 9:173-179.
Kettenmann H, Verkhratsky A (2008) Neuroglia: the 150 years after. Trends Neurosci 31:653-659.
Kidd GJ, Hauer PE, Trapp BD (1990) Axons modulate myelin protein messenger RNA levels during central nervous system myelination in vivo. Journal of neuroscience research 26:409-418.
Klein ME, Younts TJ, Castillo PE, Jordan BA (2013) RNA-binding protein Sam68 controls synapse number and local beta-actin mRNA metabolism in dendrites. Proceedings of the National Academy of Sciences of the United States of America 110:3125-3130.
Kriegstein A, Alvarez-Buylla A (2009) The glial nature of embryonic and adult neural stem cells. Annu Rev Neurosci 32:149-184.
Lamb TM, Knecht AK, Smith WC, Stachel SE, Economides AN, Stahl N, Yancopolous GD,

Harland RM (1993) Neural induction by the secreted polypeptide noggin. Science 262:713-718.

Larocque D, Galarneau A, Liu HN, Scott M, Almazan G, Richard S (2005) Protection of p27(Kip1) mRNA by quaking RNA binding proteins promotes oligodendrocyte differentiation. Nat Neurosci 8:27-33.

Lau JS, Baumeister P, Kim E, Roy B, Hsieh TY, Lai M, Lee AS (2000) Heterogeneous nuclear ribonucleoproteins as regulators of gene expression through interactions with the human thymidine kinase promoter. Journal of cellular biochemistry 79:395-406.

Laursen LS, Chan CW, Ffrench-Constant C (2011) Translation of myelin basic protein mRNA in oligodendrocytes is regulated by integrin activation and hnRNP-K. The Journal of cell biology 192:797-811.

Lee Y, Morrison BM, Li Y, Lengacher S, Farah MH, Hoffman PN, Liu Y, Tsingalia A, Jin L, Zhang PW, Pellerin L, Magistretti PJ, Rothstein JD (2012) Oligodendroglia metabolically support axons and contribute to neurodegeneration. Nature 487:443-448.

Lendahl U, Zimmerman LB, McKay RD (1990) CNS stem cells express a new class of intermediate filament protein. Cell 60:585-595.

Levine JM, Nishiyama A (1996) The NG2 chondroitin sulfate proteoglycan: a multifunctional proteoglycan associated with immature cells. Perspect Dev Neurobiol 3:245-259.

Levine JM, Stallcup WB (1987) Plasticity of developing cerebellar cells in vitro studied with antibodies against the NG2 antigen. The Journal of neuroscience : the official journal of the Society for Neuroscience 7:2721-2731.

Li J, Liu Y, Park IW, He JJ (2002) Expression of exogenous Sam68, the 68-kilodalton SRC-associated protein in mitosis, is able to alleviate impaired Rev function in astrocytes. J Virol 76:4526-4535.

Lin Q, Taylor SJ, Shalloway D (1997) Specificity and determinants of Sam68 RNA binding. Implications for the biological function of K homology domains. The Journal of biological chemistry 272:27274-27280.

Lock P, Fumagalli S, Polakis P, McCormick F, Courtneidge SA (1996) The human p62 cDNA encodes Sam68 and not the RasGAP-associated p62 protein. Cell 84:23-24.

Lukong KE, Richard S (2003) Sam68, the KH domain-containing superSTAR. Biochim Biophys Acta 1653:73-86.

Lukong KE, Richard S (2008) Motor coordination defects in mice deficient for the Sam68 RNA-binding protein. Behavioural brain research 189:357-363.

Macchi B, Marino-Merlo F, Nocentini U, Pisani V, Cuzzocrea S, Grelli S, Mastino A (2015) Role of inflammation and apoptosis in multiple sclerosis: Comparative analysis between the periphery and the central nervous system. J Neuroimmunol 287:80-87.

Macklin WB, Weill CL, Deininger PL (1986) Expression of myelin proteolipid and basic protein mRNAs in cultured cells. Journal of neuroscience research 16:203-217.

Maniatis T, Tasic B (2002) Alternative pre-mRNA splicing and proteome expansion in metazoans. Nature 418:236-243.

Manuel MN, Mi D, Mason JO, Price DJ (2015) Regulation of cerebral cortical neurogenesis by the Pax6 transcription factor. Frontiers in cellular neuroscience 9:70.

Marta CB, Adamo AM, Soto EF, Pasquini JM (1998) Sustained neonatal hyperthyroidism in the rat affects myelination in the central nervous system. Journal of neuroscience research 53:251-259.

Marty MC, Alliot F, Rutin J, Fritz R, Trisler D, Pessac B (2002) The myelin basic protein gene is expressed in differentiated blood cell lineages and in hemopoietic progenitors. Proceedings of the National Academy of Sciences of the United States of America 99:8856-8861.

Matter N, Herrlich P, Konig H (2002) Signal-dependent regulation of splicing via

phosphorylation of Sam68. Nature 420:691-695.
Matthews MA, Duncan D (1971) A quantitative study of morphological changes accompanying the initiation and progress of myelin production in the dorsal funiculus of the rat spinal cord. The Journal of comparative neurology 142:1-22.
McKinnon RD, Matsui T, Dubois-Dalcq M, Aaronson SA (1990) FGF modulates the PDGF-driven pathway of oligodendrocyte development. Neuron 5:603-614.
McMorris FA, Dubois-Dalcq M (1988) Insulin-like growth factor I promotes cell proliferation and oligodendroglial commitment in rat glial progenitor cells developing in vitro. Journal of neuroscience research 21:199-209.
Moore MJ, Sharp PA (1993) Evidence for two active sites in the spliceosome provided by stereochemistry of pre-mRNA splicing. Nature 365:364-368.
Moritz S, Lehmann S, Faissner A, von Holst A (2008a) An induction gene trap screen in neural stem cells reveals an instructive function of the niche and identifies the splicing regulator sam68 as a tenascin-C-regulated target gene. Stem Cells 26:2321-2331.
Moritz S, Lehmann S, Faissner A, von Holst A (2008b) An Induction Gene Trap Screen in Neural Stem Cells Reveals an Instructive Function of the Niche and Identifies the Splicing Regulator Sam68 as a Tenascin-C regulated Target Gene. Stem Cells.
Mudhar HS, Pollock RA, Wang C, Stiles CD, Richardson WD (1993) PDGF and its receptors in the developing rodent retina and optic nerve. Development 118:539-552.
Muller C, Bauer NM, Schafer I, White R (2013) Making myelin basic protein -from mRNA transport to localized translation. Frontiers in cellular neuroscience 7:169.
Nadarajah B (2003) Radial glia and somal translocation of radial neurons in the developing cerebral cortex. Glia 43:33-36.
Najib S, Martin-Romero C, Gonzalez-Yanes C, Sanchez-Margalet V (2005) Role of Sam68 as an adaptor protein in signal transduction. Cell Mol Life Sci 62:36-43.
Najib S, Sanchez-Margalet V (2002) Sam68 associates with the SH3 domains of Grb2 recruiting GAP to the Grb2-SOS complex in insulin receptor signaling. Journal of cellular biochemistry 86:99-106.
Nakajima K (2007) Control of tangential/non-radial migration of neurons in the developing cerebral cortex. Neurochem Int 51:121-131.
Nawaz S, Kippert A, Saab AS, Werner HB, Lang T, Nave KA, Simons M (2009) Phosphatidylinositol 4,5-bisphosphate-dependent interaction of myelin basic protein with the plasma membrane in oligodendroglial cells and its rapid perturbation by elevated calcium. The Journal of neuroscience : the official journal of the Society for Neuroscience 29:4794-4807.
Nawaz S, Sanchez P, Schmitt S, Snaidero N, Mitkovski M, Velte C, Bruckner BR, Alexopoulos I, Czopka T, Jung SY, Rhee JS, Janshoff A, Witke W, Schaap IA, Lyons DA, Simons M (2015) Actin Filament Turnover Drives Leading Edge Growth during Myelin Sheath Formation in the Central Nervous System. Dev Cell.
Neumann E, Schaefer-Ridder M, Wang Y, Hofschneider PH (1982) Gene transfer into mouse lyoma cells by electroporation in high electric fields. The EMBO journal 1:841-845.
Noctor SC, Flint AC, Weissman TA, Dammerman RS, Kriegstein AR (2001) Neurons derived from radial glial cells establish radial units in neocortex. Nature 409:714-720.
Ortega MC, Bribian A, Peregrin S, Gil MT, Marin O, de Castro F (2012) Neuregulin-1/ErbB4 signaling controls the migration of oligodendrocyte precursor cells during development. Exp Neurol 235:610-620.
Ozgen H, Kahya N, de Jonge JC, Smith GS, Harauz G, Hoekstra D, Baron W (2014) Regulation of cell proliferation by nucleocytoplasmic dynamics of postnatal and embryonic exon-II-containing MBP isoforms. Biochim Biophys Acta 1843:517-530.
Paridaen JT, Huttner WB (2014) Neurogenesis during development of the vertebrate central

nervous system. EMBO Rep 15:351-364.
Paronetto MP, Achsel T, Massiello A, Chalfant CE, Sette C (2007) The RNA-binding protein Sam68 modulates the alternative splicing of Bcl-x. The Journal of cell biology 176:929-939.
Pedraza L, Fidler L, Staugaitis SM, Colman DR (1997) The active transport of myelin basic protein into the nucleus suggests a regulatory role in myelination. Neuron 18:579-589.
Pedrotti S, Bielli P, Paronetto MP, Ciccosanti F, Fimia GM, Stamm S, Manley JL, Sette C (2010) The splicing regulator Sam68 binds to a novel exonic splicing silencer and functions in SMN2 alternative splicing in spinal muscular atrophy. The EMBO journal 29:1235-1247.
Pfeiffer SE, Warrington AE, Bansal R (1993) The oligodendrocyte and its many cellular processes. Trends Cell Biol 3:191-197.
Piaton G, Gould RM, Lubetzki C (2010) Axon-oligodendrocyte interactions during developmental myelination, demyelination and repair. J Neurochem 114:1243-1260.
Pinol-Roma S, Choi YD, Matunis MJ, Dreyfuss G (1988) Immunopurification of heterogeneous nuclear ribonucleoprotein particles reveals an assortment of RNA-binding proteins. Genes Dev 2:215-227.
Pinol-Roma S, Dreyfuss G (1992) Shuttling of pre-mRNA binding proteins between nucleus and cytoplasm. Nature 355:730-732.
Poltorak M, Sadoul R, Keilhauer G, Landa C, Fahrig T, Schachner M (1987) Myelin-associated glycoprotein, a member of the L2/HNK-1 family of neural cell adhesion molecules, is involved in neuron-oligodendrocyte and oligodendrocyte-oligodendrocyte interaction. The Journal of cell biology 105:1893-1899.
Pringle N, Collarini EJ, Mosley MJ, Heldin CH, Westermark B, Richardson WD (1989) PDGF A chain homodimers drive proliferation of bipotential (O-2A) glial progenitor cells in the developing rat optic nerve. The EMBO journal 8:1049-1056.
Pringle NP, Richardson WD (1993) A singularity of PDGF alpha-receptor expression in the dorsoventral axis of the neural tube may define the origin of the oligodendrocyte lineage. Development 117:525-533.
Quintana-Portillo R, Canfran-Duque A, Issad T, Sanchez-Margalet V, Gonzalez-Yanes C (2012) Sam68 interacts with IRS1. Biochem Pharmacol 83:78-87.
Ralston R, Bishop JM (1985) The product of the protooncogene c-src is modified during the cellular response to platelet-derived growth factor. Proceedings of the National Academy of Sciences of the United States of America 82:7845-7849.
Ranscht B, Clapshaw PA, Price J, Noble M, Seifert W (1982) Development of oligodendrocytes and Schwann cells studied with a monoclonal antibody against galactocerebroside. Proceedings of the National Academy of Sciences of the United States of America 79:2709-2713.
Relucio J, Menezes MJ, Miyagoe-Suzuki Y, Takeda S, Colognato H (2012) Laminin regulates postnatal oligodendrocyte production by promoting oligodendrocyte progenitor survival in the subventricular zone. Glia 60:1451-1467.
Remahl S, Hildebrand C (1982) Changing relation between onset of myelination and axon diameter range in developing feline white matter. J Neurol Sci 54:33-45.
Richard S, Vogel G, Huot ME, Guo T, Muller WJ, Lukong KE (2008) Sam68 haploinsufficiency delays onset of mammary tumorigenesis and metastasis. Oncogene 27:548-556.
Richard S, Yu D, Blumer KJ, Hausladen D, Olszowy MW, Connelly PA, Shaw AS (1995) Association of p62, a multifunctional SH2- and SH3-domain-binding protein, with src family tyrosine kinases, Grb2, and phospholipase C gamma-1. Molecular and cellular biology 15:186-197.
Richardson WD, Kessaris N, Pringle N (2006) Oligodendrocyte wars. Nature reviews

Neuroscience 7:11-18.
Rivers LE, Young KM, Rizzi M, Jamen F, Psachoulia K, Wade A, Kessaris N, Richardson WD (2008) PDGFRA/NG2 glia generate myelinating oligodendrocytes and piriform projection neurons in adult mice. Nat Neurosci 11:1392-1401.
Roach A, Boylan K, Horvath S, Prusiner SB, Hood LE (1983) Characterization of cloned cDNA representing rat myelin basic protein: absence of expression in brain of shiverer mutant mice. Cell 34:799-806.
Rodriguez-Pena A (1999) Oligodendrocyte development and thyroid hormone. J Neurobiol 40:497-512.
Rowitch DH, Kriegstein AR (2010) Developmental genetics of vertebrate glial-cell specification. Nature 468:214-222.
Saha MS, Spann CL, Grainger RM (1989) Embryonic lens induction: more than meets the optic vesicle. Cell Differ Dev 28:153-171.
Sanchez-Jimenez F, Sanchez-Margalet V (2013) Role of Sam68 in post-transcriptional gene regulation. Int J Mol Sci 14:23402-23419.
Sanchez-Margalet V, Najib S (1999) p68 Sam is a substrate of the insulin receptor and associates with the SH2 domains of p85 PI3K. FEBS Lett 455:307-310.
Sanchez-Margalet V, Najib S (2001) Sam68 is a docking protein linking GAP and PI3K in insulin receptor signaling. Mol Cell Endocrinol 183:113-121.
Sarlieve LL, Fabre M, Susz J, Matthieu JM (1983) Investigations on myelination in vitro: IV. "Myelin-like" or premyelin structures in cultures of dissociated brain cells from 14--15-day-old embryonic mice. Journal of neuroscience research 10:191-210.
Sasai Y, Lu B, Steinbeisser H, Geissert D, Gont LK, De Robertis EM (1994) Xenopus chordin: a novel dorsalizing factor activated by organizer-specific homeobox genes. Cell 79:779-790.
Schlessinger J (2000) Cell signaling by receptor tyrosine kinases. Cell 103:211-225.
Sette C, Messina V, Paronetto MP (2010) Sam68: a new STAR in the male fertility firmament. J Androl 31:66-74.
Shaham O, Menuchin Y, Farhy C, Ashery-Padan R (2012) Pax6: a multi-level regulator of ocular development. Prog Retin Eye Res 31:351-376.
Sharma RK, Netland PA (2007) Early born lineage of retinal neurons express class III beta-tubulin isotype. Brain Res 1176:11-17.
Simons M, Nave KA (2015) Oligodendrocytes: Myelination and Axonal Support. Cold Spring Harb Perspect Biol.
Singh R, Valcarcel J (2005) Building specificity with nonspecific RNA-binding proteins. Nat Struct Mol Biol 12:645-653.
Siomi H, Dreyfuss G (1995) A nuclear localization domain in the hnRNP A1 protein. The Journal of cell biology 129:551-560.
Smith WC, Knecht AK, Wu M, Harland RM (1993) Secreted noggin protein mimics the Spemann organizer in dorsalizing Xenopus mesoderm. Nature 361:547-549.
Sommer I, Schachner M (1981) Monoclonal antibodies (O1 to O4) to oligodendrocyte cell surfaces: an immunocytological study in the central nervous system. Dev Biol 83:311-327.
Spassky N, Goujet-Zalc C, Parmantier E, Olivier C, Martinez S, Ivanova A, Ikenaka K, Macklin W, Cerruti I, Zalc B, Thomas JL (1998) Multiple restricted origin of oligodendrocytes. The Journal of neuroscience : the official journal of the Society for Neuroscience 18:8331-8343.
Stallcup WB, Beasley L (1987) Bipotential glial precursor cells of the optic nerve express the NG2 proteoglycan. The Journal of neuroscience : the official journal of the Society for Neuroscience 7:2737-2744.
Stoykova A, Fritsch R, Walther C, Gruss P (1996) Forebrain patterning defects in Small eye

mutant mice. Development 122:3453-3465.
Tabata H (2015) Diverse subtypes of astrocytes and their development during corticogenesis. Front Neurosci 9:114.
Tang DG, Tokumoto YM, Apperly JA, Lloyd AC, Raff MC (2001) Lack of replicative senescence in cultured rat oligodendrocyte precursor cells. Science 291:868-871.
Tavanez JP, Madl T, Kooshapur H, Sattler M, Valcarcel J (2012) hnRNP A1 proofreads 3' splice site recognition by U2AF. Mol Cell 45:314-329.
Taveggia C, Feltri ML, Wrabetz L (2010) Signals to promote myelin formation and repair. Nat Rev Neurol 6:276-287.
Taylor SJ, Shalloway D (1994) An RNA-binding protein associated with Src through its SH2 and SH3 domains in mitosis. Nature 368:867-871.
Temple S, Raff MC (1985) Differentiation of a bipotential glial progenitor cell in a single cell microculture. Nature 313:223-225.
Temple S, Raff MC (1986) Clonal analysis of oligodendrocyte development in culture: evidence for a developmental clock that counts cell divisions. Cell 44:773-779.
Tole S, Christian C, Grove EA (1997) Early specification and autonomous development of cortical fields in the mouse hippocampus. Development 124:4959-4970.
Torvund-Jensen J, Steengaard J, Reimer L, Fihl LB, Laursen LS (2014) Transport and translation of MBP mRNA is regulated differently by distinct hnRNP proteins. Journal of cell science 127:1550-1564.
Trapp BD, Moench T, Pulley M, Barbosa E, Tennekoon G, Griffin J (1987) Spatial segregation of mRNA encoding myelin-specific proteins. Proceedings of the National Academy of Sciences of the United States of America 84:7773-7777.
Ulmer JB, Braun PE (1986) In vivo phosphorylation of myelin basic proteins: single and double isotope incorporation in developmentally related myelin fractions. Dev Biol 117:502-510.
Vernet C, Artzt K (1997) STAR, a gene family involved in signal transduction and activation of RNA. Trends in genetics : TIG 13:479-484.
Wake H, Lee PR, Fields RD (2011) Control of local protein synthesis and initial events in myelination by action potentials. Science 333:1647-1651.
Walters SN, Morell P (1981) Effects of altered thyroid states on myelinogenesis. J Neurochem 36:1792-1801.
Wang LL, Richard S, Shaw AS (1995) P62 association with RNA is regulated by tyrosine phosphorylation. The Journal of biological chemistry 270:2010-2013.
Watkins TA, Emery B, Mulinyawe S, Barres BA (2008) Distinct stages of myelination regulated by gamma-secretase and astrocytes in a rapidly myelinating CNS coculture system. Neuron 60:555-569.
Weaver JC (1995) Electroporation theory. Concepts and mechanisms. Methods Mol Biol 47:1-26.
White R, Gonsior C, Kramer-Albers EM, Stohr N, Huttelmaier S, Trotter J (2008) Activation of oligodendroglial Fyn kinase enhances translation of mRNAs transported in hnRNP A2-dependent RNA granules. The Journal of cell biology 181:579-586.
Wong G, Muller O, Clark R, Conroy L, Moran MF, Polakis P, McCormick F (1992) Molecular cloning and nucleic acid binding properties of the GAP-associated tyrosine phosphoprotein p62. Cell 69:551-558.
Xia H (2005) Regulation of gamma-fibrinogen chain expression by heterogeneous nuclear ribonucleoprotein A1. The Journal of biological chemistry 280:13171-13178.
Yang Y, Lewis R, Miller RH (2011) Interactions between oligodendrocyte precursors control the onset of CNS myelination. Dev Biol 350:127-138.
Ye P, Li L, Lund PK, D'Ercole AJ (2002) Deficient expression of insulin receptor substrate-1 (IRS-1) fails to block insulin-like growth factor-I (IGF-I) stimulation of brain growth

and myelination. Brain Res Dev Brain Res 136:111-121.
Yeh HJ, Ruit KG, Wang YX, Parks WC, Snider WD, Deuel TF (1991) PDGF A-chain gene is expressed by mammalian neurons during development and in maturity. Cell 64:209-216.
Zearfoss NR, Clingman CC, Farley BM, McCoig LM, Ryder SP (2011) Quaking regulates Hnrnpa1 expression through its 3' UTR in oligodendrocyte precursor cells. PLoS genetics 7:e1001269.
Zhang SC (2001) Defining glial cells during CNS development. Nature reviews Neuroscience 2:840-843.
Zhang Y, Chen K, Sloan SA, Bennett ML, Scholze AR, O'Keeffe S, Phatnani HP, Guarnieri P, Caneda C, Ruderisch N, Deng S, Liddelow SA, Zhang C, Daneman R, Maniatis T, Barres BA, Wu JQ (2014) An RNA-sequencing transcriptome and splicing database of glia, neurons, and vascular cells of the cerebral cortex. The Journal of neuroscience : the official journal of the Society for Neuroscience 34:11929-11947.
Zhou Z, Licklider LJ, Gygi SP, Reed R (2002) Comprehensive proteomic analysis of the human spliceosome. Nature 419:182-185.

Danksagung

Zuerst möchte ich PD Dr. Alexander von Holst danken, der mir die Möglichkeit gab in Heidelberg meine Doktorarbeit durchzuführen und an diesem interessanten Thema zu arbeiten. Danke für die Unterstützung und die wissenschaftlichen Ratschläge.

Herrn Prof. Kirsch möchte ich dafür danken, dass er mir ermöglicht hat meine Arbeit am Lehrstuhl für Anatomie und Zellbiologie durchzuführen.

Frau Prof. Ulrike Müller möchte ich für das Interesse an meinem Projekt und die Übernahme des Erstgutachtens danken.

Claudio Sette danke ich für die freundliche Bereitstellung der Sam68 Konstrukte.

Der Firma Lonza group und besonders Andrea Toell danke ich für die erfolgreiche Kooperation.

Denise und Richard, was hätte ich nur ohne euch gemacht. Ohne unseren Zusammenhalt wäre die ganze Zeit sicherlich sehr schwer gewesen. So aber blicke ich zurück und muss sagen, dass es großartige 3 Jahre waren. Denise, besonders dir danke ich. Unsere tiefe Freundschaft bedeutet mir so viel. Die lustigen (hier könnte man eine sehr lange Liste einfügen…) und schönen Dinge, die wir schon miteinander erlebt haben möchte ich niemals missen. Ich kann mich immer auf dich verlassen, dir vertrauen und eine ehrliche Meinung erwarten. Danke, dass es dich gibt! Patric, Christoph, Carmen, Evangelia und Sabrina, auch euch danke ich nicht nur für tolle Grillabende am Neckar, ihr habt die Zeit unvergesslich gemacht. Ihr seid so tolle Freunde, ich möchte euch alle nicht mehr missen!

Auch außerhalb unserer Arbeitsgruppe habe ich die Zeit am Institut für Anatomie sehr genossen und möchte allen jetzigen und ehemaligen Mitgliedern für die tolle Arbeitsatmosphäre danken. Den technischen Assistentinnen Andrea, Michaela, und Ingeborg möchte ich für die Unterstützung und guten Ratschläge danken.

Ganz besonders möchte ich meiner Familie danken, meinen Eltern Uwe und Petra und meinen Brüdern Marc, Marcel und Tim. Euer Rückhalt und einfach das Gefühl, dass ihr da seid wenn ich euch brauche waren für mich enorm wichtig. Ihr habt immer aufmunternde Worte gefunden, ward verständnisvoll und geduldig. Ohne euch und unseren Zusammenhalt wäre diese Zeit nicht zu meistern gewesen.